Translation 321

AD 625952

DEPARTMENT OF THE NAVY

DAVID TAYLOR MODEL BASIN
WASHINGTON, D.C.

HYDROMECHANICS

AERODYNAMICS

STRUCTURAL MECHANICS

APPLIED MATHEMATICS

ACOUSTICS AND VIBRATION

DESIGN OF SHIP RUDDERS

(Zur Formgebung von Schiffsrudern)

by

H. Thieme, Dipl.-Ing.
Shipbuilding Institute
University of Hamburg

Translated by E. N. Labouvie, Ph.D.

November 1965 Translation 321

DESIGN OF SHIP RUDDERS

(Zur Formgebung von Schiffsrudern)

by

H. Thieme, Dipl.-Ing.
Shipbuilding Institute
University of Hamburg

Presented in Supplements to the Main
Convention, Hamburg, 1961
(Jahrbuch der Schiffbautechnischen
Gesellschaft, Vol. 56, 1962)

November 1965 Translation 321

TABLE OF CONTENTS

	Page
ABSTRACT	1
A. INTRODUCTION	1
B. CRITERIA FOR ARRANGEMENT AND STRUCTURAL DESIGN	2
C. HYDROMECHANIC ASPECTS	10
D. ANALYTIC AND GRAPHIC REPRESENTATION OF PROFILE FORMS	16
E. COMPARISON AND DISCUSSION OF VARIOUS RUDDER PROFILE FORMS	18
F. SUPPLEMENTARY WIND-TUNNEL TESTS	27
G. MEASURES FOR SUBSEQUENT ALTERATION OF RUDDER CHARACTERISTICS	53
H. FUTURE TRENDS IN RUDDER FORMS	56
I. REFERENCES	57
APPENDIX - DISCUSSION BY OTHER INVESTIGATORS	60

LIST OF FIGURES

	Page
Figure 1 - Minimum Rudder Sizes for Directional Stability	3
Figure 2 - Rudder Size and Turning Ability at a 35-Degree Rudder Angle	4
Figure 3 - Rudder Effect on the Turning Ship	11
Figure 4 - Relationship between Rudder Angles δ_R, Drift Angles at the Center of Lateral Resistance ϵ_L, Drift Angles on the Rudder Axis ϵ_A, and Ship Rotation L_L/R	15
Figure 5 - Dimensional Ratios and Profile Parameter of Rudder Profiles	17
Figure 6 - Contour Equation and Contour Parameter for the Representation of Rudder Profiles	18
Figure 7 - Examples of Commonly Used Profiles of Guide-Head Rudders	22
Figure 8 - Common Profiles of Balanced Rudders of 15 Percent Relative Thickness	23
Figure 9 - Examples of Common Balanced Rudder Profiles of Greater Relative Thickness	23

		Page
Figure 10 -	Symmetrical Flow Profiles from Familiar Experimental Investigations	23
Figure 11 -	The New JfS Balanced Rudder Profiles	23
Figure 12 -	Bow Rudder Profiles	26
Figure 13 -	Profile Sections of the Plate Rudders Investigated	26
Figure 14 -	Nose Contours of Several Balanced Rudder Profiles	26
Figure 15 -	Tail Contours of Several Balanced Rudder Profiles	26
Figure 16 -	Rudder Models Tested in the Wind Tunnel, Aspect Ratio $A_R = 1$	27
Figure 17 -	Test Setup in the Former JfS Wind Tunnel at the Hamburg Engineering Institute	28
Figure 18 -	Flow Forces on Rectangular Rudder TMB 075 075 15 ...	44
Figure 19 -	Flow Forces on Rectangular Rudder TMB 075 075 15 in Astern Motion	44
Figure 20 -	Flow Forces on Rectangular Rudder NACA 0015	45
Figure 21 -	Flow Forces on Rectangular Rudder NACA 0015 in Astern Motion	45
Figure 22 -	Flow Forces on Rectangular Rudder NACA 0025	45
Figure 23 -	Flow Forces on Rectangular Rudder NACA 0025 in Astern Motion	45
Figure 24 -	Flow Forces on Rectangular Rudder JfS 58 TR 15	46
Figure 25 -	Flow Forces on Rectangular Rudder JfS 58 TR 15 in Astern Motion	46
Figure 26 -	Flow Forces on Rectangular Rudder JfS 58 TR 25	46
Figure 27 -	Flow Forces on Rectangular Rudder JfS 58 TR 25 in Astern Motion	46
Figure 28 -	Flow Forces on Rectangular Rudder JfS 61 TR 25	47
Figure 29 -	Flow Forces on Rectangular Rudder JfS 61 TR 25 in Astern Motion	47
Figure 30 -	Flow Forces on Rectangular Rudder JfS 62 TR 25	47
Figure 31 -	Flow Forces on Rectangular Rudder JfS 62 TR 25 in Astern Motion	47
Figure 32 -	Flow Forces on Rectangular Bow Rudder JfS 55 BR 15 ..	48

Page

Figure 33 - Flow Forces on Rectangular Bow Rudder JfS 55 BR 15 .. 48

Figure 34 - Flow Forces on Rectangular Bow Rudder JfS 59 BR 15 .. 48

Figure 35 - Flow Forces on Rectangular Bow Rudder JfS 57 BR 15 .. 48

Figure 36 - Flow Forces on Square Plate B/L = 0.015 49

Figure 37 - Flow Forces on Square Plate B/L = 0.03 49

Figure 38 - Flow Forces on Square Plate B/L = 0.05 49

Figure 39 - Flow Forces on Square Plate B/L = 0.07 49

Figure 40 - Efficiency of Various Rudder Profiles at Small Rudder Angles in Straight-Ahead Motion 50

Figure 41 - Comparison of the Rudder Moment Curve which Determines the Choice of the Location of the Turning Axis, for Various Rudder Profiles at Small Rudder Angles in Straight-Ahead Motion 50

Figure 42 - Drag Power Requirement of Various Rudder Profiles at Rudder Angle in Straight-Ahead Motion 51

Figure 43 - Drag Power Requirement and Efficiency of Profile JfS 5? TR 25 for Straight-Ahead Motion and for Motion along the Turning Circle $L_L/R = 0.5$ 52

Figure 44 - Influence of Aspect Ratio on the Transverse-Force Coefficient for Various Ruddars 52

Figure 45 - Influence of the Reynolds Number on the Transverse-Force Coefficient for Various Rudders 53

Figure 46 - Effect of Rudder Wedge Arrangement with and without Profile Shortening on Flow Forces Acting on Rectangular Rudder NACA 0015 55

LIST OF TABLES

Page

Table 1 - Principal Form Parameters of Familiar Balanced Rudder Profiles 19

Table 2 - Form Parameters of the JdF Profiles 20

Table 3 - Profile Offsets of the Rudder Profiles of the Present JfS Investigation 24

Table 4 - Test Results for TMB 075 075 15 32

Page

Table 5 - Test Results for NACA 0015 33

Table 6 - Test Results for NACA 0025 34

Table 7 - Test Results for JfS 58 TR 15 35

Table 8 - Test Results for JfS 58 TR 25 36

Table 9 - Test Results for JfS 61 TR 25 37

Table 10 - Test Results for JfS 62 TR 25 38

Table 11 - Test Results for JfS 55 BR 15 39

Table 12 - Test Results for JfS 54 BR 15 40

Table 13 - Test Results for JfS 59 BR 15 41

Table 14 - Test Results for JfS 57 BR 15 42

Table 15 - Test Results for Square Plate B/L = 0.015 42

Table 16 - Test Results for Square Plate B/L = 0.03 43

Table 17 - Test Results for Square Plate B/L = 0.05 43

Table 18 - Test Results for Square Plate B/L = 0.07 44

Table 19 - Rudder Efficiency and Drag Power Requirements of the Profiles Investigated 51

NOTATION

The symbols used here have been selected to avoid any confusion with the symbols used in earlier Shipbuilding Institute investigations of rudder and steering characteristics. Insofar as possible, they conform to the recommendations of the International Towing Tank Conference.

Points

o_A	Center of the turning axis of the rudder in the xy-plane of the ship
o_L	Center of lateral resistance of the ship without rudder

Lengths

A	Interval of abscissas (Figure 6)
B	Maximum breadth of ship
B	Maximum profile thickness
B_n	Thickness of profile nose at dy/dx = 0 (Figure 3)
B_s	Thickness of the trailing edge of the profile
B_{so}	Original thickness at the trailing edge of a shortened profile
g	Length of the straight profile tail
H_n	Thickness of the rudder neck (Figure 5)
H_R	Rudder height
L	Profile length, in general
$L_L = \frac{1}{A_L}\int_0^T L_z^2 \cdot dz$	Lateral length of the hull
$(L_L/R)_{35}$	Ship's rotation at 35° rudder angle
$L_{LR} = \frac{1}{A_R} \cdot \int_0^{H_R} L_{Rz}^2 \cdot dz$	Lateral length of the rudder
L_o	Original length of the shortened profile
L_{oR}	Length of the upper edge of the rudder
L_{pp}	Length between perpendiculars
L_R	Rudder length
L_{Rz}	Length of the rudder at the height z
L_{uR}	Length of the lower edge of the rudder
L_{WL}	Length in the waterline of the ship
L_z	Length of a waterline at the height z
n	Length of the profile nose
R	Radius of path, in general
R_L	Radius of the path of the center of lateral resistance
r_B	Radius of curvature of the profile contour at the maximum thickness
r_n	Radius of the profile nose
r_s	Radius of the trailing edge of the profile
s	Length of the profile tail of variable thickness (Figure 5)
T	Draft of the ship

x	Profile abscissa, longitudinal axis of the rudder, longitudinal axis of the ship
x_{Bn}	Distance of the profile nose thickness from the leading edge
x_{Hn}	Distance of the profile neck from the leading edge
x_{LA}	Horizontal distance of the turning axis of the rudder O_A from the center of lateral resistance O_L
y	Profile ordinate
z	Vertical distance of a waterline above the keel base or above the rudder base, respectively
$\eta = y/A$	Non-dimensional ordinate
ϱ_0	Contour parameter for the curvature on the profile nose (Figure 6)
$\Lambda_L = 2 \cdot T^2/A_L$	Aspect ratio of the hull
$\Lambda_R = H^2_R/A_R$	Aspect ratio of the rudder
$\Lambda_{Ro} = H^2_R/A_{Ro}$	Aspect ratio of the rudder with unshortened profile length
$\xi = x/A$	Non-dimensional abscissa

Areas

A_L	Lateral area of the hull
A_R	Rudder area
A_{Ro}	Rudder area for unshortened profile length
A_S	Cross-sectional area of the slipstream in the test section of the wind tunnel
$\tau = A_L/(L_{WL} \cdot T)$	Fullness of the lateral area

Volumes

V	Volume displacement of the ship
$\delta_L = V/(L_L \cdot B \cdot T)$	Fullness of the displacement, referred to the lateral length
$\delta_{pp} = V/(L_{pp} \cdot B \cdot T)$	Fullness of the displacement, referred to the length between perpendiculars

Angles

δ_R	Rudder angle, positive for the stern rudder in the sense of the port side rotation
ε	Angle of oblique flow, in general
ε_A	Drift angle on the rudder axis, in general
ε_{As}	Drift angle on the rudder axis, determinative for non-linear forces
ε_{Aw}	Drift angle on the rudder axis, determinative for linear forces
ε_L	Drift angle at the center of lateral resistance of the ship
ε_{max}	Flow angle at the transverse force maximum
ε_R	Flow angle of the rudder, in general
ε_{Rs}	Flow angle of the rudder, determinative for the non-linear forces
ε_{Rw}	Flow angle of the rudder, determinative for the linear forces

Velocities

v Relative velocity of the flow to the ship
v_R Relative velocity of the flow to the rudder
$Re = v \cdot L_R/\nu$ Reynolds number of the rudder

Forces and Moments

C Transverse force of the rudder perpendicular to v_R and positive toward the right, as seen against the relative flow

C_R Transverse force contribution of the rudder to the ship, perpendicular to v and positive toward the right, as seen against the relative flow
$c_C = C/(A_{Ro} \cdot v_R^2 \cdot \rho/2)$ Transverse-force coefficient of the rudder
$c_{C,Max}$ Maximum transverse-force coefficient of the rudder
$c_D = D/(A_{Ro} \cdot v_R^2 \cdot \rho/2)$ Resistance coefficient of the rudder

$c_M = M/(A_{Ro} \cdot L_o \cdot v_R^2 \cdot \rho/2)$ Coefficient of the rudder moment referred to $L_o/2$
$c_{M,25}$ Corresponding coefficient of the rudder moment referred to $L_o/4$ from the leading edge

c_{NRv} Drag power coefficient of the rudder, Equation [6]
$c_{n\varepsilon}$ Coefficient of the non-linear transverse-force gradient
$c_{w\varepsilon}$ Coefficient of the linear transverse-force gradient
$c_X = X/(A_{Ro} \cdot v \quad \cdot \rho/2)$ Longitudinal-force coefficient of the rudder
c_Y Corresponding lateral-force coefficient of the rudder
c_{YRv} Coefficient of the control force of the rudder, Equation [5]
D Resistance of the rudder, positive in the direction of the relative flow of v_R

D_R Contribution of the rudder to the ship's resistance
M Moment about the vertical axis of the rudder at $L_o/2$, positive as seen from above, clockwise direction
M_a Moment about the turning axis of the rudder of any arbitrary location
M_R Contribution of the rudder to the yawing moment about the center of lateral resistance of the ship
$M_{,25}$ Moment about the vertical axis of the rudder at $L_o/4$ from the leading edge
X Longitudinal force of the rudder, positive in the rudder-x-direction toward the bow
X_R Contribution of the rudder to the longitudinal force of the ship
Y Lateral force of the rudder, positive in the rudder-y-direction to starboard
Y_R Contribution of the rudder to the lateral force of the ship

Physical Quantities

ν Kinematic viscosity of the flow medium
ρ Density of the flow medium

ABSTRACT

Starting from present day criteria for the choice of the size and arrangement of rudders, this paper discusses the suitable streamlining of guiding-head and balanced rudders. In addition to a purely visual comparison of conventional (usual) and newly developed profiles, the report includes profile offsets that have not been published previously and contrasts the form parameters of various rudder profiles which are based on a familiar mathematical method of profile representation. Comparative studies of several familiar foreign rudder profiles and of rudder profiles which have been developed in the Shipbuilding Institute in recent years indicate that the modern profiles definitely improve rudder efficiency, both when the ship is moving astern and ahead; this also applies to bow rudder profiles. The influence of the thickness ratio (proportion of thickness to length) in the case of plate rudders--which has not been established experimentally in publications thus far--is indicated in an additional test series. To illustrate the possibilities of subsequently improving the rudder profile either in efficiency or balancing, the use of a rudder wedge arrangement, with and without profile shortening, is discussed and examples are given from a special experimental investigation.

A. INTRODUCTION

Support received from the German Research Association and an extremely effective grant from the Ministry of Transport has enabled the Shipbuilding Institute of the University of Hamburg to carry out several theoretical and experimental investigations on the characteristics of rudders over a period of several years. Moreover, it was possible to observe that during this period of time, the range of problems concerning rudder and steering qualities of ships became larger and more acute. Thus, it was easily possible that the active pursuit of these investigations was promoted and broadened by a fruitful contact with present-day requirements, on one hand, and by benefiting from the investigations started in other research institutes on similar subjects, on the other.

The result was not so much a solution of individual problems taken up consecutively, but rather the pursuit of research work on a broad front; hence, it will be understandable that the broad investigations are not entirely completed but that it is inadvisable to delay all reports until final completion. A number of findings have already been arrived at on the

basis of the results obtained in several individual fields which may have fairly useful practical applications. Hence, the purpose of this paper is to supplement the subject matter area of the intermediate results reported thus far[1,2] as well as the nearly concurrent intermediate results.[20,30] In this connection, I must therefore ask the forbearance of the reader if the timing of this report appears to be too early in view of the whole range of problems to be tackled and too late in view of the many detailed results obtained.

Since the installation of the facilities required for these and similar experimental investigations is still incomplete, many compromises regarding technical execution of the investigations were required. Staff workers of the Shipbuilding Institute, especially Messrs. Böhme, Thiemann, and Malzahn, deserve credit for the fact that the quality of the test results was not adversely affected by this circumstance.

B. CRITERIA FOR ARRANGEMENT AND STRUCTURAL DESIGN

The first consideration when designing the rudder of a ship is, of course, determination of the surface area. As a consequence of the propeller arrangement and of certain real—or assumed—requirements for maneuvering characteristics, we then obtain in relation to the preselected surface area, a more or less arbitrary arrangement of the rudder or rudders in relation to the ship and especially in relation to its propulsion system. After this determination has been made, relatively little leeway remains for selecting the aspect ratio of the rudder ($\Lambda_R = H^2_R/A_R$), the surface outline, and the type of rudder. In making these last-mentioned decisions, it will often be found that structural and operational considerations play a decisive role and that the only remaining problem of the hydromechanical design is to utilize the structural conditions to attain the best possible hydrodynamic efficiency.

If for the time being we disregard the attempts at "hydrodynamic treatments" of undesirable effects of horizontal gaps and the rare

---

[1]References are listed on page 57.

occasions to arrange for end disks and intermediate disks, then the only design element remaining for this hydrodynamic problem is the streamlining of the rudder. This last problem represents the core of this report. However, in order to see it in the proper context, we shall first consider the other problems involved in designing ship rudders.

Even today statistical data are used—probably almost exclusively—in selecting the size of the rudder surfaces. Several sources[3,4,6-9] indicate, in the "usual manner," as it were, the rudder area as a percentage of the lateral plane (A_R/A_L) as a function of the ship type or as a function of the volume displacement ∇ referred to the lateral plane A_L and and the lateral length L_L. The results of References 3 and 4, conceived to be valid for "normal" merchant ships, are shown in Figure 1. They are

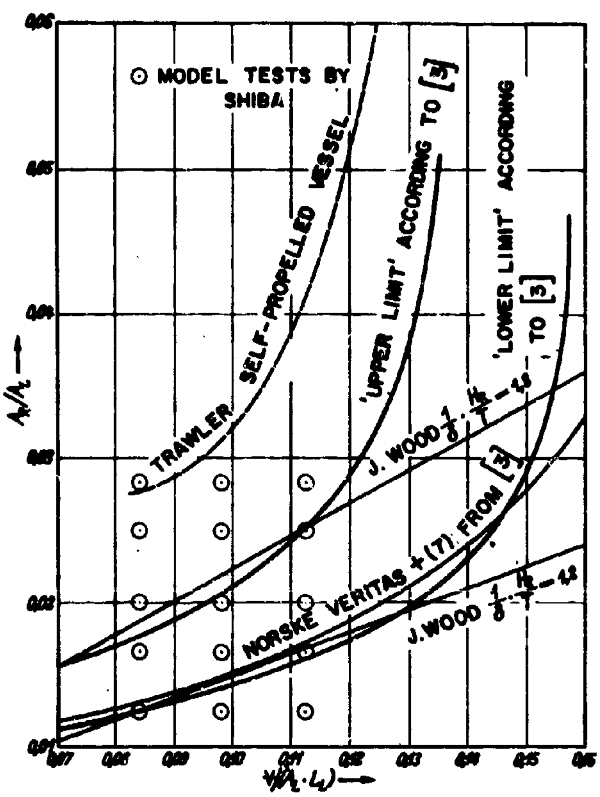

Figure 1 - Minimum Rudder Sizes for Directional Stability

reasonably consistent with one another as well as with the data of References 6 to 8. These data are based on the practical requirement of

providing ships with a high value $\Psi/(A_L \cdot L_L)$ with a rudder area which is sufficiently large for directional stability. In the case of ships with small values of $\Psi/(A_L \cdot L_L)$, on the other hand, this dimensioning criterion would result in an unusually small rudder area; it is true that directional stability of the ship would be attained, but the radius of the turning circle would be unusually large.

Thus, we have touched on the two steering qualities of a ship which are the most interesting for practical ship operation. Frequently, only the radius of the turning circle as such comes under discussion; by this we tacitly understand the smallest turning circle or, more precisely, the radius of the turning circle at approximately 35-deg rudder angle. This is represented nondimensionally as "rotation" $(L_L/R)_{35}$ in Figure 2. In

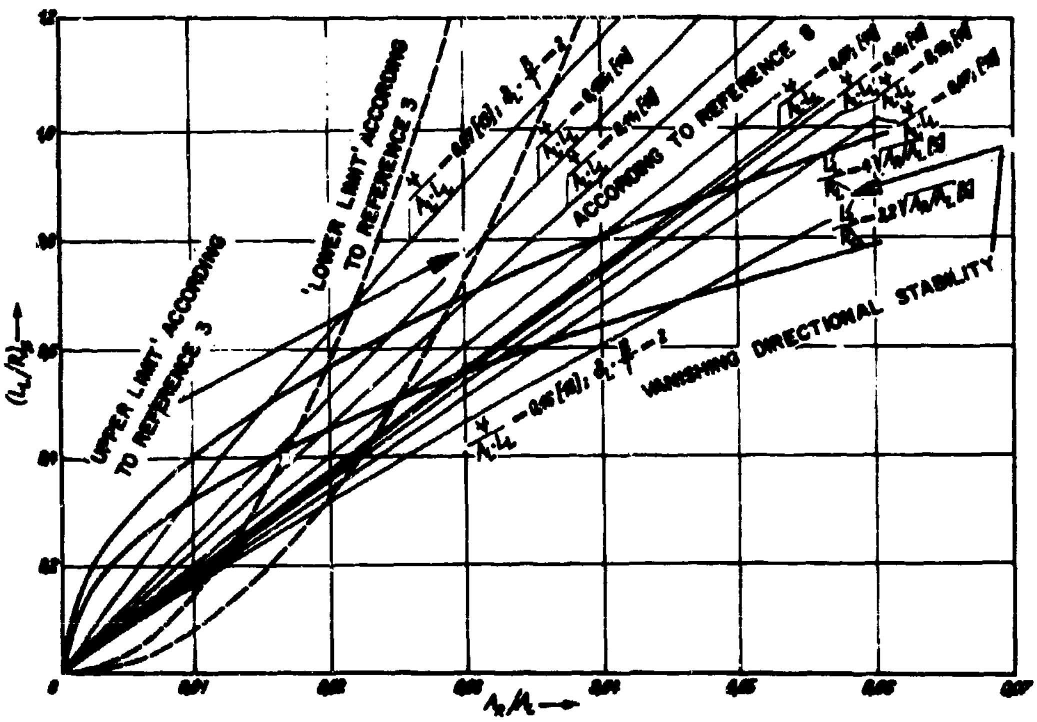

Figure 2 - Rudder Size and Turning Ability at a 35-Degree Rudder Angle

contrast to the aforementioned directional stability, this radius of the turning circle represents a clearly defined characteristic of every ship, one which can be controlled with relative ease and which at least gives a very good clue for judging its behavior. In each special case, it is possible to set size requirements which can easily be justified. The

situation is altogether different in the case of directional stability; not even the experts have agreed on the definition, let alone on the "correct measure." There is substantial agreement on the fact that a properly designed vessel must have directional stability. However, even the question of whether a ship must have "natural" directional stability, i.e., not require automatic pilot, or whether it may suffice to attain directional stability, with the aid of an automatic pilot is by no means unanimously decided as yet.

Without doubt, however, directional stability is the most significant of all the steering qualities of a ship; ultimately, of course, a ship must first of all be able to keep a fixed course in an economical way, and the ability to alter this course will have to be of secondary importance. With this in mind, it may be somewhat surprising that References 10 and 11 offer statistical data for the choice of the rudder size as a function of the desired radius of the turning circle (see Figure 2). Probably the reason for this procedure, which may not seem to be altogether logical, consists solely in the fact that the greater obviousness of the radius of the turning circle holds a certain attraction compared to directional stability. It may also be that these procedures were originally conceived in such a manner that for a given ship with a given rudder surface, the radius of the turning circle to be expected was to be determined on the basis of statistical data or of adapted theoretical considerations; see References 1^ to 14.

The diagrams of Figures 1 and 2 are based on the above-mentioned data, on an additional personal report of the Hamburg Model Basin (HSVA) on proven rudder sizes of trawlers and inland vessels (self-propelled vessels), and on qualitative derivations from the underlying theoretical principles contained in Reference 5; these diagrams serve to determine the rudder size as a function of the above-mentioned "mean breadth-length ratio"

$$\frac{V}{A_L \cdot L_L} = \frac{\delta_L \cdot L_L \cdot B \cdot T}{\tau \cdot L_{WL} \cdot T \cdot L_L} = \frac{\delta_L}{\tau} \cdot \frac{B}{L_{WL}}$$

for a specified constant or a statistical directional stability. Moreover, they serve to indicate the radii of the turning circle that are randomly obtained with this selection. In addition the changes necessary in the

rudder surface (beyond or below the size governed by directional stability) to attain a corresponding change in the radius of the turning circle may be estimated. The data of Polonski,[8] Schoenherr,[10] and Laube[14] are useful for this purpose and agree very well with the analytical results obtained by Schmitz[13] (see Figure 2). The data taken from Reference 3 are altogether different; they show implicitly the determination of A_R/A_L as a function of $\forall/(A_L \cdot L_L)$ and are thus unsuitable for determining subsequent changes in the rudder size. According to Reference 5, the two curves contain an implicit determination to the effect that the rudder size is always chosen in such manner that the directional stability barely vanishes so that directional instability prevails. Moreover, Figure 2 should not be used for values smaller than $A_R/A_L = 0.01$ and for values $(L_L/R)_{35}$ greater than approximately 1.2. In the case of every normal ship, a marked reduction in the rudder surface toward zero by no means leads to a maximum rotation approaching zero; even without rudder, a finite turning circle is still obtained. Conversely, in the case of a fixed rudder angle of 35 deg, an arbitrary increase in the rudder surface by no means produces a further increase in the obtainable rotation. As indicated in Reference 5, a rotation of approximately 1.2 represents the practical asymptotic boundary value for infinitely large rudders.

In Figures 1 and 2 the rudder surface area is presented as an obvious criterion both for attaining turning ability and for attaining directional stability and coupled with the latter for insuring "yaw-checking ability"* for the ship as well. To be sure, this is a customary, but nevertheless coarse simplification of the actual relationships. Therefore, it should be expressly pointed out that the dimensioning of the deadwood in front of the propeller and the arrangement of fixed fins behind the propeller are also to be taken into consideration, both with and without the rudder, if certain characteristics of the ship are to be produced or changed. In this connection, it should also be pointed out that these measures are not nearly equivalent. An increase of the deadwood means

---

*Translator's note: Stutzfahigkert = yaw-checking ability, ability to check swing of ship's head by laying the rudder to the opposite hand, "meeting" ability.

something totally different from an increase in the rudder area or an additional arrangement of fixed fins. Attention should also be called to ~~the danger of cutting away the deadwood which is so popular today~~; the equivalence of the deadwood area and the rudder enlargement with regard to directional stability which exists in the case of a smooth sea is easily lost in a following sea, for instance. This danger is easily intensified if the areas of keel or bilge keels are dimensioned with extreme scantiness as is customary. It is too easily forgotten that the keels not only serve to stabilize the ship against rolling but also to improve directional stability by reducing the possibility of running off course.

An additional factor is implicitly contained in the above-mentioned statistical and simplified analytical results although it is not considered in a refined form. This is the effect of the aspect ratio of the rudder

$$A_R = \left(\frac{H_R}{T}\right)^2 \cdot \frac{\frac{A_L}{3}}{A_R/A_L} = \left(\frac{H_R}{T}\right)^2 \cdot \frac{\frac{V}{A_L \cdot L_L}}{\frac{B}{T} \cdot \delta_L \cdot A_R/A_L} \qquad [1]$$

which varies with the rudder size for a given ship.

The ratio of the rudder height H_R to the draft T depends mostly on the basic design and lies in the vicinity of

$$(H_R/T)^2 = 0.3 \text{ to } 0.7 \text{ to } 0.8$$

if classified statistically by types of ships.

If we now exclude extreme cases, e.g., old river tug boats or old sailing vessels, then, according to Equation [1], we still obtain a spread of the rudder aspect ratios A_R from 0.7 for short full vessels with large rudder areas up to 2.5 for long slender ships with correspondingly small rudder areas. On the basis of the aspect ratio alone, however, the initial efficiency of the rudder is almost twice as high for a greater aspect ratio as for a smaller one. The smaller aspect ratios, on the other hand, have approximately 60 percent higher efficiency at maximum rudder angle. Thus it will indeed be possible to influence directional stability as well as turning ability and yaw-checking ability by the choice of a rudder aspect ratio. In actual practice, however, these facts can be utilized only in the transition to the multiple-surface arrangement.

While it is true, as mentioned above, that the rudder aspect ratio has a considerable effect on the efficiency of the rudder (although from a purely visual standpoint, it is not at all conspicuous in most cases), the situation is exactly the opposite as far as the rudder profile is concerned. The profile design as a rectangular or trapezoidal rudder and in certain rare cases also as an angular (broken) trapeze or as an ellipse becomes immediately conspicuous in most cases. However, the hydrodynamic effect on fundamental characteristics such as course keeping and turning ability is extremely slight. It is easier for such a design to influence the tendency of a vessel to veer off course at full speed ahead or at full speed astern when starting from the at-rest position. Obviously, however, this possibility is not interesting enough to restrain the general tendency toward the trapezoidal rudder for it is precisely the trapezoidal rudder which intensifies this tendency to veer off course compared to the rectangular rudder or even more compared to the rudder with the planform of a full ellipse. Hydrodynamically speaking, moreover, the trapezoidal rudder is somewhat inferior to the rectangular rudder because of its unfavorable pressure distribution. Superiority would be obtained only for the trapezoidal twin rudder whose upper edge would again have to be somewhat shorter than the maximum rudder length. Even the static advantages of the trapezoid are overestimated in the case of the spade rudder since the center of the application of the force for the bending moment of the rudder post is not located in the center of gravity of the surface, but always lies somewhat below.

According to a proven rule of thumb by Schrenk, this center lies between the actual center of gravity of the surface and the center of gravity of the surface of the equi-area full ellipse of equal position in a vertical sense and height. Hence, compared to the rectangular rudder, the apparent effect of the bending moment reduction through the trapezoidal form in reality is only one-half. If this factor is taken into account, it is possible that in many cases, the simpler structural design and the assured hydrodynamic improvement in the case of the rectangular rudder might influence the compromise in this direction. Of course for static reasons, the rectangular rudder calls for a greater relative profile thickness compared to the trapezoidal rudder. If, for instance, we start out

from a trapezoidal ratio of the length of the lower edge L_{uR} to the length of the upper edge L_{oR} of 2/3 ratio which is already quite large, ~~then the equi-area rectangular rudder calls for an increase in the~~ relative profile thickness of a little over 20 percent, i.e., from approximately $\delta/L = 0.20$ for the trapezoidal rudder to $\delta/L = 0.25$ for the corresponding rectangular rudder. The test data indicated in this report, however, are likely to favor such an increase in the profile thickness.

In making a hydrodynamic comparison between trapezoidal and rectangular rudder as it is practically expressed in the formation of the familiar coefficients for force components and moment, it must be borne in mind that for the trapezoidal rudder, the "lateral length" is to be used as the length in forming the moment coefficient; this "lateral length" of the rudder is obtained geometrically simply from the fundamental relation

$$L_{LR} = \frac{1}{A_R} \int_0^{H_R} \cdot L_{Rz}^2 \cdot dz \qquad [2]$$

and amounts to

$$\frac{L_{LR}}{L_{oR}} = \frac{2}{3}\left(\frac{L_{uR}}{L_{oR}} + \frac{1}{1 + L_{uR}/L_{oR}}\right) \qquad [3]$$

in the case of the trapezoidal rudder. In the case of the elliptical rudder contour, it amounts to

$$\frac{L_{LR}}{L_{oR}} = \frac{8}{3\pi} = 0.8488 \qquad [4]$$

In this case, it will be seen that fundamentally the rectangular form must always yield the smaller rudder moment since the lateral lengths L_{LR} for the trapezoid and ellipse always turn out to be somewhat greater—although for practical forms only slightly so—than the mean rudder length which, of course, is also the lateral length for the rectangular rudder.

In addition to the static criteria, the structural and operational criteria also determine the type of the rudder bearings and in turn the choice of the rudder type as well. In most cases, factors such as convenient removability and the use of antifriction bearings or sleeve-type bearings determine whether a spade rudder or a semi-balanced rudder is chosen. Although this has not yet been taken into account experimentally in this paper, our attention is nevertheless directed to the fact that

considerable efforts are still required in the area of rudder design to offset the fundamental hydrodynamic inferiority of the semi-balanced rudder or at least to minimize it. The other special rudder design— different from the normal balanced rudder—, is the one-piece through rudder with a continuous guiding head, or more briefly, the guide head rudder. It has recently lost some of its present-day significance, but it offers far greater possibilities of arriving at a hydrodynamically satisfactory design (see Figure 7).

All rudder forms have in common the structural and operational interest in choosing the location of the turning axis of the rudder in such manner that for the normal condition of ahead motion the zero position of the rudder with regard to the rudder moment curve is a stable condition in order to avoid flutter, noise, and additional bearing stresses. Unfortunately it is impossible to satisfy these desires by placing the turning axis far in front because in that case the rudder moments increase greatly at maximum rudder angles and under loadings in a seaway. Fortunately, the effect of the twist of the slipstream brings about a displacement of the pressure center to the rear; this must be borne in mind when using measurements without a propeller. Independently of this, however, there is the problem, based on structural requirements, of developing profile forms which have pressure centers, that are located as far as possible to the rear; this has, in fact, been achieved to a certain extent in the case of the measurements on newly developed profiles set forth in this report. Independently thereof or in addition thereto, experiments are to be carried forward by taking "artificial" measures such as removal by suction.[1]

C. HYDROMECHANIC ASPECTS

The hydromechanic aspects supplement the structural aspects. Any work to effectively develop good rudder forms should consider carefully all structural requirements and desires and be receptive to resultant suggestions without however adopting them directly as the fundamental condition for each and every design. The hydrodynamic rudder development must retain sufficient scope for purely hydrodynamic aspects in order that

potentially significant effects which later might become structurally possible in some modified form are not excluded at the beginning. Not only forms that are structurally possible and hydrodynamically sound are to be presented as the highlights of a development for even forms which are now considered structurally unusual or which are even hydrodynamically unsatisfactory may yield interesting data and thus lay the useful foundation for further development.

In this text then, we shall report not only on the rudder with profile JfS 58 TR 25 which is structurally possible because of its thick rear edge and which is of an altogether "advanced design," hydrodynamically speaking (the last number indicates the maximum relative thickness in percent—see Figure 11) but on profile JfS 62 TR 25 as well. Profile JfS 62 TR 25 is hydrodynamically superior but because of its very thin trailing edge it certainly will not become popular in this form, structurally speaking. Even the form of a thick plate (Figure 13) beveled in the front and rear, which an earlier investigation[2] had shown to be inferior from the hydrodynamic standpoint, and the equally inferior, newly investigated plate bow rudder JfS 57 BR 15 (Figure 12) shall not be disregarded. We should not ignore even such crude forms as JfS 59 BR 15 or JfS 54 BR 15 (Figure 12) if these even more normal bow rudder forms are hydrodynamically superior.

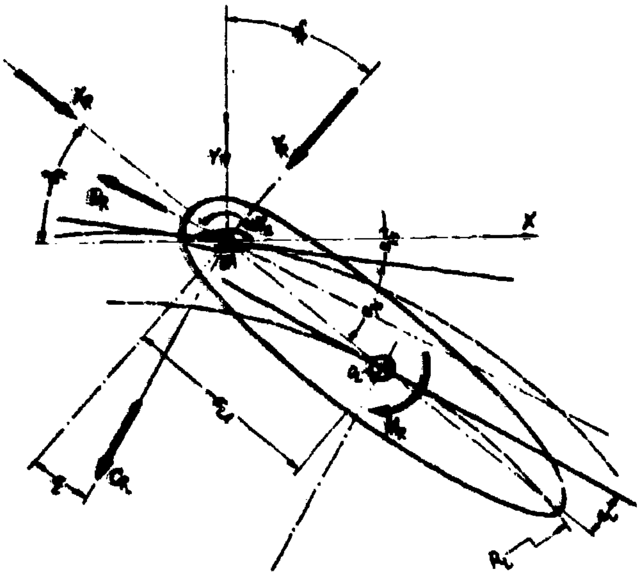

Figure 3 - Rudder Effect on the Turning Ship

The fundamental hydromechanic aspects for judging the quality of a rudder must, of course, be furnished by the purpose which the latter is to serve on the ship. The test results set forth here are immediately applicable to a ship underway in ahead motion. Customarily, such data are regarded as decisive for all of the purposes the rudder is to accomplish on the ship although the rudder effect in straight-ahead motion is only momentary and relatively weak in all cases. To round out the picture, we should also consider the rudder effect on the turning ship (Figure 3) which, after all, is more pronounced in most cases.

Figure 3 is a schematic drawing of the hydrodynamically interesting drift angles at the center of lateral resistance ε_L on the rudder axis ε_{As}, and for the rudder $-\varepsilon_{Rs}$ deflected by $-\delta_R$. The rudder forces are represented, on the one hand, as the longitudinal rudder force X and the lateral rudder force Y, and the rudder shaft moment M_a; and on the other hand, they are represented as a rudder contribution to the longitudinal force of the ship X_R, to the lateral force of the ship Y_R, and to the yawing moment about the vertical (normal) axis M_R of the center of lateral resistance. The rudder contributions to the transverse force of the ship and to the ship resistance are C_R and D_R. The hydromechanically interesting effects of the rudder on the ship as a whole are the control force Y_R, which is decisive for the contribution M_R and which thus brings about the turning of the ship, the rudder contribution to the drag power requirement of the ship N_R, which is determinative for the speed loss in the turning circle, and finally the contribution to the transverse force of the ship C_R. The contribution to the transverse force of the ship has only a very indirect effect on the steering characteristics of the ship whereas it can hardly be influenced independently of the control force; hence, it is not given any further attention in this connection. From Figure 3, it is easily possible to establish a relationship for the control force with force components referred to rudder axes.

$$c_{Y'Rr} = c_{Y'} \cdot \cos \delta_R + c_X \cdot \sin \delta_R \qquad [5]$$

In this connection, we immediately introduce the customary non-dimensional form; see the Notation. In connection with the drag

coefficient, we have disregarded in Equation [6] the contribution to the shaft moment (shaft torque) M_a which is insignificant compared to the steering moment M_R.

$$c_{NRr} = c_Y \sin(\varepsilon_L + \delta_R) - c_X \cdot \cos(\varepsilon_L + \delta_R) - \frac{L}{R_L} \cdot \frac{x_{LA}}{L_L} \cdot c_{YRr} \qquad [6]$$

According to Equation [5], when the ship is moving straight ahead, c_{YRr} is exactly equal to the transverse force coefficient of the rudder as indicated by c_C in Section F for the test results in wind tunnels; According to Equation [6] c_{NRr} becomes equal to the rudder resistance coefficient c_D from Section F when the ship moves straight ahead. In this case, the oblique inflow toward the rudder, quite generally designated as ε in Section F, coincides with the angle of rudder deflection δ_R. In accordance with the definitions of the symbols in the Notation, for a positive rotation L_L/R_L of the ship, the rudder angle in terms of the rotation must be regarded as negative.

According to Figure 3, moreover, we find that for the turning ship, the inflow at the location of the rudder axis o_A (which inflow is to be determined on a purely geometrical basis) amounts to

$$\tan \varepsilon_{Ag} = \tan \varepsilon_L + \left(\frac{-x_{LA}}{L_L}\right) \frac{L_L/R_L}{\cos \varepsilon_L} \qquad [7]$$

However, in order to determine the circulation-dependent rudder lift--characterized by the index "w" according to Equation [5]--the hydrodynamically effective angle of inflow at the rudder axis ε_{Aw} must be reduced by approximating the size of the drift angle at the center of lateral resistance ε_L.

$$\tan \varepsilon_{Aw} = \left(\frac{x_{LA}}{L_L}\right) \cdot \frac{L_L/R_L}{\cos \varepsilon_L} \qquad [8]$$

Thus, we obtain the unfortunate theoretical result, which indeed is supported experimentally, that the circulation-dependent so-called linear or "waterline" components of the rudder forces are functions of the inflow angle of the rudder

$$\varepsilon_{Rw} = \delta_R + \arctan - \left[\frac{-x_{LA}}{L_L} \cdot \frac{L_L/R_L}{\cos \varepsilon_L}\right] \qquad [9]$$

whereas the so-called nonlinear or "frame" components of the rudder forces remain functions of the purely geometrical inflow angle of the rudder.

$$\varepsilon_{Rs} = \delta_R + \arctan\left[\tan \varepsilon_L + \frac{-x_{LA}}{L_L} \cdot \frac{L_L/R_L}{\cos \varepsilon_L}\right] \qquad [10]$$

The unavoidable consequence is that the relationship between oblique inflow toward the rudder and rudder force components (polar curve of the rudder) varies somewhat with the rotation of the ship. It is necessary, therefore, that rudder measurements also be carried out behind the turning ship or ship model or that the rudder measurements for the ship moving straight ahead must be converted in a certain way to the turning circle measurement. To do so, we can fall back on the method for computing nonlinear rudder forces which is touched upon and indicated in more detail in Reference 5. With sufficient accuracy, we can neglect the effect on the c_X required in Equations [5] and [6]. In a simplified representation, c_Y is computed as:

$$c_Y = c_{w\varepsilon} \cdot \varepsilon_{Rw} + c_{s\varepsilon} \cdot \varepsilon_{Rs}^2 \cdot \frac{\varepsilon_{Rs}}{|\varepsilon_{Rs}|} \qquad [11]$$

Thereby, we obtain approximately

$$\varepsilon_{Rs} = \delta_R + \frac{1}{2}\frac{L_L}{R_L} + \varepsilon_L = \varepsilon_{Rw} + \varepsilon_L \qquad [12]$$

and finally as a correction formula

$$\begin{aligned} c_Y &= c_Y\,(\text{bei } \varepsilon = \varepsilon_{Rw}) + c_{s\varepsilon} \cdot (2\varepsilon_{Rw} \cdot \varepsilon_L + \varepsilon_L^2) \\ c_X &= c_X\,(\text{bei } \varepsilon = \varepsilon_{Rw}) \end{aligned} \qquad [13]$$

In this case, the coefficient $c_{s\varepsilon}$ as a gradient of the nonlinear component must also be determined from the measurements for straight-ahead motion. In order to convert the measurements for the ship in straight-ahead motion to turning circle measurements we must, of course, also know the drift angle and the corresponding rudder deflection. An absolute normalization is, of course, impossible in this case. However, for the

comparisons undertaken in Section F, we have drawn upon data by Shiba[15] which, comparatively speaking, represent fairly good mean values for interesting types of merchant ships. Therefore, we have used the results represented in Figure 4, namely, rudder angles with drift angles as a function of the ship rotation as well as the rudder size and the fullness of the displacement.

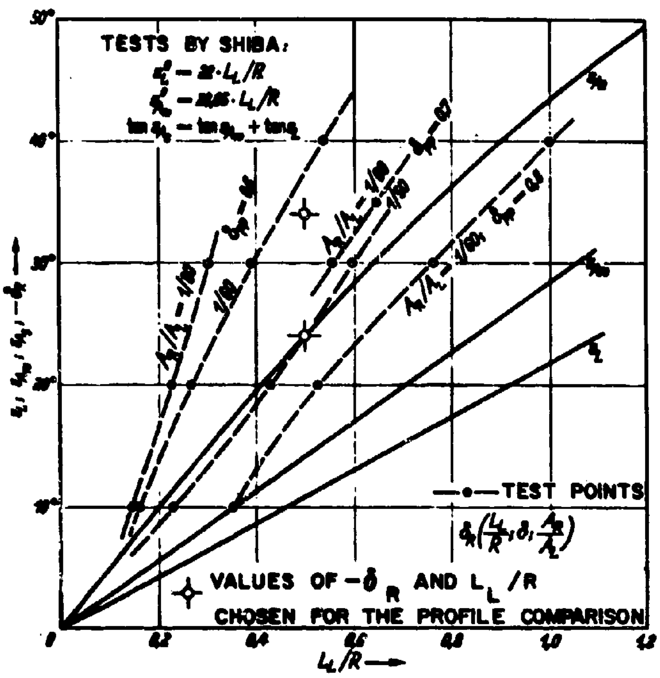

Figure 4 - Relationship between Rudder Angles δ_R, Drift Angles at the Center of Lateral Resistance ϵ_L, Drift Angles on the Rudder Axis ϵ_A, and Ship Rotation L_L/R

Thus, the results of rudder tests are then to be examined with a view to the criteria for hydrodynamic quality. A great control force and a small drag power requirement are the first prerequisites for ships moving straight ahead or going into a turn. It is true that in actual practice a high maximum transverse force is utilized during ship rotation only if rudder angles exceeding 35 deg are used. However, when checking the yaw, this characteristic has effect for almost every ship. Finally, we are to develop the astern characteristics of the rudder to as high a degree as possible, both for small rudder angles and for the maximum

transverse force. Of course, the best astern characteristics of a rudder are of no avail if this rudder is located so closely behind the deadwood that in astern motion, the transverse flow toward the rudder produces a counterforce of practically equal magnitude on the deadwood thus almost completely cancelling the rudder effect. However, the modern trend toward larger propeller apertures provides an opportunity to attain a certain control efficiency in astern motion with rudders which have good astern characteristics.

D. ANALYTIC AND GRAPHIC REPRESENTATION OF PROFILE FORMS

From the foregoing considerations, the importance of streamlining the rudder has developed into a measure for obtaining favorable rudder characteristics which may indeed be chosen rather freely. The structural limitations in this case are not so incisive as in the choice of the aspect ratio, for instance. Surprising as it may be, however, the material on ship rudder profiles scattered throughout the literature does not offer a very systematic picture. Form systematization is an effective means of utilizing practical experience quickly and effectively and with statistical accuracy; this is the more important, the fewer the quantitative hydrodynamic investigations that are available.

In view of this situation, it appears wise to use the rudder profile systematization[19,20] developed at the Hamburg Model Basin and the Shipbuilding Institute[18] and subsequently developed even further as a basis for this investigation. In Figure 5, we proceed to show this systematized notation for the dimensional ratios—the "outer" proportions of the profile, as it were—and the form parameters of the individual curved sections which comprise the total profile. Correspondingly, the form parameters might be designated as the "inner" proportions of the profile.

Figure 6 shows the notation used for the computation of the profile contours, all of which consist of polynomials and are split up into so-called influence functions, one such function being used for each form parameter. Thereby, it is possible to represent every conceivable—reasonable and unreasonable—profile form of a rudder. As an inevitable consequence, we also obtain the possib[illegible] analyzing clearly unusual

profile forms which are graphically represented and of expressing them by corresponding equations. This method (which has been described in more detail in Reference 20) also permits the analysis of the much more difficult ship lines[19] and may therefore be regarded as sufficiently accurate for rudders. The guide head rudder shown as the third form in Figure 7 may serve to prove that the method of clearly analysing arbitrary rudder profiles on the basis of polynomials is easily reproducible. It is taken from Reference 3 where the offsets are also indicated. These offsets are computed on the basis of an analysis of a small workshop drawing and they thus enable us to draw the profile with great, hydrodynamically effective accuracy.

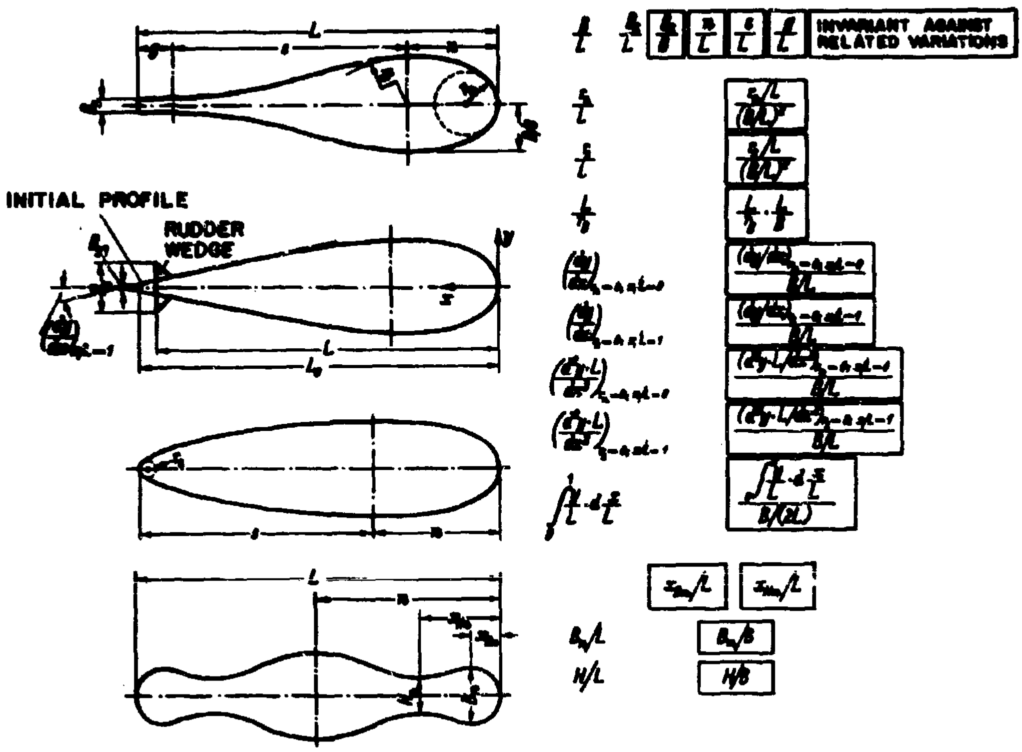

Figure 5 - Dimensional Ratios and Profile Parameter of Rudder Profiles

It should be noted, moreover, that the profiles are generally correlated with so-called profile families. In that case, the profiles of one family essentially differ only in the maximum relative thickness which,

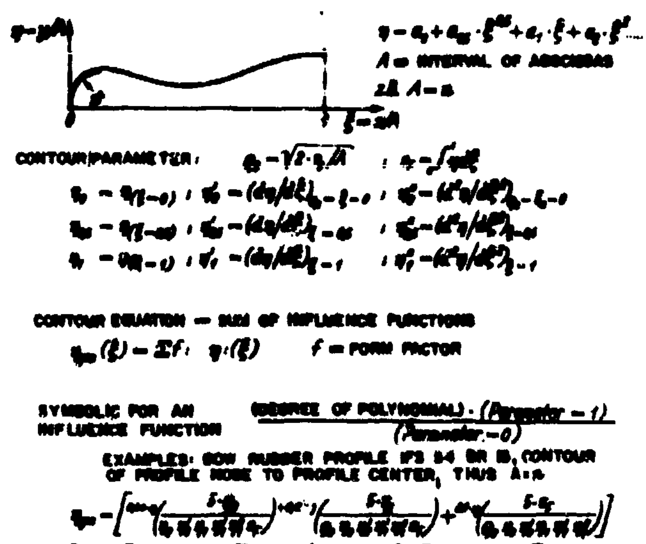

Figure 6 - Contour Equation and Contour Parameter for the Representation of Rudder Profiles

in most cases, lies between 35 and 20 percent of the total length from the front. The relative maximum thicknesses B/L which are to be considered are obtained both from available systematic test data which begin mostly at B/L = 0.12 (see Reference 26) and from extreme structural desires which lead to B/L = 0.25. Most profile families consist of simple profiles whose entire related variations differ only in the thickness ratio B/L. Such families are for instance the familiar NACA 00 .. -profiles and the more recent family JfS 58 TR .. Nonrelated families are the familiar Joukowski profiles as well as the family JfS 52 TR .. and JfS 62 TR ... from the Shipbuilding Institute. A glance at Tables 1 and 2 shows the characteristic features of these profile families.

For years profile development at the Shipbuilding Institute has always proceeded in such manner that the particular data of available profile forms are carefully examined with regard to their relation with the form parameters and that all further steps are derived from this by parameter modifications which promise to yield results.

E. COMPARISON AND DISCUSSION OF VARIOUS RUDDER PROFILE FORMS

The experiments discussed in this report (Section F) cover balanced rudders only. However, there is already a need to extend the experiments

TABLE 1

Principal Form Parameters of Familiar Balanced Rudder Profiles

	FORM PARAMETERS → / PROFILE FORM	$\frac{d}{L}$	$\frac{s}{L}$	$\frac{r_0}{L}$	$\frac{r_0/L}{(d/L)^2}$	$\left(\frac{dy}{dx}\right)_{r_0=0,\,x=L}$	$\frac{\left(\frac{dy}{dx}\right)_{r_0=0,\,x=L}}{d/L}$
RUDDER PROFILE OF COASTAL MOTOR SHIPS ACCORDING TO REF. 22	Navy Standard Nr... 15	0,15	~ 0,25	~ 0,0225	~ 1,0	0,30	1,25
	TMB 075 075 15	0,15	0,075	0,075	3,33	0,0812	0,541
	HAMBURG MODEL BASIN 50 R 15	0,15	0,30	0,02475	1,1	0,125	0,80
		0,180	0,285	~ 0,026	~ 0,80	~ 0,27	~ 1,25
		0,223	0,27	~ 0,04	~ 0,8	~ 0,25	~ 0,95
	NACA 0012	0,12	0,30	0,01584	1,1	0,1404	1,17
	NACA 0015	0,15	0,30	0,02475	1,1	0,1755	1,17
	NACA 0018	0,18	0,30	0,03564	1,1	0,2106	1,17
	NACA 0020	0,20	0,30	0,044	1,1	0,234	1,17
	NACA 0025	0,25	0,30	0,06875	1,1	0,2925	1,17
SHIPYARD RUDDER PROFILE ACCORDING TO REF. 27	Gö 409	0,120	0,25	~ 0,0144	~ 1,0	~ 0,120	~ 1,0
	[illegible]	0,194	0,25	~ 0,0376	~ 1,0	~ 0,194	~ 1,0
	[illegible] 410	0,161	0,30	~ 0,035	~ 1,35	0,1125	0,7
	Gö 429 } Joukowsky-Profile	~ 0,118	~ 0,254	~ 0,0161	~ 1,159	0	0
	Gö 535 } Joukowsky-Profile	~ 0,169	~ 0,285	~ 0,0325	~ 1,137	0	0
	Gö 539 } Joukowsky-Profile	~ 0,215	~ 0,282	~ 0,0513	~ 1,108	0	0
	Gö 549 } Joukowsky-Profile	~ 0,257	~ 0,300	~ 0,0737	~ 1,073	0	0

to guide head rudder forms as well. In any event, a sur ey of rudder profile forms cannot disregard the profiles of the guide head rudders. In Figure 7, therefore, we have summarized the guide head profiles according to References 3, 22, and 27 which are probably the most familiar ones of all. From the standpoint of the present time, a continued development would probably be worthwhile especially for Seebeck-Oertz rudders and for the HSVA guide head rudder, particularly if hollow profile flanks are used.

TABLE 2

Form Parameters of the JdF Profiles

PARAMETERS \ PROFILE	52 TR 12	52 TR 15	52 TR 18	58 TR 15	58 TR 25	61 TR 15	61 TR 25
B/L	0,12	0,15	0,18	0,15	0,25	0,15	0,25
E_n/L	0	0	0	0,03	0,05	0,03	0,05
E_n/B	0	0	0	0,2	0,2	0,2	0,2
n/L	0,25	0,25	0,25	0,25	0,25	0,2	0,2
a/L	0,75	0,75	0,75	0,65	0,65	0,7	0,7
p/L	0	0	0	0,10	0,10	0,1	0,1
r_n/L	0,0309	0,04825	0,0694	0,0804	0,134	0,0602	0,1676
$(r_n/L)/(B/L)^2$	2,146	2,146	2,146	2,146	2,146	2,68	2,68
$(r_n/n)/(B/n)^2$	0,5365	0,5365	0,5365	0,5365	0,5365	0,5365	0,5365
r_H/L	0	0	0	0	0	0	0
$(r_H/L)/(B/L)^2$	0	0	0	0	0	0	0
L/r_n	0,426	0,5236	0,64	0,5328	0,886	0,4325	1,39
$(L/r_n)/(B/L)$	3,552	3,552	3,552	3,552	3,552	5,56	5,56
$(n/r_n)/(B/n)$	0,222	0,222	0,222	0,222	0,222	0,222	0,222
$(dy/dx)\ r_a = x = 0$	−0,267	−0,333	−0,4	−0,333	−0,555	−0,417	−0,694
$(dy/dx)\ r_a = x = 0/(B/L)$	−2,22	−2,22	−2,22	−2,22	−2,22	−2,776	−2,776
$(dy/dx)\ r_a = x = 0/(B/n)$	−0,555	−0,555	−0,555	−0,555	−0,555	−0,555	−0,555
$-(dy/dx)\ r_s = 0;\ x = L$	0,1066	0,1066	0,1066	0	0	0	0
$-(dy/dx)\ r_s = 0;\ x = L/(B/L)$	0,888	0,7111	0,592	0	0	0	0
$(L \cdot d^2y/dx^2)\ r_a = x = 0$	0,1032	0,129	0,1548	0,129	0,215	0,1775	0,296
$(L \cdot d^2y/dx^2)\ r_a = x = 0/(B/L)$	0,86	0,86	0,86	0,86	0,86	1,183	1,183
$(n \cdot d^2y/dx^2)\ r_a = x = 0/(B/n)$	0,05375	0,05375	0,05375	0,05375	0,05375	0,0473	0,0473
$(L \cdot d^2y/dx^2)\ r_s = 0;\ x = L$	0	0,213	0,426	0	0	0	0
$(L \cdot d^2y/dx^2)\ r_s = 0;\ x = L/(B/L)$	0	1,42	2,366	0	0	0	0
$\int_0^1 (y/L)\, d(x/L)$	0,0396	0,0487	0,0579	0,0453	0,0755	0,0432	0,0730
$\frac{2L}{B} \int_0^1 (y/L)\, d(x/L)$	0,66	0,6493	0,6433	0,604	0,604	0,576	0,576
x_{Bm}/L	—	—	—	—	—	—	—
x_{gm}/L	—	—	—	—	—	—	—
B_m/L	—	—	—	—	—	—	—
B_m/B	—	—	—	—	—	—	—
H/L	—	—	—	—	—	—	—
H/B	—	—	—	—	—	—	—

Table 2 continued

61 TR 15	62 TR 25	65 B 15	64 BR 15	59 BR 15	57 BR 17	NACA 0015 FOR THE PURPOSE OF COMPARISON	NACA 0025	PROFILE / PARAMETERS
0,15	0,25	0,15	0,15	0,15	0,15	0,15	0,25	B/L
0,015	0,015	0	−0,1085	0,0965	0,015	0,003	0,005	B_S/L
0,10	0,06	0	−0,7233	0,6433	0,1	0,02	0,02	B_S/B
0,20	0,2	0,5	0,5	0,5	0,5	0,30	0,30	n/L
0,75	0,75	0,5	0,5	0,5	0,5	0,70	0,70	a/L
0,05	0,05	0	0	0	0	0	0	g/L
0,0602	0,1676	0,0112	0,04825	0,04825	0	0,02475	0,06875	r_n/L
2,68	2,68	0,5	2,146	2,146	0	1,1	1,1	$(r_n/L)/(B/L)^2$
0,5365	0,5365	0,25	1,073	1,072	0	0,330	0,330	$(r_n/n)/(B/n)^2$
0	0	0,0112	0,04825	0,04825	0	0	0	r_S/L
0	0	0,5	2,146	2,146	0	0	0	$(r_S/L)/(B/L)^2$
0,3325	1,20	0,3	0	6,50	1,62	0,39667	0,06436	L/r_B
5,56	5,56	2	0	43,9	10,8	2,65714	2,65714	$(L/r_B)/(B/L)$
0,222	0,222	0,5	0	10,86	2,7	0,230	0,230	$(n/r_B)/(B/n)$
−0,417	−0,694	0	0	0	0	−0,0717	−0,1195	$(dy/dx)_{r_n} = x = 0$
−2,776	−2,776	0	0	0	0	−0,4781	−0,4781	$(dy/dx)_{r_n} = x = 0/(B/L)$
−0,555	−0,555	0	0	0	0	−0,143	−0,143	$(dy/dx)_{r_n} = x = 0/(B/n)$
0	0	0	0	0	0	0,1755	0,2925	$-(dy/dx)_{r_s} = 0;\ x = L$
0	0	0	0	0	0	1,17	1,17	$-(dy/dx)_{r_s} = 0;\ x = L/(B/L)$
0,1775	0,296	0	−7,45	0	1,62	−0,81497	−1,35827	$(L \cdot d^2y/dx^2)_{r_n} = x = 0$
1,183	1,183	0	−49,6	0	10,8	−5,4331	−5,4331	$(L \cdot d^2y/dx^2)_{r_n} = x = 0/(B/L)$
0,0673	0,0673	0	12,417	0	2,7	−0,06171	−0,06171	$(n \cdot d^2y/dx^2)_{r_n} = x = 0/(B/n)$
0	0	0	−7,45	0	1,62	−0,1028	−0,1714	$(L \cdot d^2y/dx^2)_{r_s} = 0;\ x = L$
0	0	0	−49,6	0	10,8	−0,6857	−0,6857	$(L \cdot d^2y/dx^2)_{r_s} = 0;\ x = L/(B/L)$
0,0410	0,0662	0,0589	0,05	0,0406	0,04125	0,05140	0,08567	$\int_0^1 (y/L)\, d(x/L)$
0,5467	0,5296	0,7854	0,666	0,5413	0,5500	0,68536	0,68536	$\frac{2L}{B} \int_0^1 (y/L)\, d(x/L)$
—	—	—	−0,005	0,04825	—	—	—	x_{Bn}/L
—	—	—	−0,3075	0,19825	—	—	—	x_{Hn}/L
—	—	—	−0,1085	0,0965	—	—	—	B_n/L
—	—	—	−0,7233	0,6433	—	—	—	B_n/B
—	—	—	−0,065	0,05	—	—	—	H/L
—	—	—	−0,433	0,33	—	—	—	H/B

Balanced rudder profiles are summarised as profile sketches in Figures 8 to 11. Table 3 contains the profile offsets of all of the IfS rudder profiles with the exception of the offsets of the IfS 52 TR... family already published in Reference 3. The form parameters are summarised in their entirety in Table 2. The principal form ratios of

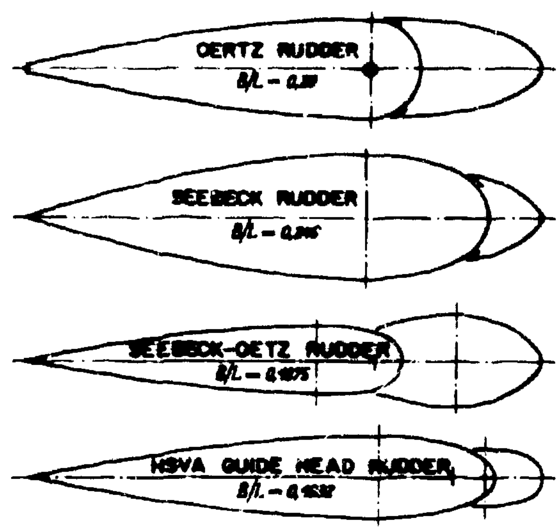

Figure 7 – Examples of Commonly Used Profiles of Guide-Head Rudders

foreign profiles are indicated in Table 1. Figure 12 shows the profiles of bow rudders and Figure 13 the profile sections of the plate rudders investigated or taken into consideration. In order to demonstrate more clearly and graphically the development into profiles with a relatively thick "nose" and a relatively flat "tail" (which proved successful according to the experiments reported here), Figure 14 shows a greatly enlarged representation of the nose contours and Figure 15 shows the tail contours of the old and new balanced rudders of particular interest to us.

The rudder profiles[22,27] shown in Figure 9 are very ineffective on the basis of all practical experience and theoretical analysis. In spite of their "aesthetic" contours, the two profiles do not exhibit any

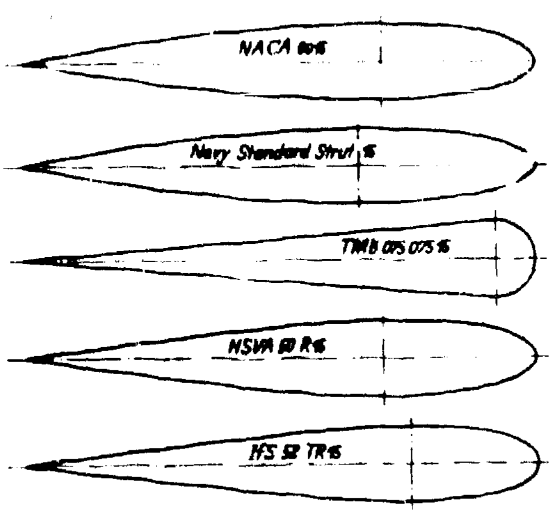

Figure 8 - Common Profiles of Balanced Rudders of 15 Percent Relative Thickness

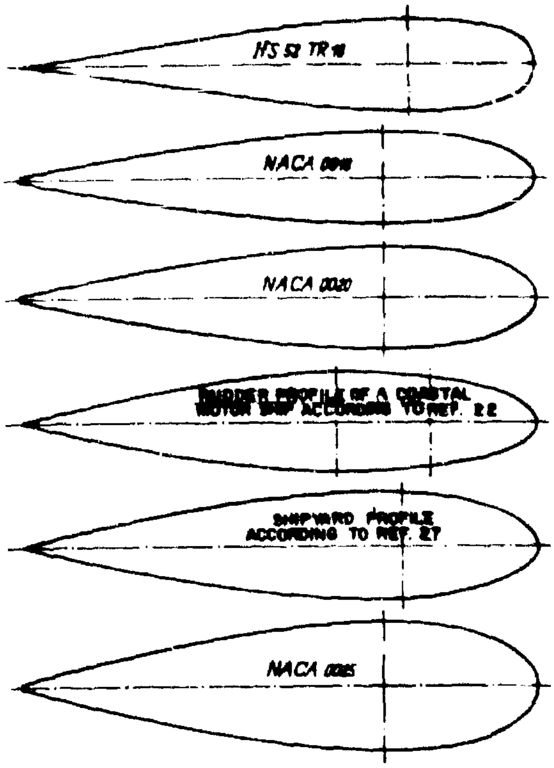

Figure 9 - Examples of Common Balanced Rudder Profiles of Greater Relative Thickness

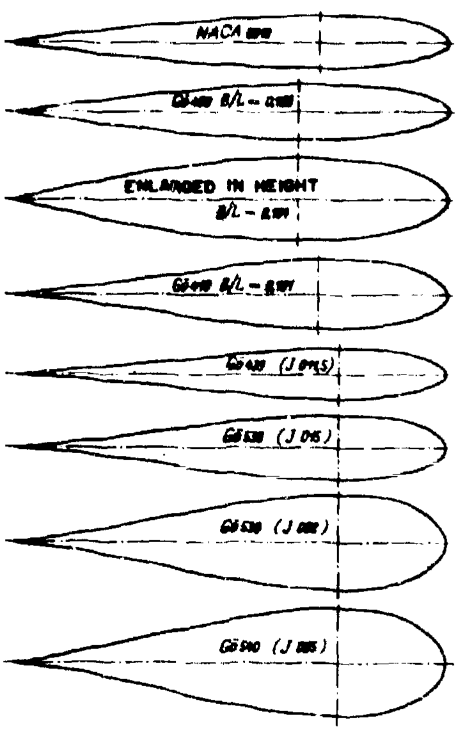

Figure 10 - Symmetrical Flow Profiles from Familiar Experimental Investigations

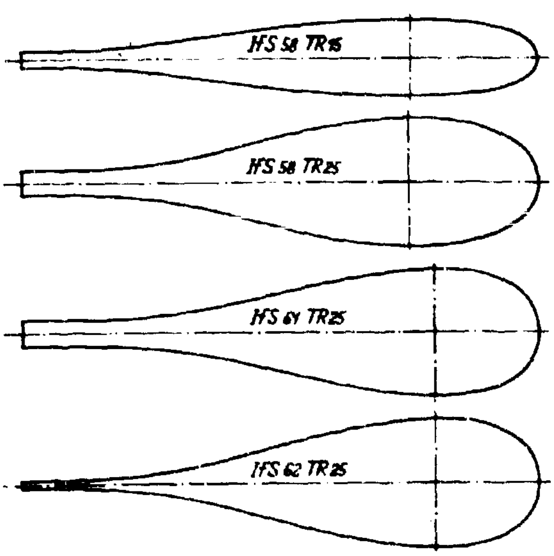

Figure 11 - The New JfS Balanced-Rudder Profiles

TABLE 3

Profile Offsets of the Rudder Profiles of the Present JfS Investigation

JfS 62 TR 15 / 25

$\frac{x}{L}$	$\frac{x}{n}$	$\frac{y}{L}$ (15)	$\frac{y}{L}$ (25)
0	0	0	0
0,004	0,02	0,02025	0,03374
0,010	0,05	0,03063	0,05104
0,020	0,1	0,04059	0,06814
0,040	0,2	0,05301	0,08835
0,060	0,3	0,06045	0,10075
0,080	0,4	0,06549	0,10916
0,120	0,6	0,07140	0,11915
0,160	0,8	0,07494	0,12374
0,200	1,0	0,07500	0,12500
	$\frac{x-n}{e}$		
0,200	0	0,07500	0,12500
0,275	0,1	0,07271	0,12115
0,350	0,2	0,06629	0,11050
0,425	0,3	0,05676	0,09378
0,500	0,4	0,04547	0,07420
0,575	0,5	0,03302	0,05406
0,650	0,6	0,02253	0,03580
0,725	0,7	0,01541	0,02150
0,800	0,8	0,01021	0,01231
0,875	0,9	0,00789	0,00819
0,950	1,0	0,00750	0,00750
1,000		0,00750	0,00750

IfS 55 BR 15

$\frac{x}{L}$	$\frac{y}{L}$
0	0
0,01	0,01492
0,025	0,02342
0,05	0,03369
0,10	0,04500
0,15	0,05356
0,20	0,06000
0,30	0,06874
0,40	0,07349
0,50	0,07500

IfS 54 BR 15

$\frac{x}{L}$	$\frac{y}{L}$
0	0
0,01	[illegible]
0,02	0,04091
0,05	0,05314
0,10	0,04875
0,15	0,03766
0,20	0,03170
0,25	0,03431
0,30	0,04405
0,35	0,05679
0,40	0,06781
0,45	0,07285
0,50	0,07500

IfS 59 BR 15

$\frac{x}{L}$	$\frac{x}{x_{Bn}}$	$\frac{y}{L}$
0	0	0
0,00096	0,02	0,00959
0,00241	0,05	0,01505
0,00482	0,10	0,02101
0,00964	0,20	0,02893
0,01446	0,30	0,03443
0,01928	0,40	0,03857
0,02893	0,60	0,04419
0,03857	0,80	0,04724
0,04821	1,00	0,04821
	$\frac{x-x_{Bn}}{x_{Hn}-x_{Bn}}$	
0,04821	0	0,04821
0,06317	0,1	0,04632
0,07813	0,2	0,04211
0,10805	0,4	0,03282
0,13797	0,6	0,02702
0,16789	0,8	0,02516
0,19781	1,0	0,02500
	$\frac{x-x_{Hn}}{n-x_{Hn}}$	
0,19781	0	0,02500
0,25825	0,2	0,02637
0,31869	0,4	0,03396
0,37912	0,6	0,04876
0,43956	0,8	0,06596
0,46978	0,9	0,07239
0,50000	1,0	0,07500

IfS 57 BR 15

$\frac{x}{L}$	$\frac{y}{L}$
0	0,00750
0,05	0,00939
0,10	0,01452
0,15	0,02158
0,20	0,03126
0,25	0,04125
0,30	0,05124
0,35	0,06042
0,40	0,06798
0,45	0,07311
0,50	0,07500

Table 3 Continued

JfS 58 TR		15	25
$\frac{x}{L}$	$\frac{x}{n}$	$\frac{y}{L}$	$\frac{y}{L}$
0	0	0	0
0,0050	0,02	0,02025	0,03374
0,1025	0,05	0,03062	0,05104
0,0250	0,1	0,04089	0,06814
0,0500	0,2	0,05301	0,08835
0,0750	0,3	0,06045	0,10075
0,1000	0,4	0,06550	0,10916
0,1500	0,6	0,07149	0,11915
0,2000	0,8	0,07425	0,12374
0,2500	1,0	0,07500	0,12500
	$\frac{x-n}{s}$		
0,2500	0	0,07500	0,12500
0,3150	0,1	0,07366	0,12277
0,3800	0,2	0,06922	0,11536
0,4450	0,3	0,06174	0,10290
0,5100	0,4	0,05206	0,08677
0,5750	0,5	0,04148	0,06913
0,6400	0,6	0,03145	0,05242
0,7050	0,7	0,02330	0,03882
0,7700	0,8	0,01790	0,02983
0,8350	0,9	0,01542	0,02570
0,9000	1,0	0,01500	0,02500
1,0000		0,01500	0,02500

JfS 61 TR		15	25
$\frac{x}{L}$	$\frac{x}{n}$	$\frac{y}{L}$	$\frac{y}{L}$
0	0	0	0
0,004	0,02	0,02025	0,03374
0,010	0,05	0,03062	0,05104
0,020	0,1	0,04089	0,06814
0,040	0,2	0,05301	0,08835
0,060	0,3	0,06045	0,10075
0,080	0,4	0,06549	0,10916
0,120	0,6	0,07149	0,11915
0,160	0,8	0,07424	0,12374
0,200	1,0	0,07500	0,12500
	$\frac{x-n}{s}$		
0,200	0	0,07500	0,12500
0,270	0,1	0,07300	0,12166
0,340	0,2	0,06734	0,11224
0,410	0,3	0,05891	0,09819
0,480	0,4	0,04890	0,08149
0,550	0,5	0,03862	0,06437
0,620	0,6	0,02934	0,04890
0,690	0,7	0,02209	0,03681
0,760	0,8	0,01743	0,02905
0,830	0,9	0,01535	0,02558
0,900	1,0	0,01500	0,02500
1,000		0,01500	0,02500

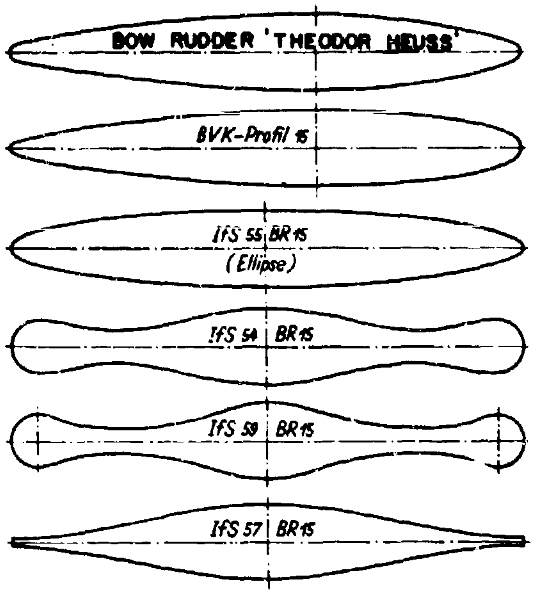

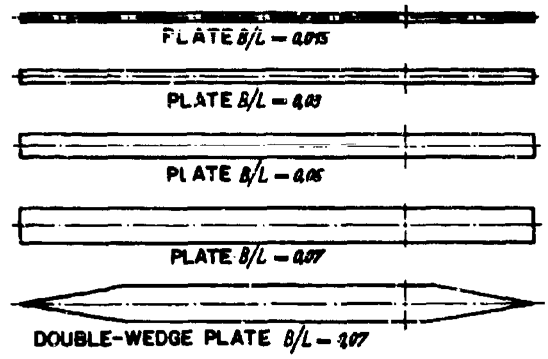

Figure 13 - Profile Sections of the Plate Rudders Investigated

Figure 12 - Bow-Rudder Profiles

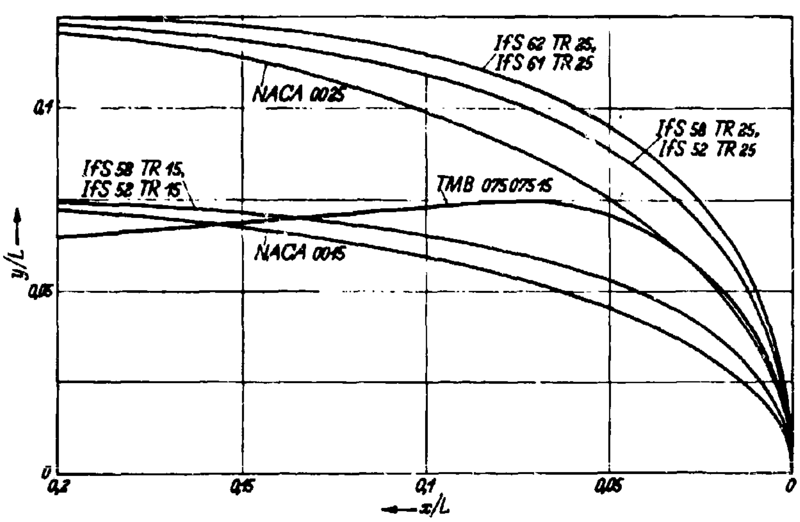

Figure 14 - Nose Contours of Several Balanced Rudder Profiles

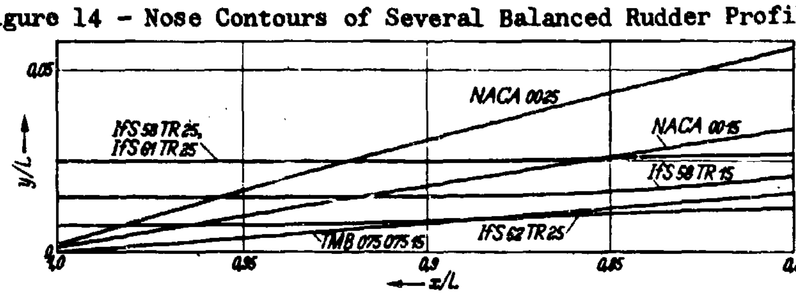

Figure 15 - Tail Contours of Several Balanced Rudder Profiles

great performances in the experiments carried out in the place cited. Conversely, profile TMB 075 075 15 which is a fairly primitive design (consisting only of a leading-edge circle and two tangent straight profile flanks) shows fairly good results if the Reynolds numbers are sufficiently large.[25] The good characteristics with respect to astern motion proved their worth even at the smaller Reynolds numbers of the JfS investigation. Therefore, the TMB profile is included in Figure 8 as well as in Figures 14 and 15.

F. SUPPLEMENTARY WIND-TUNNEL TESTS

Our published literature does not contain an excessively large number of special and systematic tests with free-running ship rudders. Not very much new material has been published since a summary of such test results was made in 1955.[26] Now that it has become pretty clear what the fundamental influence of the aspect ratio and Reynolds number amounts to (see Figures 44 and 45 in this connection), the need has arisen for carrying out comparative profile investigations. The fact that the profiles of the NACA 00.. series which, after all, had originally been intended for other purposes in the field of aeronautics, suggested the question whether it might not be possible to produce even more suitable profiles for use as ship rudders. Thus, new profile forms were produced at the Shipbuilding Institute which, however, were not yet sufficiently verified experimentally although, on occasion, they had already been used for comparative tests[1,22,30] and have found practical application as well.

Figure 16 - Rudder Models Tested in the Wind Tunnel, Aspect Ratio $A_R = 1$

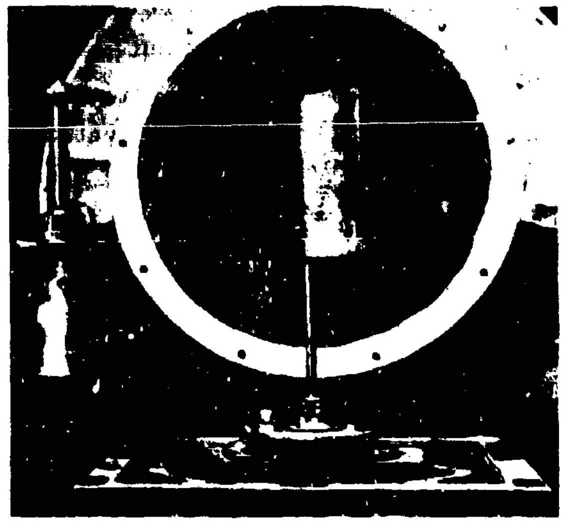

Figure 17 - Test Setup in the Former JfS
Wind Tunnel at the Hamburg Engineering Institute

For the supplementary tests which appeared to be necessary in view of the influence of profile forms, the following JfS profiles newly developed in recent years were used:

Balanced-rudder profiles	JfS 58 TR 15
	25
	JfS 61 TR 25
	JfS 62 TR 25
Bow-rudder profiles	JfS 54 BR 15
	JfS 29 BR 15
	JfS 57 BR 15

For purposes of comparison, the following profiles were investigated:

Balanced-rudder profiles	TMB 075 075 15
	NACA 00 15
	25
Bow-rudder profile	JfS 55 BR 15 (ellipse)
Plate rudder	B/L = 0.015
	0.03
	0.05
	0.07

The large number of tests were carried out in the wind tunnel of the Hamburg Engineering Institute (formerly JfS Wind Tunnel). Figures 16 and 17 indicate the models and test setup used. All of the models had a square planform of 0.4 X 0.4 m. The slipstream cross section had a diameter

of 1 m so that a tank blockage of $A_R/A_S = 0.204$ was obtained. As a scale for these measurements we used a flexible-joint spring balance with electrical metering elements, which is also suitable for tank experiments. The testing path is practically zero so that it is not necessary to make any geometrical correction for the rudder angle. The capacity of the tunnel permitted a Reynolds number of approximately 0.8×10^6. Several characteristic values for the profiles were investigated to obtain a clue to their dependence on the characteristic in question. By way of supplementing these tests, we also carried out experiments in a slipstream diameter of 0.5 m with the profiles NACA 0015 and JfS 58 TR 15 with models of 0.1 X 0.1 m. Thereby, for a tunnel blockage of $A_R/A_S = 0.0501$, a Reynolds number of approximately 0.13×10^6 was included as the minimum. The rudder measuring device for small ship models as used for the small rudders of the investigation[2] served as a wind-tunnel scale.

All of the data obtained are included in Tables 4-18 in the form of the familiar coefficients c_C for the transverse force, c_D for the resistance, c_Y for the lateral force, c_X for he longitudinal force, and $c_{M,25}$ for the moment about an imaginary turning axis referred to the L/4 point of the rudder length. As examples for the graphical representation, Figures 18 to 39 show these coefficients as a function of the angle of attack ϵ. In doing so, we have generally represented the largest of the Reynolds numbers investigated. In the case of the profiles designated as bow rudders, we have measured and plotted the moment coefficient c_M which represents in nondimensional form the moment referred to the center of the rudder length rather than plotting the coefficient c_M,25. These bow rudders and the plate with $B/L = 0.05$ were provided with a shaft at $L_R/2$ for mounting support on the scale (all the other rudders had the shaft at $L_R/4$ from the front). A rod correction for this rudder shaft was deducted from the measured resistance. No further corrections were made since at the time the measurements were undertaken no sufficiently reliable procedures had yet been worked out for correcting the wind tunnel measurements of rudder surfaces with small aspect ratios. Since it is a fact, on the other hand (see Reference 26) that the use of the wind tunnel corrections for measurements on airfoils (hydrofoils) with larger aspect ratios would lead to an undercorrection for the transverse force maximum in the case of

rudders with an aspect ratio of 1 and to an overcorrection within the remaining range, the method used here probably represents the lesser of two evils. In any event, the omission of the correction is of minor importance for comparing the profile forms investigated here.

However, if we compare the data with foreign measurements, as in Figures 44 and 45, for instance, this factor should be borne in mind. The foreign measurements used in these figures are all corrected in the usual manner; that is to say that the transverse forces are somewhat too low in the case of the maximum transverse force and otherwise somewhat too high. However, since the tunnel blockages are lower there for the most part, than in the case of the JfS measurements with the 0.4 m rudders, the corrections are not so great either and therefore they cannot be decisive for the quality of the comparison with the new measurements.

As for the rest, the results of the measurements have been represented exactly as they have been measured geometrically. In doing so, we have used the definitions which have been recommended by the International Towing Tank Conference (ITTC). Thus, in each case a clockwise moment—clockwise as seen from above—is figured positive. The resistance is always calculated positive in the direction of the relative flow. The longitudinal force is figured positive in the direction from the profile center toward the nose of the profile. The lateral force, accordingly, is figured positive at a right angle toward the right starting from the positive x-direction. It should be borne in mind especially that the transverse force is figured positive to the right—always seen contrary to the relative flow—and that a positive angle of flow always results from a rotation which is positive in the direction of the moment. Thus, for instance, all of the measurements for astern motion indicated here have been measured and represented with flow angles between 180 and 90 deg.

We decided not to undertake here a comparative tabulation of precise force coefficients of the individual profiles. In most cases, the performance differences of the various profiles are obvious enough in the figures. Thus, the greatest transverse force coefficient measured was 1.478 for the JfS 62 TR 25 profile and the lowest transverse force maximum of the balanced-rudder profiles was 0.88 for the TMB 075 075 15 profile if the Reynolds number was equally high. In astern motion, however, the TMB

075 075 15 profile with $c_{C,Max}$ = 1.115 is the best of these profiles whereas the NACA profile 0025 yields the poorest value, that is, 0.908. Among the bow rudders, JfS 57 BR 15 is best (maximum transverse force of 1.03) and the elliptical profile JfS 55 BR 15 is the worst (maximum transverse force of 0.743). For the purpose of carrying out a curve comparison, exact profiles have been selected. As for the effectiveness at smaller rudder angles, Figure 40 shows that the JfS 62 TR 15 profile is particularly good and the figure also shows the relatively good position of the two JfS 58 TR profiles. Figure 41 indicates the balancing possibility for the new JfS profiles, clearly an improvement over the NACA profiles; the turning axis may lie farther back without risking any danger of overbalance. The form of the familiar polar curves (Figure 42) indicates the effectiveness and the drag power requirement, especially at larger angles.

Profile JfS 58 TR 25 whose practical application is sturdy in form and performs very well; Figure 43 compares the polar curves in straight-ahead motion and motion along the turning circle with $L_L/R_L = 0.5$. In doing so, we have made the conversions starting out from the straight-ahead motion and using Equations [5] to [13]. In this case, we have introduced a drift angle on the ship ϵ_L = 11 deg (see Figure 4) as well as a standard value $x_{LA}/L_L = -1/2$ and a (value) $c_{s\epsilon} = 1.0$ as it may be derived from Figure 40 with the aid of the method of Reference 26. This cautious method of estimating the rudder effect when turning and when checking the yaw in the turning circle already confirms the empirical fact that the drag power requirement is greater when checking the yaw than when turning. By way of supplementing the above data, Table 19 lists several comparative values for the control force and the drag power requirement for various profiles at a 35 deg rudder angle, both in straight-ahead motion and in motion along the turning circle. The method of calculation is the same as for Figure 43. Note that the superiority of the more recent profiles over the NACA profiles is also retained in the turning circle.

Figures 44 and 45 serve to compare foreign measurements and to illustrate the influence of the aspect ratio and Reynolds number. The results are in line with the general trend; thus there is every indication that the comparable results obtained here will remain valid even if the Reynolds numbers are extended further and if other aspects ratios are used.

TABLE 4

Test Results for TMB 075 075 15

Re $= 0{,}38 \cdot 10^6$

$\varepsilon°$	c_C	c_D	c_Y	c_X	$c_{M,25}$
−2	−0,065	0,040	−0,056	−0,038	0,002
0	0	0,040	0,000	−0,040	0
2	0,050	0,040	0,051	−0,038	0,002
5	0,134	0,065	0,139	−0,053	−0,006
10	0,271	0,109	0,286	−0,061	−0,037
15	0,438	0,179	0,469	−0,060	−0,071
20	0,562	0,259	0,617	−0,051	−0,105
25	0,662	0,363	0,753	−0,049	−0,129
30	0,776	0,482	0,913	−0,029	−0,153
35	0,851	0,602	1,042	−0,006	−0,176
40	0,856	0,682	1,093	0,028	−0,183
41	0,806	0,672	1,049	0,021	−0,181
42	0,756	0,682	1,019	−0,001	−0,181
45	0,662	0,692	0,957	−0,021	−0,174
50	0,642	0,726	0,969	0,025	−0,176
55	0,577	0,756	0,950	0,040	−0,176
60	0,502	0,786	0,931	0,042	−0,178
70	0,348	0,806	0,876	0,051	−0,181
80	0,229	0,881	0,908	0,073	−0,215
90	0,090	0,960	0,960	0,090	−0,261

Re $= 0{,}56 \cdot 10^6$

$\varepsilon°$	c_C	c_D	c_Y	c_X	$c_{M,25}$
−2	−0,052	0,038	−0,053	−0,036	−0,002
0	0	0,031	0	−0,031	−0,001
2	0,052	0,033	0,053	−0,031	0,004
5	0,130	0,054	0,135	−0,043	−0,004
10	0,291	0,111	0,205	−0,059	−0,034
15	0,435	0,175	0,465	−0,056	−0,069
20	0,567	0,262	0,623	−0,052	−0,013
25	0,667	0,357	0,756	−0,042	−0,131
30	0,776	0,475	0,910	−0,023	−0,150
35	0,847	0,603	1,040	−0,008	−0,173
40	0,861	0,700	1,110	0,018	−0,189
43	0,743	0,678	1,006	0,011	−0,175
44	0,719	0,667	0,981	0,019	−0,169
45	0,716	0,672	0,981	0,031	−0,164
50	0,648	0,719	0,967	0,034	−0,172
55	0,582	0,755	0,952	0,044	−0,175
60	0,502	0,766	0,914	0,052	−0,173
70	0,350	0,792	0,865	0,058	−0,176
80	0,225	0,873	0,899	0,071	−0,212
90	0,097	0,972	0,972	0,097	−0,256

Re $= 0{,}69 \cdot 10^6$

$\varepsilon°$	c_C	c_D	c_Y	c_X	$c_{M,25}$
−2	−0,058	0,033	−0,059	−0,030	−0,002
0	0	0,030	0	−0,030	0
2	0,055	0,030	0,056	−0,028	0,003
5	0,136	0,058	0,141	−0,046	−0,001
10	0,294	0,108	0,309	−0,055	−0,030
15	0,441	0,182	0,473	−0,062	−0,069
20	0,575	0,260	0,629	−0,047	−0,102
25	0,670	0,361	0,760	−0,044	−0,122
30	0,780	0,491	0,921	−0,035	−0,154
35	0,856	0,617	1,055	−0,014	−0,178
40	0,862	0,715	1,170	0,007	−0,194
41	0,824	0,694	1,077	0,016	−0,184
42	0,772	0,680	1,029	0,012	−0,178
45	0,717	0,686	0,992	0,022	−0,171
50	0,664	0,717	0,976	0,048	−0,170
55	0,586	0,745	0,946	0,052	−0,171
60	0,515	0,772	0,926	0,060	−0,174
70	0,364	0,788	0,864	0,073	−0,177
80	0,226	0,879	0,905	0,070	−0,213
90	0,096	0,963	0,963	0,096	−0,250

ASTERN MOTION Re $= 0{,}56 \cdot 10^6$

$180° - \varepsilon°$	c_C	c_D	c_Y	c_X	$c_{M,25}$
0	−0,010	0,057	0,010	0,057	−0,050
5	−0,182	0,073	0,188	0,057	−0,073
10	−0,336	0,121	0,352	0,061	−0,148
15	−0,532	0,213	0,569	0,068	−0,224
20	−0,705	0,319	0,772	0,059	−0,317
25	−0,885	0,466	0,999	0,052	−0,387
30	−1,033	0,634	1,211	0,032	−0,429
35	−1,104	0,811	1,370	0,031	−0,467
40	−1,095	0,972	1,464	0,041	−0,483
45	−1,022	1,081	1,487	0,041	−0,473
50	−0,624	0,861	1,062	0,076	−0,341
55	−0,539	0,910	1,054	0,080	−0,335
60	−0,447	0,942	1,040	0,084	−0,324
70	−0,272	0,996	1,029	0,085	−0,307
80	−0,088	1,017	1,016	0,091	−0,289
90	−0,092	0,982	0,982	0,092	−0,259

TABLE 5

Test Results for NACA 0015

$Re = 0{,}30 \cdot 10^6$

$\alpha°$	c_C	c_D	c_Y	c_X	$c_{M,\infty}$
−2	−0,076	0,040	−0,077	−0,037	−0,017
0	−0,016	0,040	−0,016	−0,040	−0,009
2	0,042	0,046	0,042	−0,055	−0,009
5	0,143	0,074	0,148	−0,061	−0,004
10	0,345	0,123	0,361	−0,061	−0,009
15	0,408	0,208	0,508	−0,077	−0,025
20	0,554	0,316	0,628	−0,108	−0,105
25	0,662	0,428	0,780	−0,108	−0,132
30	0,715	0,525	0,862	−0,097	−0,159
35	0,722	0,608	0,941	−0,084	−0,171
40	0,704	0,675	0,973	−0,085	−0,176
45	0,655	0,744	0,989	−0,083	−0,202
50	0,619	0,811	1,019	−0,047	−0,022
55	0,606	0,890	1,076	−0,014	−0,224
60	0,543	0,924	1,072	0,008	−0,255
90	0	1,000	1,000	0	−0,350

$Re = 0{,}56 \cdot 10^6$

$\alpha°$	c_C	c_D	c_Y	c_X	$c_{M,\infty}$
−2	−0,047	0,021	−0,048	−0,020	−0,001
0	0	0,019	0	−0,019	0,004
2	0,057	0,021	0,057	−0,019	0,006
5	0,140	0,028	0,142	−0,016	0,016
10	0,279	0,047	0,283	0,002	0,002
15	0,442	0,083	0,446	0,034	0,021
20	0,622	0,147	0,634	0,075	0,004
25	0,762	0,215	0,781	0,127	−0,002
28	0,837	0,277	0,866	−0,140	−0,013
29	0,667	0,417	0,785	−0,041	−0,036
30	0,672	0,428	0,796	−0,033	−0,009
35	0,705	0,537	0,896	−0,035	−0,129
40	0,662	0,612	0,917	−0,031	−0,137
45	0,620	0,657	0,903	−0,027	−0,140
50	0,558	0,719	0,910	−0,035	−0,149
55	0,502	0,738	0,893	−0,011	−0,152
60	0,440	0,768	0,885	−0,003	−0,157
70	0,307	0,799	0,856	0,015	−0,170
80	0,185	0,866	0,865	0,032	−0,213
90	0,0615	0,960	0,960	0,062	−0,256

$Re = 0{,}67 \cdot 10^6$

$\alpha°$	c_C	c_D	c_Y	c_X	$c_{M,\infty}$
−2	−0,052	0,025	−0,053	−0,023	−0,001
0	0	0,022	0	−0,022	0,003
2	0,062	0,024	0,063	−0,021	0,007
5	0,144	0,027	0,145	−0,014	0,014
10	0,284	0,039	0,287	0,011	0,018
15	0,453	0,074	0,456	0,046	0,018
20	0,632	0,138	0,641	0,087	0,001
25	0,762	0,220	0,784	0,123	−0,004
30	0,927	0,325	0,966	0,183	−0,029
32	0,982	0,387	1,038	0,192	−0,063
33	0,692	0,491	0,848	−0,034	−0,122
35	0,719	0,538	0,897	−0,028	−0,129
40	0,689	0,610	0,920	−0,025	−0,139
45	0,631	0,658	0,911	−0,019	−0,141
50	0,574	0,706	0,910	−0,014	−0,149
55	0,512	0,741	0,901	−0,006	−0,153
60	0,441	0,768	0,886	−0,002	−0,163
70	0,314	0,809	0,867	0,019	−0,175
80	0,186	0,894	0,912	0,028	−0,214
90	0,061	0,991	0,991	0,061	−0,261

$Re = 0{,}79 \cdot 10^6$

$\alpha°$	c_C	c_D	c_Y	c_X	$c_{M,\infty}$
−2	−0,055	0,021	−0,055	−0,019	−0,001
0	0	0,020	0	−0,020	0,003
2	0,056	0,023	0,056	−0,021	0,008
5	0,141	0,026	0,143	−0,014	0,014
10	0,289	0,042	0,292	0,009	0,021
15	0,441	0,069	0,444	0,048	0,019
20	0,622	0,135	0,630	0,086	0,006
25	0,775	0,217	0,795	0,130	−0,004
30	0,926	0,320	0,962	0,186	−0,026
33	1,025	0,405	1,081	0,218	−0,060
34	1,052	0,505	1,153	0,111	−0,121
35	0,713	0,528	0,887	−0,023	−0,126
40	0,685	0,605	0,914	−0,023	−0,137
45	0,631	0,645	0,902	−0,010	−0,141
50	0,583	0,700	0,911	−0,004	−0,152
55	0,528	0,731	0,902	0,013	−0,155
60	0,448	0,761	0,883	0,007	−0,161
70	0,322	0,791	0,853	0,031	−0,175
80	0,209	0,875	0,898	0,054	−0,211
90	0,065	0,969	0,969	0,065	−0,255

ASTERN MOTION $Re = 0{,}56 \cdot 10^6$

$180° - \alpha°$	c_C	c_D	c_Y	c_X	$c_{M,\infty}$
0	−0	0,050	0	0,050	0,001
5	−0,241	0,069	0,246	0,047	−0,077
10	−0,385	0,102	0,397	0,033	−0,157
15	−0,532	0,180	0,561	0,036	−0,222
20	−0,643	0,258	0,692	0,022	−0,287
25	−0,771	0,376	0,857	0,015	−0,339
30	−0,918	0,532	1,061	0,002	−0,418
35	−1,022	0,719	1,249	0,003	−0,458
40	−1,059	0,885	1,380	−0,003	−0,489
45	−1,010	1,041	1,450	0,022	−0,492
50	−0,572	0,806	0,986	0,079	−0,347
55	−0,511	0,861	0,908	0,076	−0,341
60	−0,431	0,911	1,005	0,063	0,336
70	−0,277	0,981	1,017	0,075	0,315
80	−0,111	1,024	1,028	0,068	0,297
90	−0,059	0,989	0,980	0,059	0,263

TABLE 6

Test Results for NACA 0025

$Re = 0{,}56 \cdot 10^6$

ε°	c_C	c_D	c_Y	c_X	$c_{M,m}$
−2	−0,052	0,036	−0,053	−0,034	−0,004
0	0	0,033	0	0,033	−0,002
2	0,052	0,036	0,053	−0,034	0,003
5	0,130	0,036	0,133	−0,036	0,008
10	0,269	0,050	0,275	−0,012	0,014
15	0,421	0,080	0,430	0,022	0,014
20	0,572	0,144	0,587	0,060	0,009
25	0,728	0,222	0,754	0,107	−0,006
30	0,882	0,317	0,922	0,167	−0,025
35	1,057	0,440	1,117	0,245	−0,060
40	1,178	0,593	1,283	0,300	−0,102
45	1,318	0,809	1,497	0,386	−0,162
47	1,313	0,847	1,515	0,362	−0,173
48	1,308	0,880	1,529	0,384	−0,186
49	0,534	0,664	0,851	−0,032	−0,130
50	0,521	0,669	0,847	−0,031	−0,132
55	0,485	0,724	0,871	−0,018	−0,147
60	0,423	0,745	0,857	−0,007	−0,154
70	0,306	0,788	0,844	0,028	−0,169
80	0,194	0,861	0,882	0,039	−0,210
90	0,085	0,936	0,936	0,085	−0,255

$Re = 0{,}69 \cdot 10^6$

ε°	c_C	c_D	c_Y	c_X	$c_{M,m}$
−2	−0,050	0,036	−0,051	−0,034	−0,004
0	0	0,034	0	−0,034	−0,001
2	0,053	0,034	0,054	−0,032	0,004
5	0,129	0,040	0,132	−0,029	0,009
10	0,272	0,055	0,278	−0,006	0,015
15	0,423	0,090	0,431	0,022	0,012
20	0,577	0,138	0,589	0,065	0,005
25	0,732	0,221	0,757	0,109	−0,007
30	0,895	0,317	0,933	0,174	−0,028
35	1,039	0,447	1,107	0,229	−0,062
40	1,188	0,600	1,296	0,305	−0,104
45	1,315	0,778	1,480	0,380	−0,150
48	1,320	0,874	1,532	0,396	−0,177
49	1,313	0,910	1,548	0,394	−0,186
50	1,305	0,935	1,555	0,398	−0,190
51	0,527	0,679	0,859	−0,017	−0,133
55	0,485	0,719	0,867	−0,015	−0,144
60	0,435	0,746	0,863	0,003	−0,151
70	0,319	0,780	0,842	0,033	−0,165
80	0,198	0,851	0,872	0,047	−0,206
90	0,083	0,928	0,928	0,083	−0,254

$Re = 0{,}78 \cdot 10^6$

ε°	c_C	c_D	c_Y	c_X	$c_{M,m}$
−2	−0,050	0,032	−0,051	−0,030	−0,005
0	0	0,031	0	−0,031	0,001
2	0,055	0,035	0,056	−0,033	0,003
5	0,132	0,036	0,134	−0,034	0,010
10	0,270	0,052	0,275	−0,005	0,015
15	0,419	0,069	0,428	0,023	0,015
20	0,586	0,145	0,599	0,065	0,008
25	0,732	0,217	0,756	0,112	−0,004
30	0,883	0,319	0,916	0,166	−0,026
35	1,033	0,446	1,102	0,227	−0,058
40	1,192	0,595	1,294	0,310	−0,099
45	1,325	0,768	1,479	0,393	−0,146
46	1,336	0,805	1,507	0,401	−0,153
47	1,321	0,832	1,509	0,398	−0,165
48	1,315	0,864	1,521	0,399	−0,177
49	1,312	0,894	1,535	0,404	−0,183
50	1,310	0,918	1,545	0,413	−0,187
51	1,292	0,947	1,549	0,409	−0,194
52	0,515	0,685	0,857	−0,016	−0,135
55	0,495	0,710	0,864	−0,001	−0,139
60	0,434	0,747	0,855	0,002	−0,152
70	0,341	0,771	0,841	0,056	−0,164
80	0,216	0,815	0,840	0,071	−0,197
90	0,066	0,924	0,924	0,066	−0,247

ASTERN MOTION $Re = 0{,}56 \cdot 10^6$

$180^\circ - \varepsilon^\circ$	c_C	c_D	c_Y	c_T	$c_{M,m}$
0	0	0,064	0	0,064	−0,004
5	−0,267	0,095	−0,274	0,071	−0,088
10	−0,412	0,142	−0,431	0,068	−0,165
15	−0,553	0,199	−0,585	0,049	−0,235
20	−0,672	0,289	−0,730	0,041	−0,300
25	−0,738	0,381	−,0830	0,033	−0,340
30	−0,767	0,511	−0,921	0,059	−0,362
35	−0,672	0,548	−0,864	0,064	−0,332
37	−0,908	0,719	−1,157	0,028	−0,436
40	−0,894	0,816	−1,210	0,050	−0,447
45	−0,529	0,705	−0,872	0,124	−0,333
50	−0,478	0,773	−0,899	0,131	−0,335
55	−0,412	0,828	−0,915	0,138	−0,332
60	−0,341	0,858	−0,914	0,134	−0,323
70	−0,203	0,937	−0,949	0,130	−0,311
80	−0,055	0,956	−0,952	0,112	−0,284
90	−0,085	0,901	−0,901	0,085	−0,252

TABLE 7

Test Results for Jfs TR 15

Re = 0,13 · 10^6

ε°	c_C	c_D	c_Y	c_X	$c_{M,m}$
−1,3	[illegible]	[illegible]	−0,087	[illegible]	0,011
0,7	[illegible]	[illegible]	0,017	[illegible]	[illegible]
2,7	[illegible]	[illegible]	0,075	[illegible]	[illegible]
5,7	0,170	[illegible]	0,175	−0,045	[illegible]
10,7	[illegible]	0,119	[illegible]	−0,065	−0
15,7	[illegible]	0,156	[illegible]	−0,073	[illegible]
20,7	[illegible]	[illegible]	0,675	[illegible]	−0,117
25,7	0,717	[illegible]	[illegible]	[illegible]	−0,147
30,7	0,704	[illegible]	[illegible]	[illegible]	−0,177
35,7	0,704	[illegible]	1,031	−0,075	[illegible]
40,7	[illegible]	0,723	[illegible]	−0,070	−0,210
45,7	0,677	0,775	[illegible]	[illegible]	−0,227
50,7	[illegible]	[illegible]	1,040	−0,057	[illegible]
55,7	[illegible]	[illegible]	1,070	−0,030	−0,257
60,7	0,540	0,947	1,076	−0,018	[illegible]
90,7	0	[illegible]	[illegible]	0,012	[illegible]

Re = [illegible] · 10^6

ε°	c_C	c_D	c_Y	c_X	$c_{M,m}$
−2	−0,087	[illegible]	[illegible]	[illegible]	[illegible]
0	[illegible]	[illegible]	[illegible]	[illegible]	[illegible]
[illegible]	[illegible]	[illegible]	[illegible]	[illegible]	[illegible]
[illegible]	[illegible]	[illegible]	[illegible]	[illegible]	[illegible]
2	0,076	[illegible]	0,078	[illegible]	[illegible]
5	0,175	0,074	[illegible]	[illegible]	[illegible]
10	[illegible]	0,128	[illegible]	[illegible]	0
15	[illegible]	0,274	[illegible]	−0,120	[illegible]
20	[illegible]	0,431	0,717	[illegible]	−0,123
25	0,720	[illegible]	[illegible]	[illegible]	−0,145
30	[illegible]	0,675	1,013	[illegible]	−0,194
35	[illegible]	[illegible]	1,042	−0,113	[illegible]
40	0,784	0,751	1,061	[illegible]	[illegible]
45	[illegible]	0,776	1,017	[illegible]	[illegible]
50	0,612	[illegible]	1,047	−0,079	[illegible]
55	[illegible]	0,915	1,114	[illegible]	−0,351
60	0,578	[illegible]	1,130	0,081	[illegible]
90	0	1,000	1,000	0	−,0370

Re = [illegible] · 10^6

ε°	c_C	c_D	c_Y	c_X	$c_{M,m}$
−2	−0,087	0,031	−0,088	−0,030	−0,003
0	0	0,026	0	−0,026	−0,001
2	0,082	0,028	0,082	−0,026	0
5	0,186	0,033	0,186	−0,019	0,001
10	0,315	0,067	0,330	−0,001	0,001
15	0,463	0,085	0,491	0,033	−0,010
20	0,677	0,106	0,683	0,076	−0,022
25	0,856	0,256	0,884	0,128	−0,066
30	1,034	0,378	1,083	0,192	−0,083
31	0,837	0,534	0,983	−0,036	−0,256
35	0,884	0,634	1,088	−0,007	−0,189
40	0,885	0,764	1,160	−0,016	−0,215
42	0,809	0,731	1,080	−0,002	−0,190
45	0,736	0,721	1,032	0,012	−0,191
50	0,636	0,755	0,967	0,001	−0,189
55	0,558	0,776	0,936	0,012	−0,188
60	0,460	0,785	0,919	0,019	−0,184
70	0,321	0,813	0,873	0,024	−0,190
80	0,206	0,918	0,946	0,044	−0,231
90	0,082	0,998	0,998	0,082	−0,271

Re = 0,65 · 10^6

ε°	c_C	c_D	c_Y	c_X	$c_{M,m}$
−2	−0,064	0,032	−0,055	−0,030	−0,002
0	0	0,030	0	−0,030	−0,001
2	0,061	0,034	0,062	−0,032	0
5	0,136	0,039	0,138	−0,034	0
10	0,315	[illegible]	0,330	−0,002	0,001
15	0,494	0,102	0,503	0,030	−0,007
20	0,667	0,100	0,703	0,076	−0,023
25	0,853	0,262	0,883	0,128	−0,047
30	1,044	0,364	1,086	0,190	−0,077
31	1,061	0,416	1,131	0,206	−0,087
32	1,112	0,448	1,118	0,210	−0,097
33	0,875	0,603	1,056	−0,019	−0,179
35	0,883	0,638	1,097	−0,011	0,191
40	0,900	0,749	1,171	0,004	0,279
42	0,834	0,734	1,111	0,012	0,204
45	0,741	0,731	1,071	0,007	0,195
50	0,639	0,751	0,966	0,007	0,188
55	0,545	0,778	0,961	0,017	0,187
60	0,477	0,790	0,931	0,013	0,187
70	0,323	0,817	0,878	0,023	0,188
80	0,213	0,922	0,945	0,050	0,230
90	0,059	1,000	1,000	0,059	0,266

Re = 0,78 · 10^6

ε°	c_C	c_D	c_Y	c_X	$c_{M,m}$
−2	0,055	0,033	0,056	−0,031	0,001
0	0	0,029	0	0,029	0
2	0,060	0,032	0,062	0,030	0
5	0,161	0,034	0,164	−0,030	0,001
10	0,322	0,053	0,327	0,001	0,001
15	0,500	0,066	0,508	0,035	0,007
20	0,670	0,106	0,686	0,073	0,023
25	0,867	0,263	0,897	0,129	−0,046
30	1,051	0,387	1,104	0,191	0,074
33	1,140	0,477	1,230	0,223	0,100
34	1,182	0,512	1,265	0,237	0,100
35	0,891	0,637	1,095	0,011	0,188
40	0,906	0,762	1,184	0,001	0,210
45	0,740	0,728	1,036	0,006	−0,193
50	0,636	0,756	0,990	0,001	0,190
55	0,576	0,765	0,973	0,021	0,188
60	0,492	0,801	0,940	0,025	0,185
70	0,329	0,811	0,875	0,032	−0,196
80	0,216	0,912	0,937	0,055	−0,226
90	0,062	0,998	0,998	0,062	0,204

ASTERN MOTION Re = 0,56 · 10^6

180° − ε°	c_C	c_D	c_Y	c_X	$c_{M,m}$
0	0	0,052	0	0,052	0
5	0,132	0,062	0,137	0,050	0,063
10	0,272	0,092	0,284	0,044	0,157
15	0,537	0,196	0,570	0,051	0,225
20	−0,648	0,288	0,707	0,047	0,281
25	−0,771	0,468	0,868	0,038	−0,335
30	−0,932	0,558	1,066	0,017	−0,415
35	−1,059	0,735	1,289	0,005	0,463
40	−1,114	0,865	1,422	0,037	−0,494
45	1,000	1,043	1,492	0,018	0,498
50	0,610	0,821	1,021	0,061	0,353
55	0,525	0,868	1,012	0,008	0,342
60	0,445	0,933	1,022	0,007	0,339
70	0,290	0,999	1,036	0,073	0,325
80	0,111	1,015	1,019	0,066	0,297
90	+0,062	0,994	0,994	0,062	0,269

TABLE 8

Test Results for JfS 58 TR 25

Re = 0,56 · 10⁶

ε°	c_C	c_D	c_Y	c_X	$c_{M,m}$
−2	−0,062	0,045	−0,064	−0,043	−0,006
0	0	0,045	0	−0,045	−0,006
2	0,062	0,045	0,063	−0,043	−0,008
5	0,156	0,050	0,160	−0,036	−0,009
10	0,317	0,078	0,326	−0,022	−0,014
15	0,483	0,123	0,498	0,006	−0,025
20	0,672	0,192	0,697	0,050	−0,045
25	0,856	0,293	0,899	0,097	−0,069
30	1,060	0,418	1,118	0,163	−0,102
35	1,222	0,572	1,330	0,233	−0,143
40	1,296	0,796	1,460	0,277	−0,177
41	1,320	0,719	1,466	0,323	−0,185
42	0,766	0,679	1,023	0,007	−0,204
45	0,661	0,696	0,975	−0,011	−0,200
50	0,629	0,707	0,947	0,027	−0,205
55	0,577	0,778	0,968	0,027	−0,208
60	0,506	0,799	0,945	0,038	−0,207
70	0,359	0,818	0,892	0,057	−0,202
80	0,220	0,887	0,912	0,063	−0,231
90	0,099	0,956	0,956	0,099	−0,265

Re = 0,67 · 10⁶

ε°	c_C	c_D	c_Y	c_X	$c_{M,m}$
−2	−0,060	0,046	−0,062	−0,044	−0,005
0	0	0,044	0	−0,044	−0,006
2	0,062	0,044	0,064	−0,042	−0,007
5	0,161	0,044	0,165	−0,030	−0,011
10	0,319	0,075	0,327	−0,019	−0,014
15	0,491	0,126	0,507	0,006	−0,025
20	0,670	0,197	0,696	0,044	−0,043
25	0,846	0,290	0,890	0,095	−0,070
30	1,021	0,404	1,086	0,161	−0,105
35	1,206	0,568	1,313	0,226	−0,139
40	1,321	0,719	1,474	0,298	−0,163
41	1,324	0,747	1,489	0,305	−0,169
42	1,354	0,778	1,527	0,328	−0,177
43	1,364	0,805	1,547	0,341	−0,181
44	1,379	0,839	1,574	0,354	−0,189
45	1,399	0,880	1,611	0,367	−0,196
46	0,692	0,704	0,987	0,010	−0,196
50	0,645	0,728	0,971	0,025	−0,197
55	0,570	0,778	0,964	0,021	−0,205
60	0,512	0,787	0,937	0,049	−0,202
70	0,367	0,810	0,887	0,068	−0,199
80	0,229	0,864	0,891	0,076	−0,224
90	0,078	0,936	0,936	0,098	−0,258

Re = 0,78 · 10⁶

ε°	c_C	c_D	c_Y	c_X	$c_{M,m}$
−2	−0,059	0,047	−0,061	−0,045	−0,006
0	0	0,043	0	−0,043	−0,006
2	0,062	0,044	0,063	−0,042	−0,009
5	0,149	0,050	0,153	−0,037	−0,009
10	0,313	0,076	0,321	−0,020	−0,014
15	0,488	0,123	0,503	0,007	−0,024
20	0,660	0,191	0,685	0,047	−0,042
25	0,844	0,288	0,887	0,096	−0,067
30	1,022	0,411	1,091	0,156	−0,100
35	1,206	0,559	1,309	0,233	−0,132
40	1,324	0,711	1,472	0,307	−0,160
45	1,410	0,877	1,617	0,377	−0,194
46	1,416	0,906	1,635	0,389	−0,197
47	1,431	0,941	1,664	0,405	−0,206
48	1,448	0,972	1,691	0,425	−0,211
49	0,654	0,756	1,000	−0,003	−0,206
50	0,643	0,743	0,983	0,015	−0,200
55	0,590	0,785	0,982	0,033	−0,204
60	0,530	0,803	0,960	0,057	−0,205
70	0,377	0,821	0,901	0,073	−0,202
80	0,253	0,873	0,903	0,097	−0,227
90	0,105	0,954	0,954	0,105	−0,263

ASTERN MOTION Re = 0,56 · 10⁶

180° − ε°	c_C	c_D	c_Y	c_X	$c_{M,m}$
0	−0,014	0,085	0,014	0,085	−0,005
5	−0,151	0,099	0,160	0,086	−0,069
10	−0,293	0,139	0,313	0,087	−0,168
15	−0,428	0,196	0,464	0,079	−0,233
20	−0,674	0,356	0,755	0,096	−0,297
25	−0,785	0,475	0,912	0,098	−0,361
30	−0,885	0,589	1,071	0,067	−0,415
35	−0,927	0,714	1,169	0,053	−0,437
40	−0,975	0,873	1,308	0,041	−0,461
45	−0,610	0,735	0,952	0,088	−0,345
50	−0,558	0,797	0,970	0,085	−0,344
55	−0,478	0,863	0,980	0,104	−0,340
60	−0,385	0,892	0,966	0,113	−0,329
70	−0,229	0,952	0,972	0,111	−0,311
80	−0,069	0,987	0,984	0,104	−0,293
90	+0,104	0,952	0,952	0,104	−0,263

TABLE 9

Test Results for JfS 61 TR 25

Re = $0{,}56 \cdot 10^6$

$\varepsilon°$	c_C	c_D	c_Y	c_X	$c_{M,u}$
− 2	−0,054	0,052	−0,056	−0,050	0,005
0	0	0,047	0	−0,047	0,004
2	0,066	0,050	0,066	−0,047	0,004
5	0,161	0,054	0,165	−0,040	0,004
10	0,317	0,083	0,326	−0,027	−0,002
15	0,501	0,133	0,516	0,002	−0,014
20	0,676	0,203	0,704	0,040	−0,033
25	0,866	0,307	0,915	0,088	−0,058
30	1,059	0,442	1,137	0,147	−0,094
31	1,083	0,475	1,174	0,151	−0,102
32	1,131	0,508	1,227	0,170	−0,109
33	1,166	0,539	1,270	0,183	−0,118
34	1,188	0,572	1,305	0,190	−0,127
25	0,780	0,638	1,005	−0,074	−0,191
40	0,799	0,723	1,077	−0,040	−0,203
45	0,691	0,717	0,996	−0,018	−0,191
50	0,633	0,755	0,985	−0,001	−0,196
55	0,579	0,780	0,970	0,027	−0,194
60	0,506	0,808	0,953	0,034	−0,200
70	0,355	0,818	0,890	0,053	−0,194
80	0,229	0,880	0,907	0,072	−0,224
90	0,104	0,963	0,963	0,104	−0,263

Re = $0{,}70 \cdot 10^6$

$\varepsilon°$	c_C	c_D	c_Y	c_X	$c_{M,u}$
− 2	−0,056	0,050	−0,058	−0,048	0,006
0	0	0,049	0	−0,049	−0,004
2	0,062	0,050	0,064	−0,048	0,004
5	0,161	0,058	0,166	−0,043	0,003
10	0,323	0,084	0,333	−0,027	−0,002
15	0,509	0,130	0,526	0,006	−0,015
20	0,692	0,204	0,719	0,045	−0,034
25	0,873	0,309	0,921	0,089	−0,059
30	1,047	0,437	1,126	0,145	−0,091
35	1,231	0,598	1,352	0,216	−0,132
36	1,254	0,636	1,388	0,222	−0,139
37	1,269	0,658	1,409	0,238	−0,142
38	1,292	0,691	1,444	0,250	−0,150
39	0,801	0,710	1,069	−0,048	−0,202
40	0,795	0,725	1,075	−0,044	−0,206
45	0,707	0,736	1,021	−0,021	−0,201
50	0,640	0,756	0,990	0,004	−0,195
55	0,599	0,783	0,984	0,042	−0,197
60	0,512	0,806	0,954	0,041	−0,200
70	0,365	0,807	0,884	0,067	−0,195
80	0,226	0,884	0,909	0,069	−0,227
90	0,101	0,953	0,953	0,101	−0,259

Re = $0{,}79 \cdot 10^6$

$\varepsilon°$	c_C	c_D	c_Y	c_X	$c_{M,u}$
− 2	−0,058	0,047	−0,060	−0,045	0,004
0	0	0,046	0	−0,046	0,003
2	0,060	0,047	0,061	−0,045	0,004
5	0,147	0,051	0,151	−0,038	0,002
10	0,322	0,076	0,330	−0,019	−0,002
15	0,495	0,126	0,511	0,007	−0,014
20	0,678	0,192	0,703	0,052	−0,031
25	0,856	0,295	0,900	0,095	−0,057
30	1,037	0,422	1,109	0,154	−0,087
35	1,213	0,578	1,325	0,223	−0,125
40	1,327	0,732	1,487	0,292	−0,154
41	1,342	0,731	1,083	−0,027	−0,208
45	0,720	0,728	1,024	−0,006	−0,200
50	0,646	0,738	0,980	0,021	−0,195
55	0,602	0,795	0,996	0,037	−0,204
60	0,530	0,810	0,966	0,054	−0,201
70	0,377	0,818	0,898	0,074	−0,198
80	0,256	0,868	0,899	0,101	−0,222
90	0,109	0,943	0,109	0,109	−0,260

ASTERN MOTION Re = $0{,}56 \cdot 10^6$

$180° - \varepsilon°$	c_C	c_D	c_Y	c_X	$c_{M,u}$
0	+0,005	0,086	−0,005	0,088	0,001
5	−0,142	0,102	0,150	0,089	−0,077
10	−0,298	0,149	0,319	0,095	−0,153
15	−0,444	0,222	0,486	0,099	−0,219
20	−0,662	0,376	0,751	0,127	−0,281
25	−0,771	0,475	0,900	0,105	−0,333
30	−0,894	0,593	1,071	0,066	−0,412
35	−0,955	0,709	1,189	0,033	−0,436
40	−0,999	0,870	1,324	0,024	−0,466
45	−0,636	0,728	[illegible]	0,064	−0,342
50	−0,596	0,820	1,011	0,070	−0,349
55	−0,502	0,880	1,009	0,094	−0,345
60	−0,413	0,910	0,995	0,093	−0,332
70	−0,248	0,967	0,994	0,098	−0,313
80	−0,078	0,995	0,994	0,096	−0,294
90	−0,104	0,963	0,963	0,104	−0,265

TABLE 10

Test Results for JfS 62 TR 25

Re = 0,56 · 10^6

ε°	c_C	c_D	c_Y	c_X	c_M
− 2	−0,052	0,038	−0,053	−0,036	0,002
0	0	0,036	0	−0,036	0,001
2	0,062	0,036	0,063	−0,033	0,001
5	0,161	0,040	0,164	−0,026	0
10	0,324	0,073	0,332	−0,016	−0,007
15	0,516	0,123	0,531	0,015	−0,020
20	0,698	0,196	0,713	0,055	−0,039
25	0,894	0,307	0,940	0,100	−0,067
30	1,088	0,449	1,167	0,155	−0,105
35	1,254	0,617	1,383	0,213	−0,145
38	1,320	0,712	1,478	0,251	−0,164
39	0,799	0,705	1,065	−0,045	−0,202
40	0,790	0,707	1,060	−0,034	−0,220
45	0,714	0,705	1,004	0,006	−0,191
50	0,648	0,745	0,988	0,017	−0,192
55	0,596	0,792	0,992	0,034	−0,200
60	0,527	0,806	0,962	0,053	−0,200
70	0,381	0,823	0,903	0,075	−0,197
80	0,251	0,892	0,923	0,092	−0,226
90	0,111	0,960	0,960	0,111	−0,256

Re = 0,69 · 10^6

ε°	c_C	c_D	c_Y	c_X	c_M
− 2	−0,055	0,040	−0,056	−0,038	0,001
0	0	0,036	0	−0,036	0
2	0,065	0,039	0,066	−0,036	0,001
5	0,166	0,043	0,169	−0,028	0
10	0,334	0,071	0,341	−0,012	−0,008
15	0,521	0,123	0,535	0,016	−0,020
20	0,706	0,200	0,731	0,054	−0,039
25	0,894	0,305	0,940	0,102	−0,068
30	1,072	0,442	1,149	0,153	−0,099
35	1,236	0,608	1,361	0,210	−0,135
40	1,373	0,762	1,541	0,290	−0,156
41	1,379	0,783	1,554	0,314	−0,155
42	1,397	0,828	1,592	0,320	−0,162
45	1,461	0,925	1,687	0,379	−0,174
46	0,698	0,723	1,006	0	−0,195
50	0,651	0,747	0,997	0,025	−0,194
55	0,605	0,780	0,986	0,047	−0,196
60	0,532	0,803	0,961	0,059	−0,197
70	0,381	0,824	0,904	0,076	−0,197
80	0,248	0,868	0,897	0,093	−0,218
90	0,117	0,952	0,952	0,117	−0,255

Re = 0,78 · 10^6

ε°	c_C	c_D	c_Y	c_X	c_M
− 2	−0,056	0,039	−0,057	−0,037	0,001
	0	0,036	0	−0,035	0,001
2	0,064	0,037	0,065	−0,034	0,001
5	0,162	0,042	0,165	−0,027	0
10	0,329	0,072	0,337	−0,014	−0,005
15	0,516	0,122	0,530	0,016	−0,019
20	0,708	0,199	0,733	0,055	−0,039
25	0,893	0,305	0,938	0,101	−0,064
30	1,084	0,442	1,159	0,159	−0,097
35	1,259	0,601	1,376	0,230	−0,131
40	1,378	0,751	1,538	0.311	−0,153
45	1,467	0,930	1,695	0,379	−0,181
46	1,478	0,966	1,721	0,382	−0,188
47	1,457	1,004	1,728	0,381	−0,194
48	1,451	1,010	1,720	0,402	−0,198
49	0,673	0,739	1,000	0,023	−0,195
50	0,668	0,743	0,998	0,034	−0,194
55	0,613	0,794	1,002	0,047	−0,202
60	0,548	0,818	0,982	0,065	−0,202
70	0,405	0,855	0,942	0,088	−0,205
80	0,278	0,872	0,907	0,123	−0,219
90	0,120	0,960	0,960	0,120	−0,255

ASTERN MOTION Re 0,56 10^6

$180^\circ - \varepsilon^\circ$	c_C	c_D	c_Y	c_X	c_M
0	0	0,073	0	0,073	−0,001
5	−0,147	0,078	0,153	0,085	−0,082
10	−0,423	0,166	0,445	0,090	−0,163
15	−0,577	0,240	0,620	0,083	−0,236
20	−0,705	0,345	0,780	0,073	−0,305
25	−0,866	0,466	0,982	0,056	−0,387
30	−0,976	0,603	1,147	0,034	−0,448
35	−1,039	0,747	1,290	0,016	−0,475
40	[illegible]	0,903	1,382	0,015	−0,498
45	0,975	1,050	1,431	0,053	−0,481
50	−0,553	0,820	0,983	0,104	−0,342
55	−0,471	0,875	0,987	0,116	−0,336
60	−0,388	0,922	0,992	0,125	−0,330
70	−0,225	0,988	1,005	0,176	−0,313
80	−0,050	1,003	0,997	0,125	−0,288
90	−0,111	0,963	0,963	0,111	−0,259

TABLE 11

Test Results for JfS 55 BR 15

$Re = 0{,}56 \cdot 10^6$

α	c_C	c_D	c_Y	c_X	c_M
− 2	−0,073	0,031	−0,074	−0,028	−0,010
0	0,005	0,033	0,005	−0,033	−0,002
2	0,083	0,031	0,084	−0,028	0,010
5	0,203	0,040	0,206	−0,022	0,027
10	0,352	0,069	0,359	−0,006	0,064
15	0,506	0,106	0,517	0,028	0,101
20	0,608	0,185	0,634	0,025	0,133
25	0,674	0,329	0,749	−0,013	0,103
30	0,743	0,447	0,867	−0,015	0,124
35	0,690	0,542	0,876	−0,049	0,102
36	0,681	0,548	0,873	−0,043	0,101
37	0,657	0,568	0,867	−0,059	0,097
40	0,648	0,601	0,882	−0,043	0,097
45	0,582	0,645	0,868	−0,044	0,095
50	0,548	0,712	0,897	−0,039	0,089
55	0,478	0,754	0,891	−0,041	0,085
60	0,407	0,775	0,875	−0,036	0,073
70	0,277	0,840	0,884	−0,027	0,052
80	0,137	0,856	0,867	−0,014	0,029
90	0	0,870	0,870	0	−0,002

$Re = 0{,}71 \cdot 10^6$

$\alpha°$	c_C	c_D	c_Y	c_X	c_M
− 2	−0,080	0,031	−0,081	−0,028	−0,012
0	0	0,028	0	−0,028	−0,001
2	0,080	0,031	0,081	−0,028	0,011
5	0,186	0,037	0,189	−0,021	0,030
10	0,335	0,059	0,340	−0,000	0,068
15	0,478	0,097	0,486	0,029	0,105
20	0,601	0,182	0,627	0,035	0,139
22	0,618	0,244	0,664	0,005	0,013
25	0,664	0,331	0,742	−0,019	0,110
30	0,721	0,438	0,844	−0,018	0,119
35	0,692	0,529	0,870	−0,036	0,098
36	0,670	0,541	0,860	−0,044	0,097
37	0,668	0,560	0,870	−0,045	0,099
30	0,640	0,594	0,872	−0,043	0,095
45	0,595	0,654	0,883	−0,041	0,097
50	0,538	0,704	0,885	−0,041	0,090
55	0,485	0,751	0,893	−0,034	0,083
60	0,411	0,790	0,890	−0,039	0,072
70	0,284	0,840	0,886	−0,020	0,050
80	0,141	0,849	0,860	−0,009	0,029
90	0	0,876	0,876	0	0,001

TABLE 12

Test Results for JfS 54 BR 15

Re = 0,56 · 10^6

ε°	c_C	c_D	c_Y	c_X	c_M
− 2	−0,059	0,073	−0,062	−0,071	−0,017
0	0	0,069	0	−0,069	−0,003
2	0,064	0,071	0,066	−0,069	0,009
5	0,163	0,083	0,170	−0,068	0,029
10	0,333	0,121	0,349	−0,061	0,057
15	0,492	0,185	0,523	−0,051	0,075
20	0,629	0,277	0,686	−0,045	0,093
25	0,762	0,395	0,858	−0,036	0,093
30	0,873	0,534	1,023	−0,025	0,114
35	0,967	0,688	1,187	−0,008	0,114
40	0,965	0,820	1,266	−0,007	0,094
41	0,861	0,783	1,163	−0,026	0,087
42	0,799	0,750	1,095	−0,022	0,086
45	0,723	0,759	1,040	−0,026	0,086
50	0,652	0,792	1,026	−0,009	0,075
55	0,577	0,825	1,007	0	0,068
60	0,489	0,844	0,976	0,001	0,060
70	0,326	0,884	0,941	0,004	0,045
80	0,163	0,879	0,894	0,010	0,026
90	0,005	0,901	0,901	0,005	0,001

Re = 0,71 · 10^6

ε°	c_C	c_D	c_Y	c_X	c_M
− 2	−0,056	0,071	−0,059	−0,069	−0,018
0	0,003	0,067	0,003	−0,067	−0,003
2	0,068	0,068	0,070	−0,066	0,017
5	0,167	0,073	0,173	−0,059	0,031
10	0,340	0,117	0,355	−0,056	0,060
15	0,449	0,182	0,481	−0,059	0,078
20	0,633	0,277	0,689	−0,043	0,096
25	0,760	0,404	0,860	−0,045	0,102
30	0,864	0,540	1,018	−0,036	0,116
35	0,945	0,692	1,171	−0,025	0,117
40	0,922	0,826	1,237	−0,040	0,103
41	0,840	0,795	1,155	−0,049	0,103
42	0,789	0,772	1,103	−0,046	0,092
45	0,720	0,754	1,042	−0,024	0,088
50	0,654	0,795	1,030	−0,010	0,078
55	0,577	0,828	1,009	−0,002	0,073
60	0,491	0,858	0,989	−0,004	0,063
70	0,321	0,890	0,946	−0,003	0,049
80	0,158	0,887	0,901	0,002	0,029
90	0,003	0,908	0,908	0,003	0,002

Re = 0,78 · 10^6

ε°	c_C	c_D	c_Y	c_X	c_M
− 2	−0,064	0,069	−0,066	−0,067	−0,014
0	0	0,060	0	−0,060	−0,003
2	0,060	0,063	0,061	−0,061	0,014
5	0,149	0,065	0,154	−0,052	0,035
10	0,341	0,121	0,357	−0,060	0,038
15	0,492	0,189	0,524	−0,056	0,075
20	0,630	0,284	0,689	−0,052	0,083
25	0,767	0,406	0,867	−0,044	0,094
30	0,863	0,544	1,019	−0,039	0,104
35	0,965	0,700	1,192	−0,020	0,111
40	0,962	0,837	1,275	−0,024	0,088
41	0,905	0,837	1,232	−0,038	0,079
42	0,812	0,778	1,124	−0,035	0,077
45	0,732	0,769	1,082	−0,026	0,070
50	0,649	0,803	1,032	−0,019	0,061
55	0,576	0,838	1,016	−0,009	0,053
60	0,489	0,867	0,995	−0,011	0,048
70	0,317	0,904	0,957	−0,011	0,034
80	0,165	0,890	0,906	0,007	0,016
90	0,006	0,905	0,905	0,006	−0,002

TABLE 13

Test Results for JfS 59 BR 15

$Re = 0{,}56 \cdot 10^6$

$\varepsilon°$	c_C	c_D	c_Y	c_X	c_M
−2	−0,059	0,078	0,062	−0,076	−0,008
0	0	0,080	0	−0,080	0,002
2	0,066	0,080	0,069	−0,078	0,011
5	0,163	0,095	0,171	−0,080	0,026
10	0,338	0,140	0,357	−0,079	0,046
15	0,492	0,199	0,526	−0,064	0,064
20	0,634	0,289	0,695	−0,055	0,083
25	0,785	0,404	0,883	−0,034	0,086
30	0,953	0,570	1,110	−0,016	0,113
35	1,022	0,738	1,260	−0,018	0,106
40	1,029	0,887	1,358	−0,018	0,089
41	1,023	0,908	1,368	−0,014	0,090
42	0,792	0,752	1,091	−0,029	[illegible]
45	0,743	0,776	1,074	−0,025	0,068
50	0,669	0,802	1,045	−0,004	0,061
55	0,574	0,830	1,009	−0,006	0,052
60	0,487	0,854	0,983	−0,005	0,051
70	0,321	0,894	0,950	−0,005	0,035
80	0,159	0,903	0,917	−0,001	0,014
90	0	0,913	0,913	0	0,002

$Re = 0{,}71 \cdot 10^6$

$\varepsilon°$	c_C	c_D	c_Y	c_X	c_M
−2	−0,058	0,084	−0,061	−0,082	−0,008
0	0	0,080	0	−0,080	0,002
2	0,065	0,083	0,068	−0,080	0,011
5	0,152	0,096	0,160	−0,083	0,027
10	0,342	0,138	0,361	−0,076	0,047
15	0,494	0,193	0,528	−0,064	0,064
20	0,640	0,300	0,704	−0,063	0,087
25	0,782	0,429	0,890	−0,058	0,093
30	0,930	0,577	1,094	−0,035	0,115
35	1,024	0,757	1,273	−0,033	0,113
40	1,020	0,906	1,364	−0,039	0,098
41	1,009	0,923	1,366	−0,037	0,091
42	0,806	0,747	1,099	−0,015	0,074
45	0,729	0,775	1,063	−0,033	0,065
50	0,661	0,809	1,045	−0,014	0,061
55	0,581	0,835	1,017	−0,003	0,053
60	0,492	0,858	0,989	−0,003	0,047
70	0,315	0,881	0,935	−0,005	0,037
80	0,160	0,899	0,913	0,001	0,012
90	0	0,921	0,921	0	−0,001

$Re = 0{,}78 \cdot 10^6$

$\varepsilon°$	c_C	c_D	c_Y	c_X	c_M
−2	−0,059	0,088	−0,062	−0,086	−0,012
0	0	0,085	0	−0,085	0
2	0,066	0,087	0,069	−0,084	0,012
5	0,173	0,096	0,181	−0,081	0,028
10	0,341	0,140	0,360	−0,078	0,049
15	0,502	0,209	0,539	−0,072	0,071
20	0,649	0,296	0,711	−0,056	0,089
25	0,791	0,428	0,898	−0,053	0,096
30	0,928	0,573	1,090	−0,032	0,116
35	1,019	0,749	1,263	−0,029	0,109
40	1,019	0,891	1,353	−0,027	0,094
41	1,005	0,926	1,365	−0,039	0,089
42	0,808	0,779	1,121	−0,039	0,075
45	0,747	0,780	1,079	−0,023	0,067
50	0,660	0,820	1,052	−0,022	0,063
55	0,583	0,852	1,032	−0,011	0,056
60	0,503	0,874	1,008	−0,002	0,047
70	0,322	0,901	0,956	−0,007	0,033
80	0,163	0,910	0,924	0,002	0,017
90	0,005	0,918	0,918	0,005	−0,000

TABLE 14

Test Results for JfS 57 BR 15

$Re = 0{,}56 \cdot 10^6$

$\varepsilon°$	c_C	c_D	c_Y	c_X	c_M
−2	−0,057	0,028	−0,058	−0,026	−0,013
0	0	0,026	0	−0,026	0,001
2	0,059	0,031	0,060	−0,029	0,019
5	0,147	0,043	0,150	−0,029	0,044
10	0,293	0,069	0,300	−0,017	0,078
15	0,435	0,123	0,452	−0,006	0,099
20	0,579	0,213	0,617	−0,002	0,106
25	0,717	0,336	0,792	−0,002	0,092
30	0,894	0,511	1,030	0,015	0,121
35	1,010	0,688	1,222	0,016	0,130
40	1,053	0,875	1,370	0,006	0,124
42	1,046	0,922	1,394	0,014	0,102
43	0,705	0,707	0,997	−0,036	0,078
45	0,672	0,726	0,988	−0,038	0,078
50	0,601	0,776	0,982	−0,038	0,070
55	0,534	0,825	0,981	−0,036	0,062
60	0,454	0,868	0,978	−0,041	0,058
70	0,300	0,908	0,956	−0,028	0,047
80	0,149	0,929	0,941	−0,014	0,023
90	−0,005	0,964	0,964	−0,005	−0,002

$Re = 0{,}72 \cdot 10^6$

$\varepsilon°$	c_C	c_D	c_Y	c_X	c_M
−2	−0,056	0,030	−0,057	−0,028	−0,011
0	0,003	0,028	0,003	−0,028	0,005
2	0,059	0,031	0,060	−0,029	0,022
5	0,148	0,037	0,150	−0,024	0,045
10	0,293	0,068	0,300	−0,016	0,081
15	0,435	0,123	0,452	−0,006	0,101
20	0,572	0,217	0,612	−0,008	0,111
25	0,698	0,349	0,780	−0,021	0,097
27	0,735	0,401	0,837	−0,023	0,101
28	0,751	0,427	0,863	−0,024	0,104
29	0,825	0,470	0,949	−0,011	0,117
30	0,877	0,506	1,013	0,001	0,123
35	0,985	0,703	1,210	−0,011	0,140
40	1,038	0,889	1,366	−0,014	0,127
42	0,996	0,965	1,385	−0,051	0,120
43	0,704	0,724	1,009	−0,050	0,086
45	0,667	0,736	0,992	−0,048	0,086
50	0,603	0,794	0,995	−0,048	0,077
55	0,535	0,841	0,996	−0,045	0,073
60	0,455	0,880	0,990	−0,046	0,067
70	0,307	0,940	0,987	−0,033	0,048
80	0,154	0,944	0,956	−0,013	0,030
90	0,001	0,962	0,962	−0,002	0

TABLE 15

Test Results for Square Plate B/L = 0.015

$Re = 0{,}56 \cdot 10^6$

$\varepsilon°$	c_C	c_D	c_Y	c_X	$c_{M,25}$
−2	−0,057	0,018	−0,057	−0,016	0,004
0	0	0,017	0	−0,017	0,001
2	0,057	0,017	0,057	−0,015	−0,003
5	0,156	0,024	0,158	−0,010	−0,004
10	0,338	0,071	0,345	−0,011	−0,008
15	0,553	0,149	0,573	−0,001	−0,037
20	0,762	0,272	0,809	0,006	−0,082
25	0,929	0,423	1,021	0,010	−0,129
30	1,070	0,587	1,220	0,027	−0,175
35	1,155	0,762	1,382	0,038	−0,213
40	1,178	0,939	1,505	0,038	−0,256
41	1,153	0,939	1,486	0,049	−0,256
42	0,803	0,714	1,123	0,050	−0,202
45	0,773	0,747	1,074	0,018	−0,201
50	0,681	0,768	1,026	0,020	−0,194
55	0,596	0,785	0,985	0,038	−0,188
60	0,502	0,802	0,945	0,034	−0,184
70	0,336	0,863	0,926	0,021	−0,192
80	0,180	0,975	0,991	0,008	−0,234
90	0	1,048	1,048	0	−0,265

$Re = 0{,}71 \cdot 10^6$

$\varepsilon°$	c_C	c_D	c_Y	c_X	$c_{M,25}$
−2	−0,056	0,022	−0,057	−0,020	−0,002
0	0	0,018	0	−0,018	0,001
2	0,056	0,019	0,057	−0,017	0,004
5	0,151	0,030	0,153	−0,016	0,007
10	0,349	0,077	0,357	−0,015	−0,005
15	0,544	0,155	0,565	−0,009	−0,034
20	0,749	0,271	0,797	0,001	−0,077
25	0,925	0,413	1,013	0,017	−0,120
30	1,047	0,587	1,201	0,016	−0,165
35	1,159	0,758	1,384	0,043	−0,002
40	1,177	0,944	1,508	0,033	−0,230
41	1,157	0,936	1,487	0,052	−0,247
42	0,354	0,725	1,119	0,032	−0,199
45	0,785	0,748	1,083	0,027	−0,195
50	0,689	0,768	1,031	0,034	−0,187
55	0,599	0,784	0,985	0,042	−0,181
60	0,506	0,821	0,964	0,027	−0,186
70	0,334	0,840	0,903	0,027	−0,186
80	0,182	0,946	0,964	0,015	−0,223
90	0,003	1,036	1,036	0,003	−0,262

TABLE 16

Test Results for Square Plate B/L = 0.03

$Re = 0{,}57 \cdot 10^6$

ε°	c_C	c_D	c_Y	c_X	$c_{M,u}$
−2	−0,064	0,033	−0,056	−0,031	−0,002
0	0,007	0,033	0,007	−0,033	0,002
2	0,062	0,035	0,063	−0,033	0,005
5	0,156	0,050	0,159	−0,031	0,005
10	0,338	0,092	0,349	−0,032	−0,009
15	0,539	0,170	0,565	−0,025	−0,036
20	0,724	0,286	0,778	−0,022	−0,077
25	0,887	0,428	0,965	−0,013	−0,116
30	1,036	0,592	1,193	0,005	−0,160
35	1,119	0,762	1,353	0,018	−0,202
40	1,154	0,920	1,476	0,038	−0,246
41	1,147	0,951	1,489	0,035	−0,253
42	0,853	0,716	1,112	0,038	−0,194
45	0,816	0,743	1,103	0,053	−0,194
50	0,681	0,771	1,028	0,026	−0,186
55	0,582	0,780	0,973	0,029	−0,176
60	0,489	0,797	0,935	0,024	−0,176
70	0,321	0,863	0,921	0,007	−0,188
80	0,177	0,953	0,970	0,009	−0,217
90	0,007	1,062	1,062	0,007	−0,259

$Re = 0{,}71 \cdot 10^6$

ε°	c_C	c_D	c_Y	c_X	$c_{M,u}$
−2	−0,061	0,036	−0,062	−0,033	−0,002
0	0,008	0,033	0,003	−0,033	0,001
2	0,061	0,036	0,063	−0,033	0,004
5	0,155	0,044	0,159	−0,031	0,005
10	0,342	0,092	0,353	−0,031	−0,009
15	0,527	0,167	0,552	−0,025	−0,036
20	0,722	0,269	0,778	−0,024	−0,080
25	0,876	0,404	0,965	0,004	−0,117
30	1,016	0,584	1,171	0,002	−0,164
35	1,106	0,764	1,343	0,008	−0,203
40	1,142	0,914	1,463	0,034	−0,240
41	1,132	0,937	1,468	0,035	−0,243
42	0,849	0,728	1,118	0,027	−0,198
45	0,796	0,756	1,097	0,029	−0,198
50	0,695	0,784	1,047	0,028	−0,187
55	0,604	0,798	0,999	0,037	−0,182
60	0,494	0,807	0,946	0,024	−0,177
70	0,333	0,855	0,917	0,020	−0,182
80	0,175	0,960	0,975	0,005	−0,217
90	0,005	1,066	1,006	0,005	−0,263

TABLE 17

Test Results for Square Plate B/L = 0.05

$Re = 0{,}56 \cdot 10^6$

ε°	c_C	c_D	c_Y	c_X	c_M	$c_{M,u}$
−2	−0,054	0,052	−0,056	−0,050	−0,013	0,002
0	0,005	0,050	0,005	−0,050	0,001	−0,000
2	0,062	0,057	0,063	−0,055	0,018	0,002
5	0,161	0,069	0,166	−0,054	0,039	−0,003
10	0,336	0,116	0,351	−0,056	0,066	−0,003
15	0,518	0,192	0,550	−0,051	0,085	−0,053
20	0,690	0,291	0,749	−0,037	0,086	−0,089
25	0,844	0,428	0,946	−0,031	0,098	−0,139
30	0,991	0,619	1,168	−0,040	0,114	−0,178
35	1,069	0,788	1,327	−0,032	0,107	−0,225
40	1,100	0,948	1,459	−0,013	0,102	−0,263
41	1,105	0,972	1,472	−0,009	0,098	−0,270
42	1,095	0,979	1,469	0,004	0,094	−0,274
43	0,894	0,809	1,206	0,019	0,089	−0,212
45	0,785	0,804	1,123	−0,013	0,082	−0,200
50	0,714	0,842	1,103	0,006	0,069	−0,207
55	0,624	0,884	1,082	0,004	0,083	−0,207
60	0,530	0,922	1,063	−0,003	0,061	−0,205
70	0,338	0,946	1,005	−0,007	0,045	−0,206
80	0,161	0,958	0,972	−0,008	0,023	−0,220
90	0	0,998	0,998	0	0	−0,250

$Re = 0{,}67 \cdot 10^6$

ε°	c_C	c_D	c_Y	c_X	c_M	$c_{M,u}$
−2	−0,051	0,056	−0,053	−0,054	−0,012	0,001
0	0	0,054	0	−0,054	0,003	0,0025
2	0,061	0,058	0,063	−0,055	0,018	0,0021
5	0,166	0,071	0,171	−0,056	0,040	0,0027
10	0,345	0,117	0,360	−0,055	0,068	−0,0218
15	0,514	0,193	0,456	−0,053	0,086	−0,0506
20	0,697	0,315	0,763	−0,047	0,102	−0,0889
25	0,859	0,460	0,972	−0,054	0,109	−0,1343
30	0,995	0,624	1,173	−0,042	0,111	−0,1821
35	1,070	0,793	1,332	−0,037	0,107	−0,22[illegible]0
40	1,125	0,954	1,475	−0,008	0,101	−0,3677
41	1,109	1,010	1,498	−0,035	0,112	−0,2624
42	1,079	1,019	1,482	−0,036	0,103	−0,2673
43	0,832	0,790	1,148	−0,010	0,072	−0,2151
45	0,798	0,795	1,126	0,002	0,070	−0,2115
50	0,731	0,844	1,117	0,017	0,065	−0,2144
55	0,616	0,879	1,073	0,001	0,062	−0,2059
60	0,521	0,917	1,055	−0,008	0,054	−0,2097
70	0,342	0,942	1,002	−0,001	0,039	−0,2111
80	0,162	0,964	0,977	−0,008	0,023	−0,2214
90	0	0,996	0,996	0	0,001	−0,2484

TABLE 18

Test Results for Square Plate B/L = 0.07

$\delta°$	c_C	c_D	c_Y	c_X	$c_{M.n}$
Re = 0,56 · 10⁶					
−2	−0,062	0,071	−0,064	−0,069	0,005
0	0	0,069	0	−0,069	0,003
2	0,062	0,071	0,064	−0,069	−0,002
5	0,156	0,080	0,163	−0,067	−0,006
10	0,315	0,125	0,332	−0,069	−0,020
15	0,482	0,199	0,517	−0,067	−0,048
20	0,648	0,305	0,712	−0,065	−0,093
25	0,783	0,440	0,895	−0,068	−0,140
30	0,908	0,586	1,079	−0,054	−0,184
35	0,969	0,728	1,228	−0,030	−0,213
40	1,024	0,889	1,356	−0,023	−0,247
41	1,010	0,889	1,346	−0,008	−0,247
42	0,823	0,754	1,116	−0,010	−0,205
45	0,738	0,738	1,044	0	−0,195
50	0,681	0,761	1,021	0,033	−0,197
55	0,601	0,792	0,994	0,039	−0,192
60	0,497	0,818	0,957	0,021	−0,189
70	0,315	0,856	0,912	0,003	−0,194
80	0,173	0,975	0,990	0,001	−0,236
90	0	1,071	1,071	0	−0,275

$\delta°$	c_C	c_D	c_Y	c_X	$c_{M.n}$
Re = 0,71 · 10⁶					
0	0	0,074	0	−0,074	0,002
2	0,065	0,077	0,068	−0,074	−0,001
5	0,160	0,086	0,167	−0,072	−0,006
10	0,323	0,132	0,341	−0,073	−0,018
15	0,485	0,206	0,521	−0,073	−0,047
20	0,654	0,311	0,721	−0,068	−0,095
25	0,788	0,442	0,901	−0,068	−0,142
30	0,915	0,593	1,089	−0,055	−0,187
35	0,988	0,738	1,232	−0,049	−0,222
40	1,000	0,873	1,327	−0,025	−0,247
41	1,003	0,901	1,348	−0,021	−0,255
42	0,788	0,788	1,106	−0,051	−0,215
45	0,757	0,749	1,066	−0,006	−0,202
50	0,698	0,768	1,037	0,040	−0,199
55	0,618	0,806	1,014	0,044	−0,200
60	0,512	0,828	0,972	0,029	−0,198
70	0,319	0,871	0,927	0,002	−0,202
80	0,175	0,972	0,987	0,003	−0,238
90	0,002	1,076	1,076	0,002	−0,279

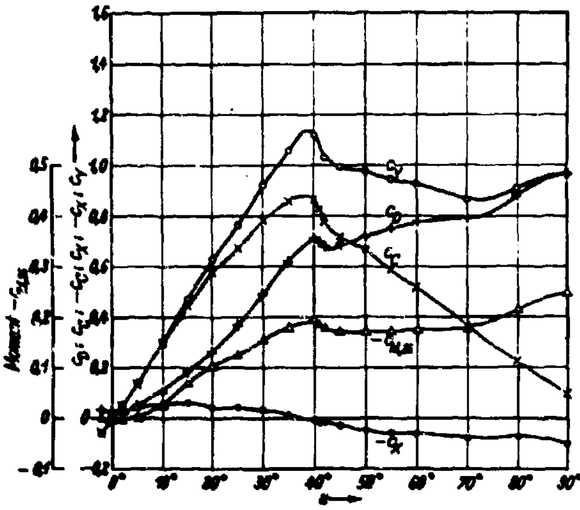

Figure 18 - Flow Forces on Rectangular Rudder TMB 075 075 15 $\Lambda_R = 1$, Re = 0.69 . 10^6, JfS wind tunnel measurement, uncorrected, $A_R/A_S = 0.204$. (Numerical values in Table 4)

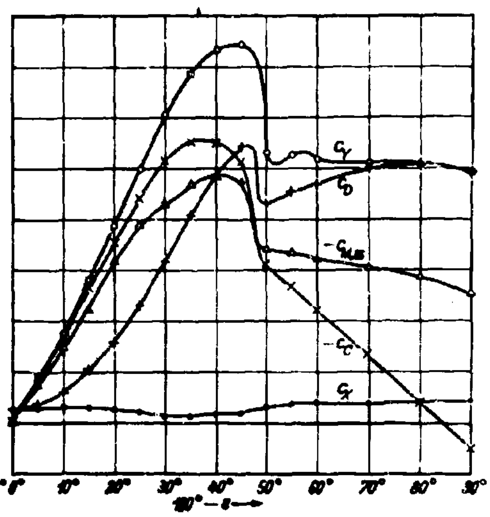

Figure 19 - Flow Forces on Rectangular Rudder TMB 075 075 15 in Astern Motion $\Lambda_R = 1$, Re = 0.56 . 10^6, JfS wind tunnel measurement, uncorrected, $A_R/A_S = 0.204$. (Numerical values in Table 4)

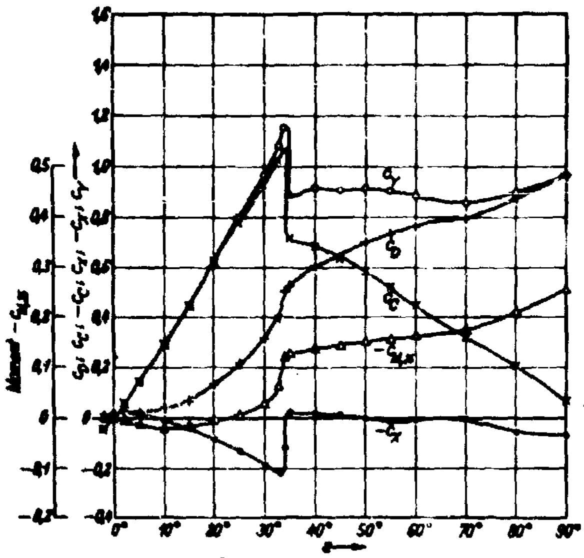

Figure 20 - Flow Forces on Rectangular Rudder NACA 0015 $_R = 1$, Re = $0.79 \cdot 10^6$, JfS wind tunnel measurement, uncorrected, $A_R/A_S = 0.204$. (Numerical values in Table 5).

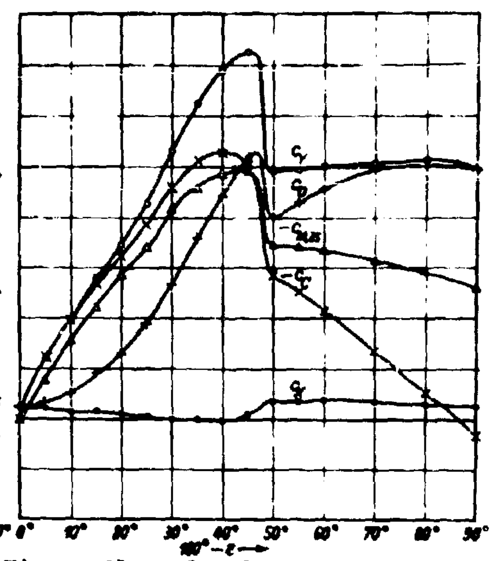

Figure 21 - Flow Forces on Rectangular Rudder NACA 0015 in Astern Motion

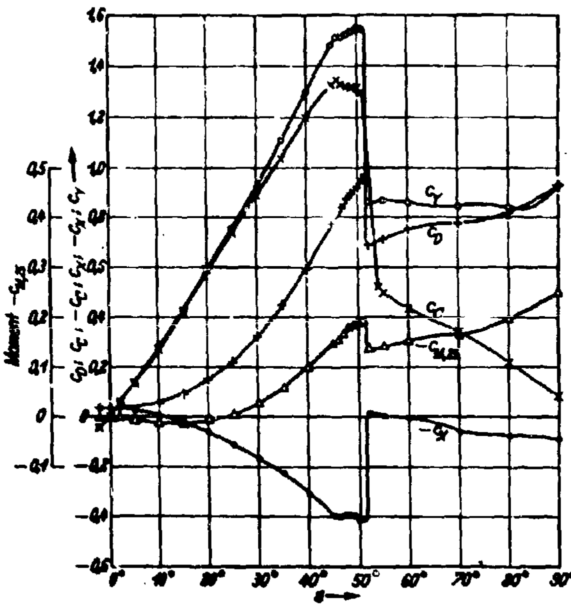

Figure 22 - Flow Forces on Rectangular Rudder NACA 0025

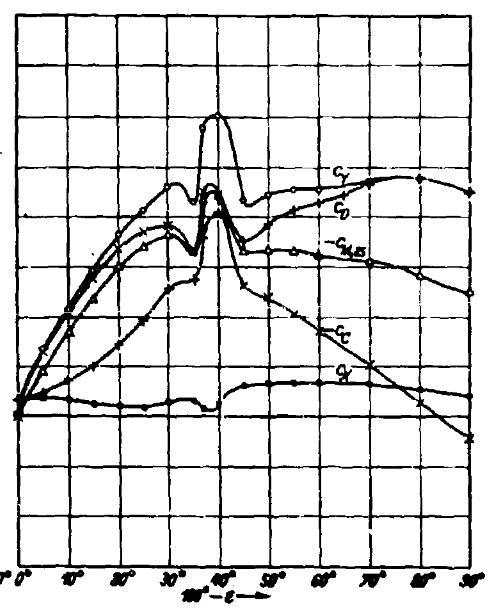

Figure 23 - Flow Forces on Rectangular Rudder NACA 0025 in Astern Motion

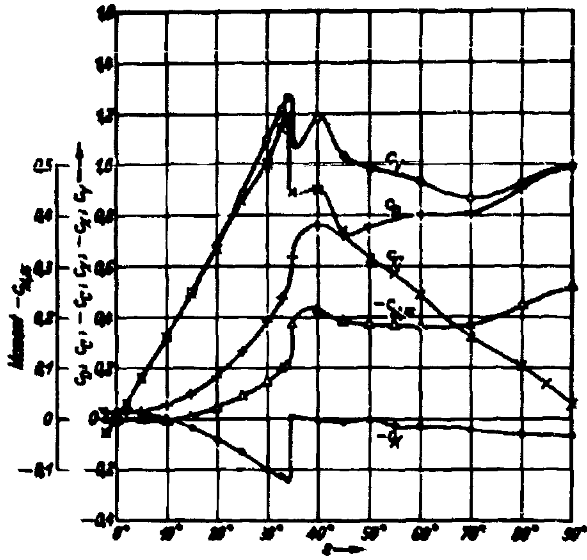

Figure 24 - Flow Forces on Rectangular Rudder JfS 58 TR 15

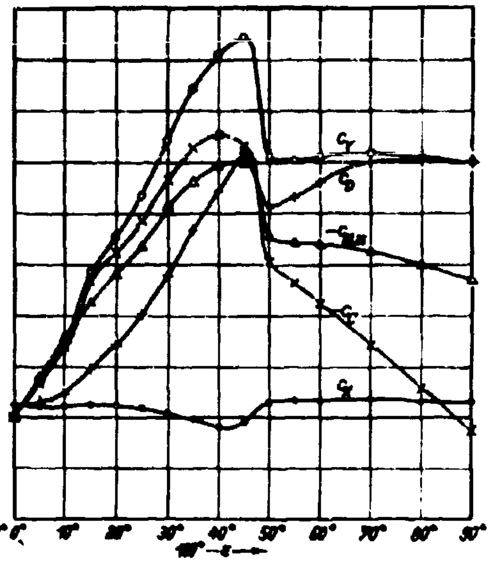

Figure 25 - Flow Forces on Rectangular Rudder JfS 58 TR 15 in Astern Motion

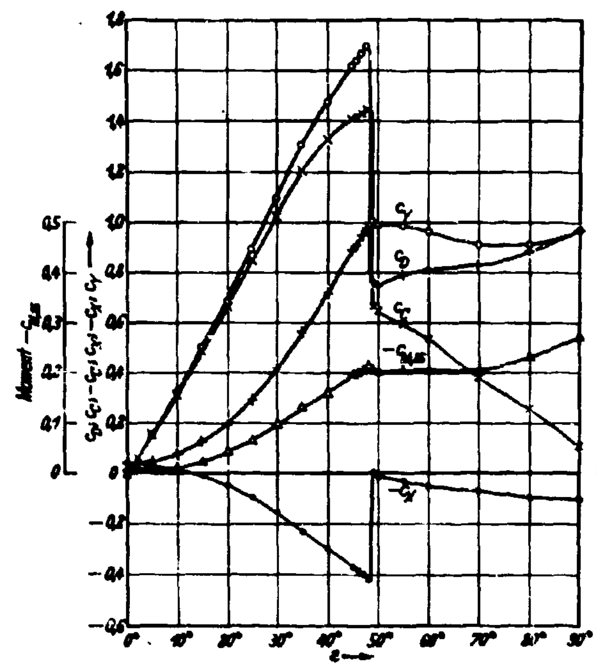

Figure 26 - Flow Forces on Rectangular Rudder JfS 58 TR 25

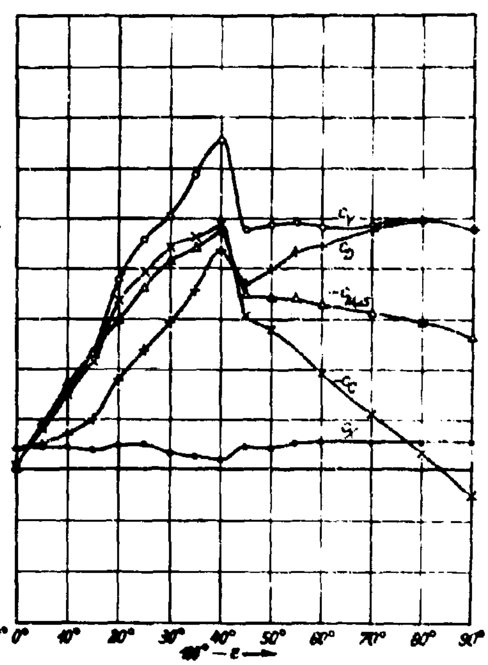

Figure 27 - Flow Forces on Rectangular Rudder JfS 58 TR 25 in Astern Motion

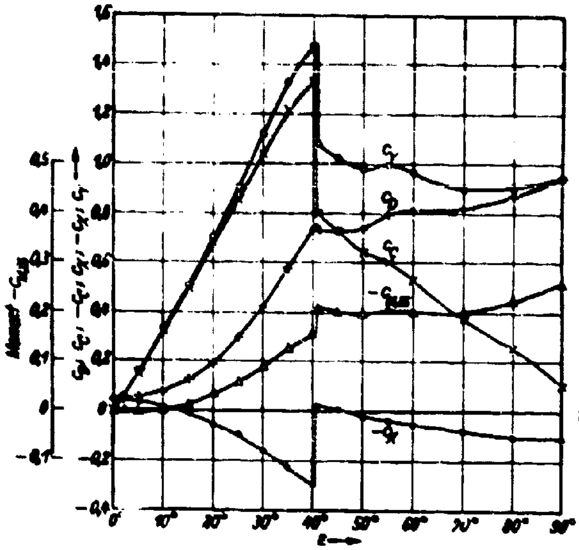

Figure 28 - Flow Forces on Rectangular Rudder JfS 61 TR 25

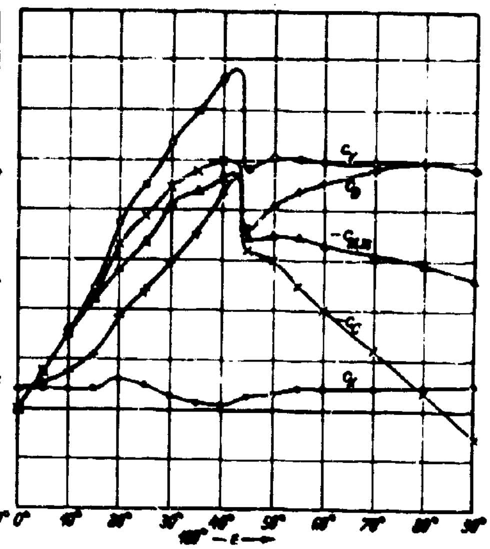

Figure 29 - Flow Forces on Rectangular Rudder JfS 61 TR 25 in Astern Motion

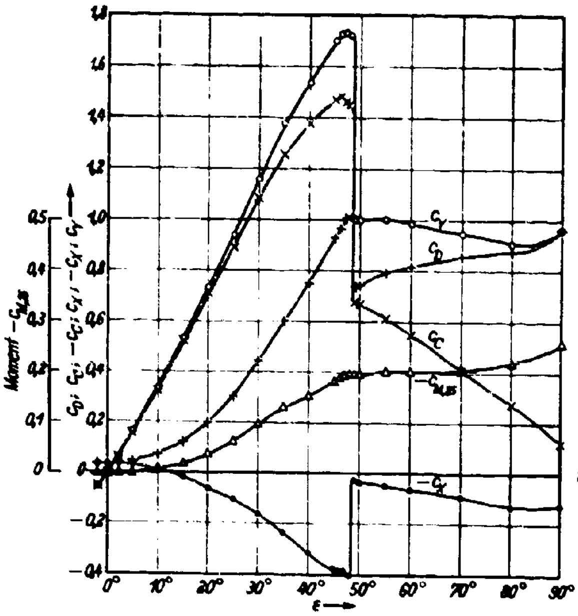

Figure 30 - Flow Forces on Rectangular Rudder JfS 62 TR 25

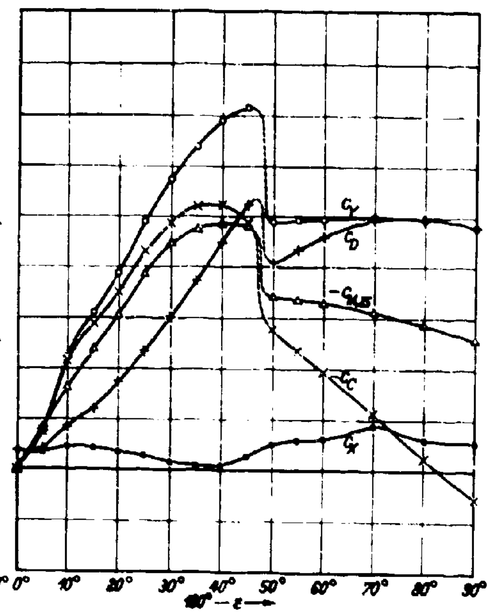

Figure 31 - Flow Forces on Rectangular Rudder JfS 62 TR 25 in Astern Motion

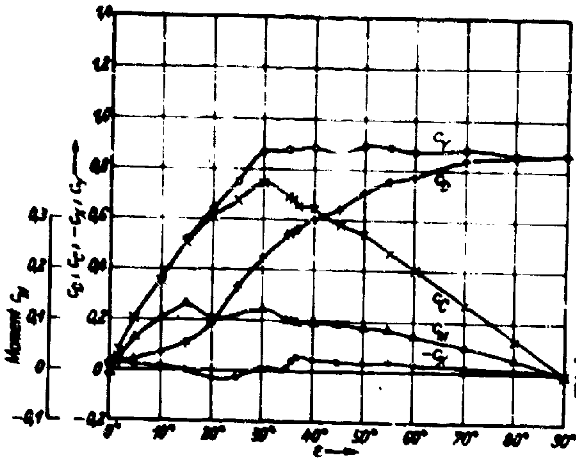

Figure 32 - Flow Forces on Rectangular Bow Rudder JfS 55 BR 15

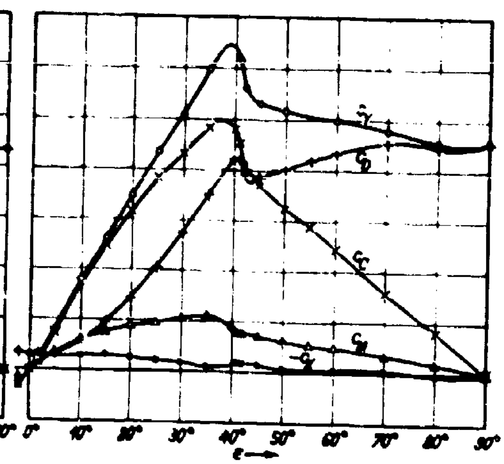

Figure 33 - Flow Forces on Rectangular Bow Rudder JfS 54 BR 15

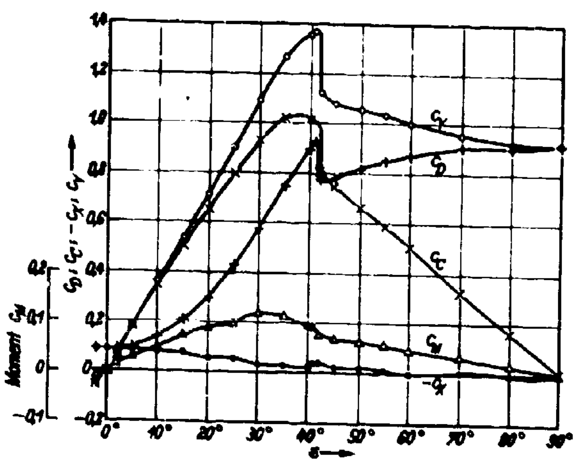

Figure 34 - Flow Forces on Rectangular Bow Rudder JfS 59 BR 15

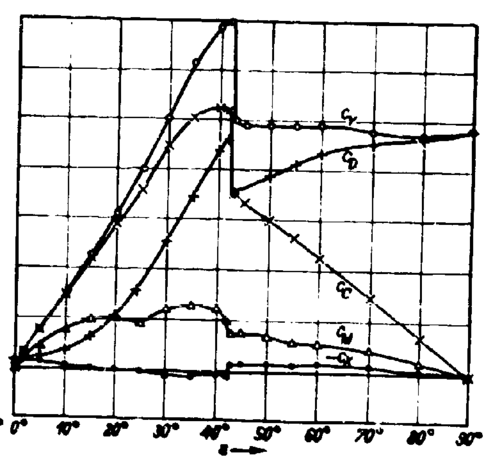

Figure 35 - Flow Forces on Rectangular Bow Rudder JfS 57 BR 15

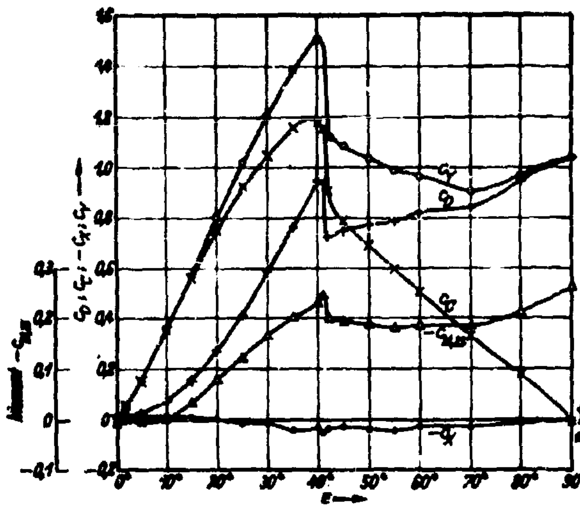

Figure 36 - Flow Forces on Square Plate B/L = 0.015

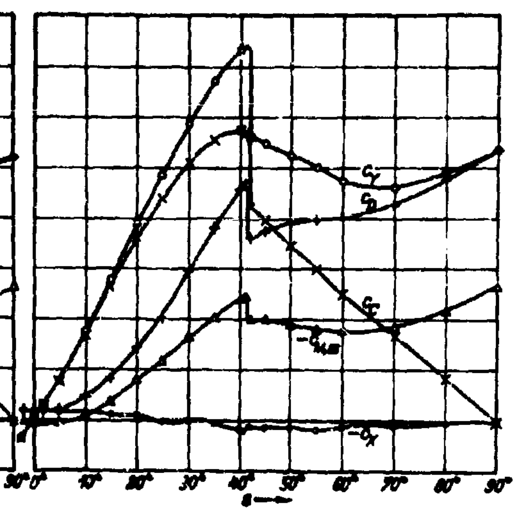

Figure 37 - Flow Forces on Square Plate B/L = 0.03

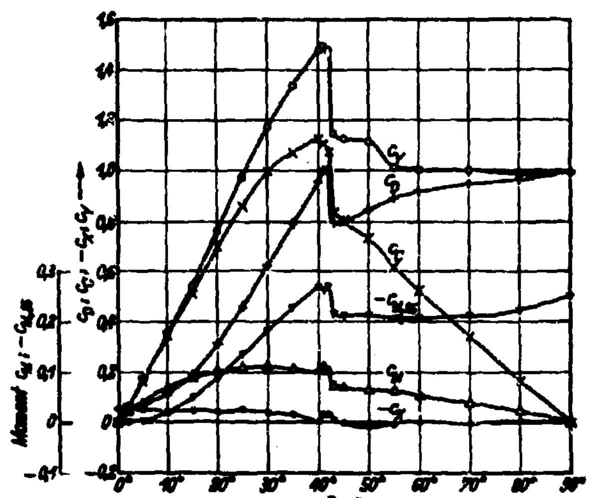

Figure 38 - Flow Forces on Square Plate B/L = 0.05

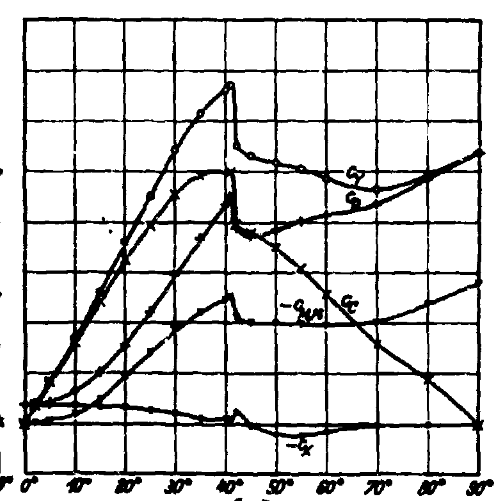

Figure 39 - Flow Forces on Square Plate B/L = 0.07

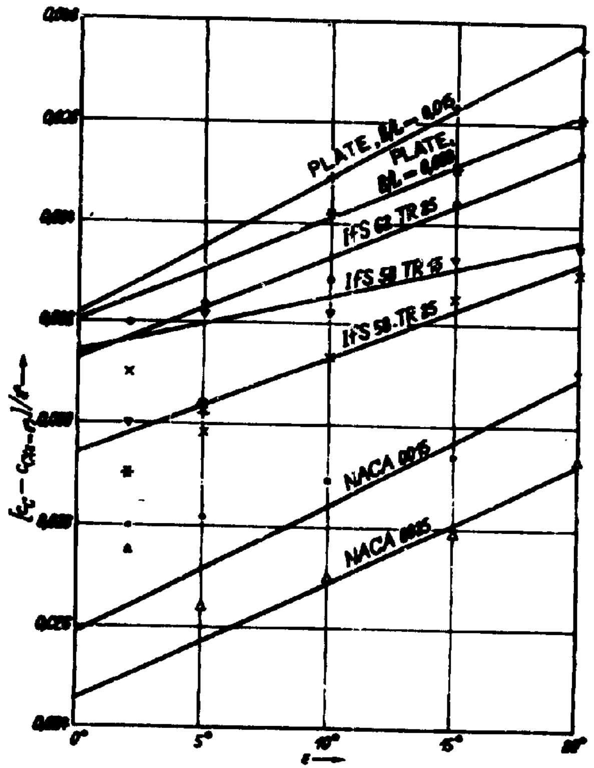

Figure 40 - Efficiency of Various Rudder Profiles at Small Rudder Angles in Straight-Ahead Motion

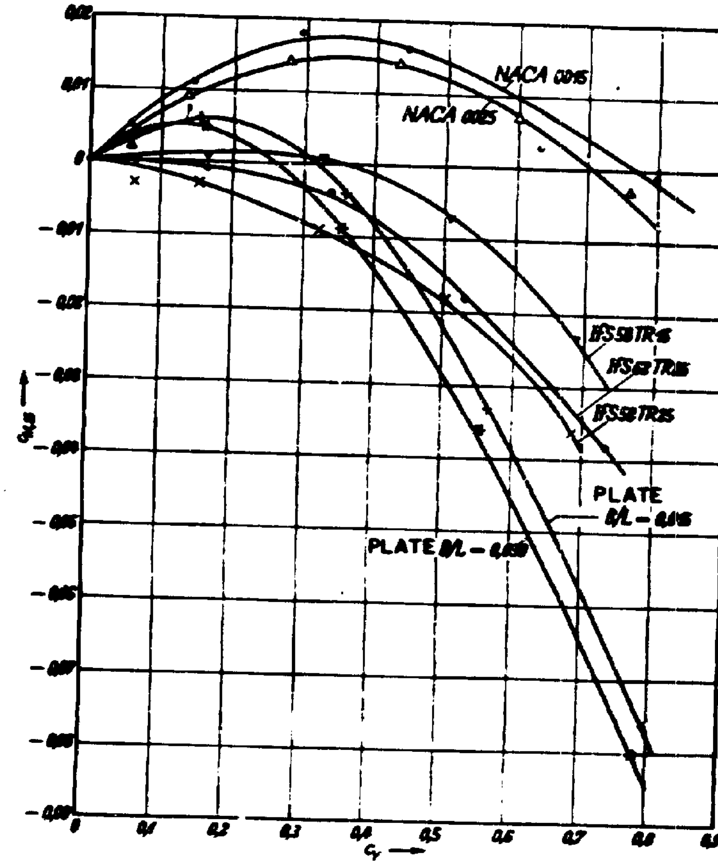

Figure 41 - Comparison of the Rudder Moment Curve which Determines the Choice of the Location of the Turning Axis, for Various Rudder Profiles at Small Rudder Angles in Straight-Ahead Motion

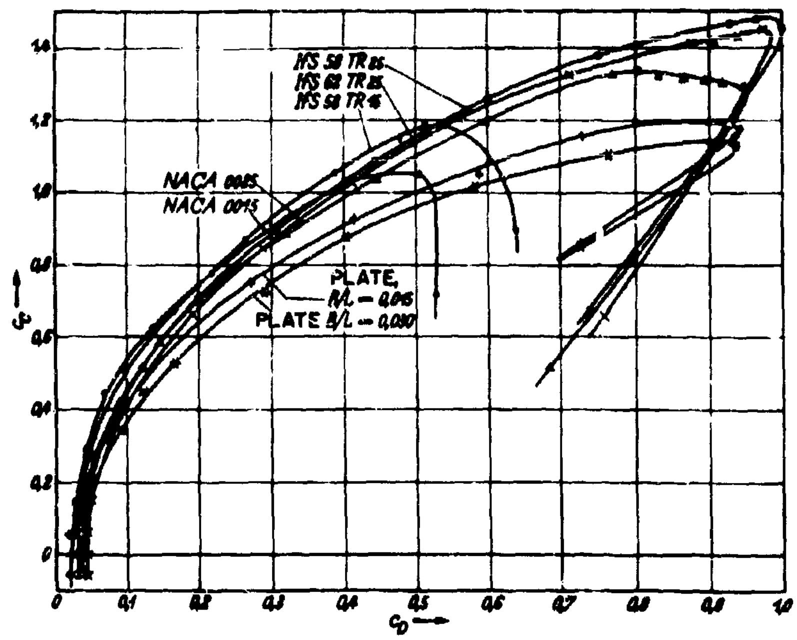

Figure 42 - Drag Power Requirement of Various Rudder Profiles at Rudder Angle in Straight-Ahead Motion

TABLE 19

Rudder Efficiency and Drag Power Requirements of the Profiles Investigated

PROFILE	$\frac{Re}{10^6}$	RUDDER ANGLE $\delta_R = -35°$ STRAIGHT-AHEAD MOTION: $c_{YRr} = c_C$ CONTROL FORCE	$c_{NRr} = c_D$ DRAG POWER REQUIREMENT	MOTION ALONG THE TURNING CIRCLE $L_L/R_L = 0,5$: c_{YRr} CONTROL FORCE	c_{NRr} DRAG POWER REQUIREMENT
NACA 0015	0,79	– 0,622	0,135	– 0,675	0,062
0025	0,78	– 0,586	0,145	– 0,637	0,060
JfS 58 TR 15	0,78	– 0,670	0,166	– 0,714	0,087
*) 25	0,78	– 0,660	0,191	– 0,698	0,115
JfS 62 TR 25	0,78	– 0,708	0,199	– 0,742	0,116

*) SEE ALSO FIGURE 43.

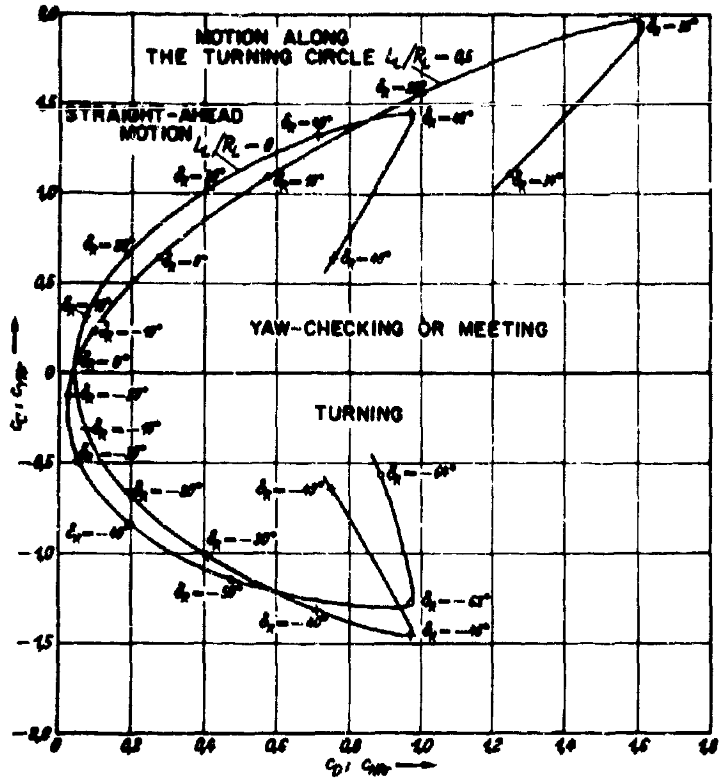

Figure 43 - Drag Power Requirement and Efficiency of Profile JfS 58 TR 25 for Straight-Ahead Motion and for Motion along the Turning Circle $L_L/R = 0.5$

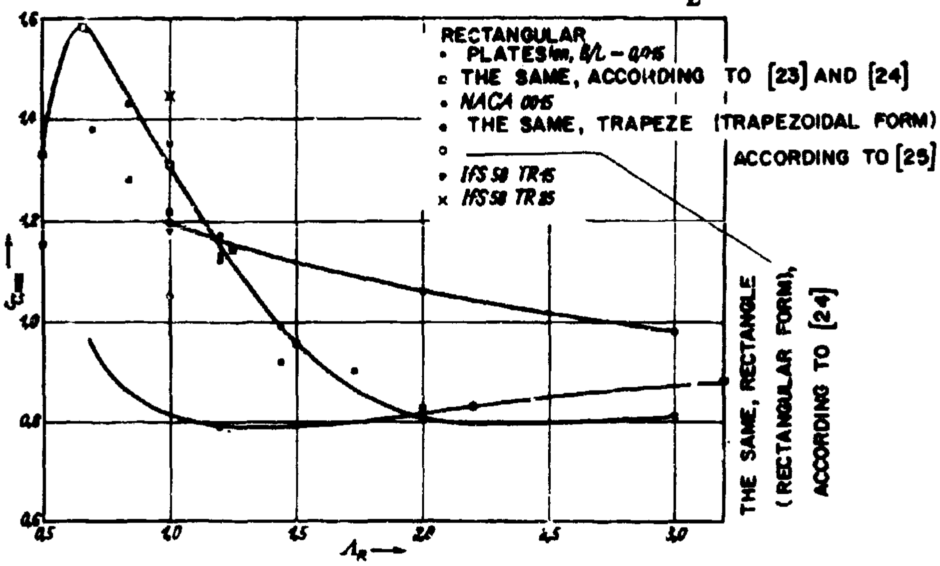

Figure 44 - Influence of Aspect Ratio on the Transverse-Force Coefficient for Various Rudders

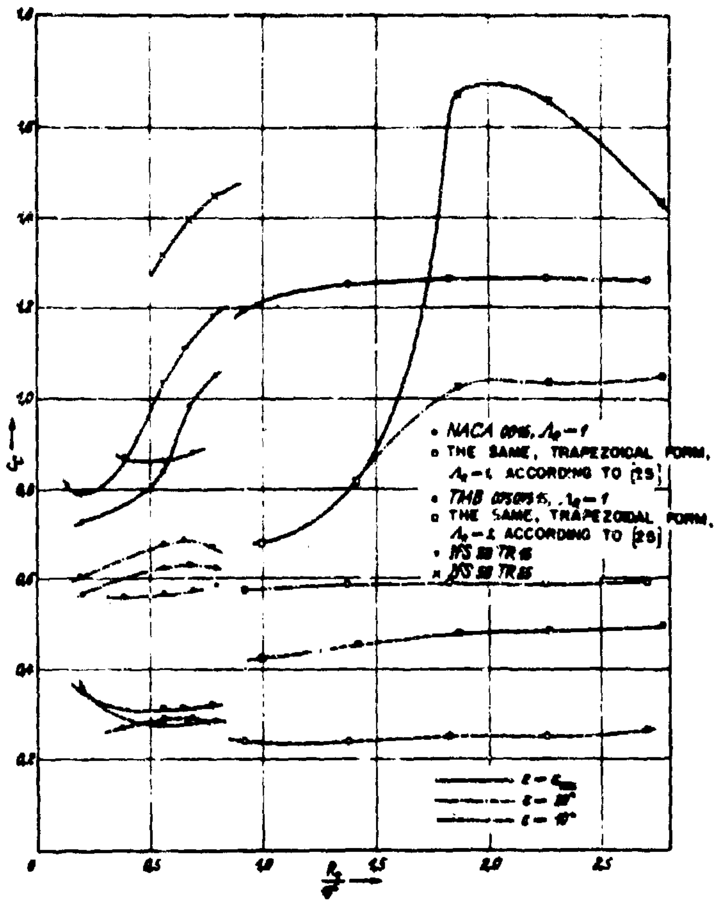

Figure 45 - Influence of the Reynolds Number on the Transverse-Force Coefficient for Various Rudders

G. MEASURES FOR SUBSEQUENT ALTERATION OF RUDDER CHARACTERISTICS

This catch word was adopted after the last war in order to resume research work on the problems concerning ship rudders. Even today there arises again and again the problem of improving the qualities and the efficiency of a rudder, with the aid of limited means in most cases.

Frequently, an improvement in directional stability is what is desired. The most inexpensive means to achieve this is by the so-called rudder wedge arrangement.* Figure 46 shows an example taken from the extensive investigation by Thiemann.[30] Figures 46a, b, and c indicate,

---

*Translator's note: Stankeil - "stagnation" wedge.

moreover, how this brings about a change in transverse force, resistance, and moment. Of course, the improvement of the transverse force and directional stability entails a certain additional resistance and a higher rudder moment. Moreover, it must be borne in mind that the effect of the wedge arrangement is all the greater, the poorer the design of the initial profile which is to be improved. That is a unique disadvantage of the more recent profiles; they can no longer be improved so easily later on by fitting a wedge on the profile.

The development of the wedges fitted on the trailing edge of rudders will hardly be clarified entirely by the statements made here. After the last war it was a prestige question at one time whether this procedure originated in the model basin or in the shipyards building coastal vessels. It must be admitted, however, that evolutionally the procedure of the model basin was based on the trailing-edge control mechanism developed a number of years before for missiles by Herbert Wagner which makes this procedure about 20 years old now. Meanwhile, however, the author following a friendly suggestion was able to ascertain that even as early as 1934 the Howaldt Co. of Hamburg (Howaldt Shipyard at Hamburg) had fitted the seaside resort ship KÖNIGIN LUISÉ with a kind of alternately step-like rudder wedge to compensate for a reduction of the rudder area.

In the meantime, the shape of the rudder wedge has undergone a considerable evolution. First, the combination of a shortening of the profile at the trailing edge and the simultaneous fitting of a wedge at the new trailing edge, as shown in Form II in Figure 46, was successfully used in actual practice and later investigated experimentally. Thereby it is possible by the skillful application of these measures not only to increase the transverse force in the entire angular range, but also to reduce the rudder moment at the same time, as seen again in Figures 46a, b, and c.

It should be pointed out nevertheless that the astern characteristics are affected somewhat adversely by the wedge arrangement. On the other hand, steering ability in astern motion depends less on the form of the rudder than on the rudder arrangement. In the case of a narrow propeller aperture or a twin-screw single rudder immediately behind the deadwood, shortening the deadwood helps more than changing the rudder profile.

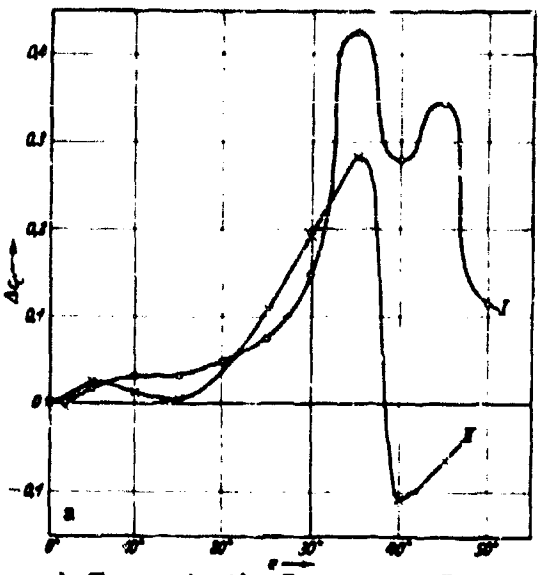

a) Change in the Transverse-Force Coefficient

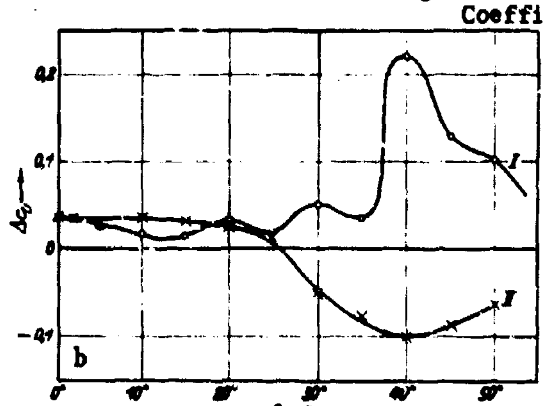

b) Change in the Resistance Coefficient

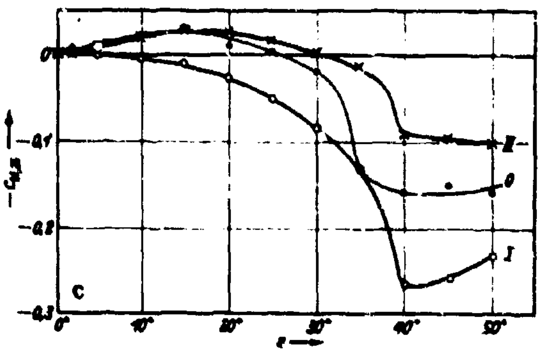

c) Change in the Moment Coefficient

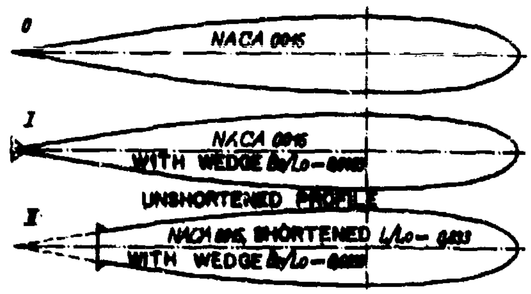

SHORTENED PROFILE

Figure 46 - Effect of Rudder Wedge Arrangement with and without Profile Shortening on Flow Forces Acting on Rectangular Rudder NACA 0015

We might mention in this connection one other inexpensive and already proven method of changing the rudder, that is, the use of end disks. In any event, this increases the contribution of the rudder to directional stability although it produces some additional resistance, especially for larger aspect ratios. At smaller aspect ratios, say, at 1.0 or even below that, the resistance increase is small in relation to the increase in the transverse force; in that case, however, the maximum rudder effect decreases so that we must count on a decrease in the maximum turning ability.

H. FUTURE TRENDS IN RUDDER FORMS

The optimum which was approximately obtained for balanced-rudder profiles with such forms as IfS 58 TR 25 and IfS 62 TR 25 will have to be investigated further in view of the influence of structural desires for a thick trailing edge and possibly for even greater profile thicknesses. In this connection, the danger of cavitation or air penetration, when rudders operate near the surface will have to be considered as the Froude number increases.

A parallel development for guide head rudders and semi-balanced rudders may be based on these results. In the case of the guide head rudders, a certain measure of balancing is urgently desirable as a particular goal of the development; thus far, this has been obtained in the highest degree with the HSVA form according to Figure 74.

In view of the bow-rudder development and the control of the astern motion with normal stern rudders, it is not enough to continue the development of the bow-rudder forms now begun. The effect of the deadwood in front of the stern rudder and of the ship hull behind the bow rudder warrants investigation. In both cases, a certain interspace must remain in order that the cross flow in the wake of the rudder does not react upon the hull with full force.

The above-mentioned fundamental influence exerted on the rudder forces by the turning of the ship which deforms the entire rudder polar curve must be investigated still further, especially in view of the maximum rudder effect, since possibly the simple conversion process used here does not encompass the overall improvement which might be obtained.

A special objective for model tests at particularly small Reynolds numbers, on one hand, and for certain types of ships, on the other, consists in the development of rudders which, for structural reasons, must have adequate shaft thickness while acting supposedly like thin plate rudders. Rudder IfS 57 TR 15 investigated here has not yet proved to be satisfactory in this sense; it still remains at a disadvantage compared to the plates of equal or even greater edge thickness.

It goes without saying, that additional effects due to the influence of the propeller slipstream, a greater Reynolds number, and natural roughness must be kept in mind for all further developments. In this connection the question becomes interesting as to the extent to which a partial flow separation may be quickly compensated for by giving a limited amount of rudder angle if the maximum transverse force is exceeded. If adequate safety can be provided in this area, the operational performance of rudders can also be increased in a simple manner by stepping up appreciably the permissible hard-over position of the rudder.

I. REFERENCES

1. Baillitis, E., "Ruder mit versetztem Druckpunkt," Schiffstechnik 1960, H. 36, S. 71/78.

2. Thiemann, H. and Thieme, H., "Windkanaluntersuchung von Rechteckplattenrudern," Schiff und Hafen (1959) S. 1071/1083.

3. Thieme, H., "Ruder." Handbuch der Werften (1952) S. 89/94.

4. Rankine: Zitat 1866.

5. Thieme, H., "Kennzahlen von Steuereigenschaften," Schiff und Hafen 1957, S. 81/100.

6. Lamb, B. J., and S. B. Cook, "A Practical Approach to Rudder Design," Shipb. a. Shipp. Record 1961. Sep, S. 334/336.

7. Saunders, H., "The Design of the Movable Appendages and Control Surfaces," Hydrodynamics in Ship Design Vol. II. New York 1957, S. 706/737.

8. Polonski, W. L., "Elektrische Antriebe auf Schiffen." Berlin 1958.

9. Phillips-Birt, D., "The Naval Architecture of Small Craft," London 1957.

10. Schoenherr, K., "Steering," Principles of Naval Architecture, Vol. II, New York 1949, S. 197.

11. Newton, R. N., "Turning and Maneuvering Trials," N.E.C. Inst. of Eng. a. Shipb. Vol. 76, 1960, S. 79/94 und SD 61/SD 70.

12. Lindgren, H. and N. Norrbin, "Model T ts and Ship Correlation for a Cargo Liner," T.R.I.N.A. 1962, S. 141/181. (read on 5.9.61).

13. Schmitz, G., "Anwendung der Theorie des schlanken Korpers auf die dynamische Gierstabilität und Steuerbarkeit von Schiffen," Wiss. Zeitschrift d. Universität Rostock. Math. Nat. Reihe. Heft 2/3 (1961). S. 175/190.

14. Laube, R., "Rechenverfahren für vorläufige Bestimmung des Drehkreises für Binnenschiffe," Schiffbautechnik 1961, S. 396/397.

15. Shiba, H., "Model Experiments about the Maneuverability and Turning of Ships," David Taylor Model Basin Report 1461, 1960, S. 49/126.

16. Jacobs, E. and Ward, K and Pinkerton, R., "The Characteristics of 78 Related Airfoil Sections from Tests in the Variable Density Wind Tunnel," NACA Report 460, 1933.

17. Stack, J. and A. v. Doenhoff, "Tests of 19 Related Airfoils at High Speeds," NACA Report 492, 1934.

18. Thieme, H., "Systematik für Ruder und Propellerprofile," Schiff und Hafen 1952, S. 165/166.

19. Thieme, H., "Über Grundlagen für den mathematischen Linienriss eines Frachtschiffes," Schiffstechnik 1956, H. 18, S. 288/299.

20. Kwik, K., "Darstellung der Profilform von Schiffsrudern," Schiff und Hafen 1962, S. 853/859.

21. Flügel, G., "Vergleichsversuche an Rudermodellen," Schiffbau 1940, S. 167 und S. 189.

22. Möckel, W., "Über die Steuereigenschaften von Küstenmotorschiffen," Schiffstechnik 1959, H. 34. S. 217/227.

23. Winter, H., "Strömungsvorgänge an glatten und profilierten Korpern bei kleinen Spannweiten," Forschung 1935, S. 40 und S. 67.

24. Scholz, N., "Kraft und Druckverteilungsmessungen an Tragflächen Kleiner Streckung," Forschung 1949/50, S. 85.

25. Whicker, L., and Fehlner, L., "Free-Stream Characteristics of a Family of Low-Aspect-Ratio, All-Movable Control Surfaces for Application to Ship Design," David Taylor Model Basin Report 933, 1958.

26. Thieme, H., "Zur Behandlung von Ruderproblemen," Schiff und Hafen 1955, S. 605/618.

27. Flügel, G., "Neue Erkenntnisse der Ruderforschung," Hansa 1950, S. 1432.

28. Oelert, W., Theodor Heuss, "Das neue Eisenbahn- und Auto-Fährschiff der Deutschen Bundesbahn. Hansa 1957, S." 2295/2321, Schiff und Hafen 1957, S. 981-923.

29. Thieme, H., "BVK-Profil. Blohm und Voss Profilatlas," Ae N 1025 (1944).

30. Thiemann, H., "Windkanaluntersuchungen von Rudern mit Staukeilen und Profilkurzungen," Schiff und Hafen 1962, S. 42/60.

APPENDIX

DISCUSSION BY OTHER INVESTIGATORS

Dr. Eng. Dr. Aschenbach, Frankfort (expanded in writing)

In 1943, I was engaged in experiments on new types of rudders on the basis of two German Reich patents; these experiments were altogether different from those discussed in the present paper.

One of the patents dealt with perforated and staggered rudder surfaces and the other with a 'spreading rudder' (German 'Spreizruder') which served as an anti-roll stabilizer.

The tests with the slotted rudder were undertaken at the request of the Reich Ministry of Transport and were carried out by the Hamburg Model Basin (HSVA).

In these tests, the slotted rudder was investigated in comparison to a conventional rudder of a barge; the former had only 89 percent of the area of the conventional rudder. The greatest profile thickness of the conventional rudder amounted to 1/30 while that of the slotted rudder amounted to 1/11 of the rudder length; in both cases it was located in the turning axis which was arranged approximately 17.5 percent of the length behind the leading edge of the rudder.

The balancing surface was equally large for both rudders; however, the slotted rudder exhibited a greater equilibration due to the slot and to the pressure increase in the forward zone of the flow which occurs in the case of streamlined profiles. The body plan of the barge and the two rudders are represented in Figure 1.

Two series of tests were carried out. First, the steering moments and the rudder turning moments were measured for various rudder angles with the model running straight ahead and then Z-maneuvers were carried out.

The curve of the steering moments are presented in Figure 2, and a curve of the rudder turning moments for both types of rudders is shown in Figure 3. From these, the energy expended in shifting the rudder was computed and is represented graphically for both types of rudders in

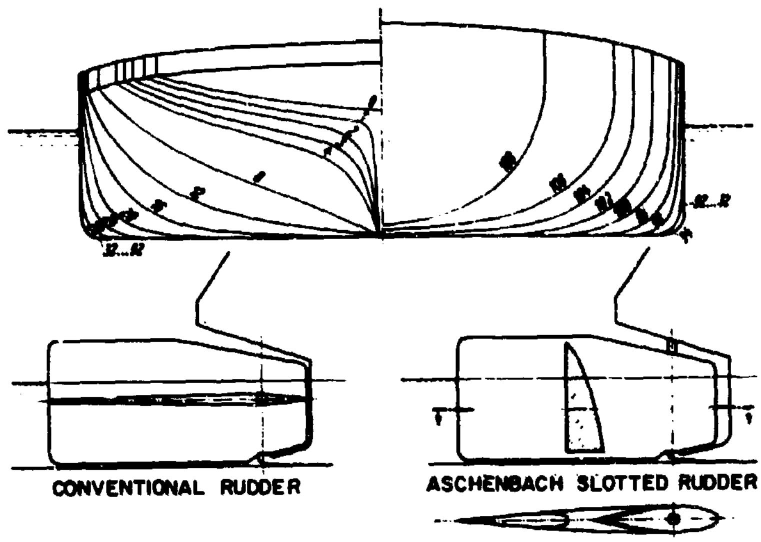

Figure 1 - Body Plan of the Barge and of the Two Rudders

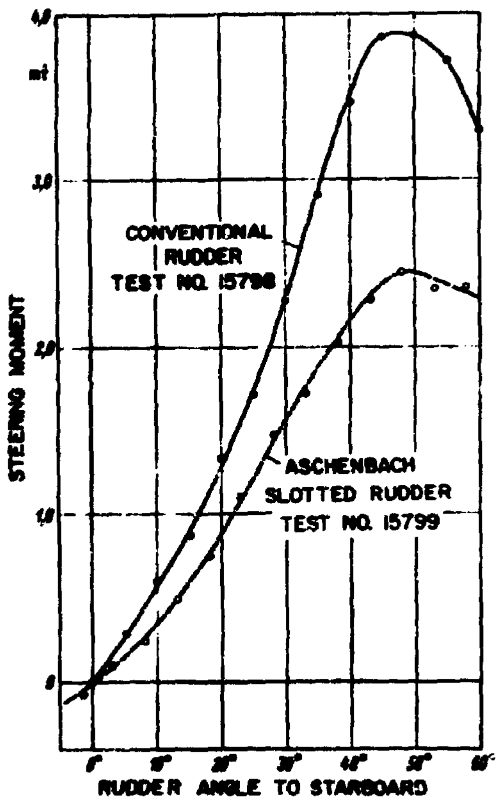

Figure 2 - Curve of the Steering Moments

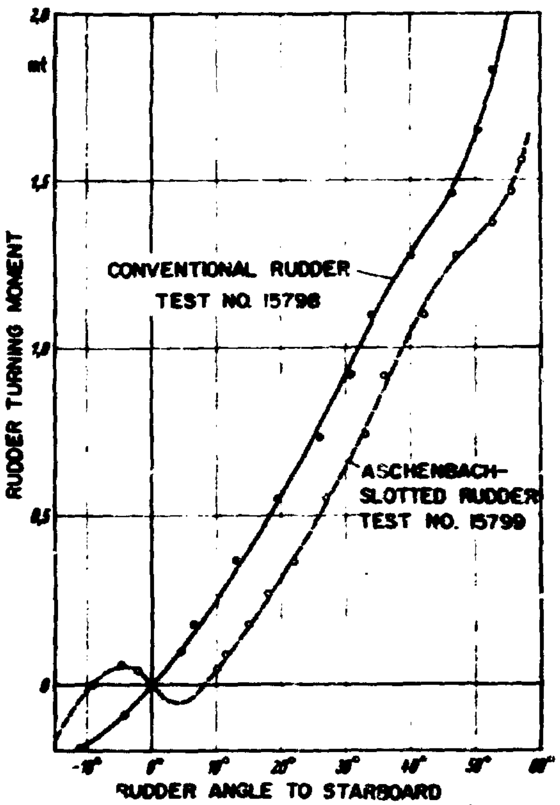

Figure 3 - Curve of the Turning Moments of the Rudder

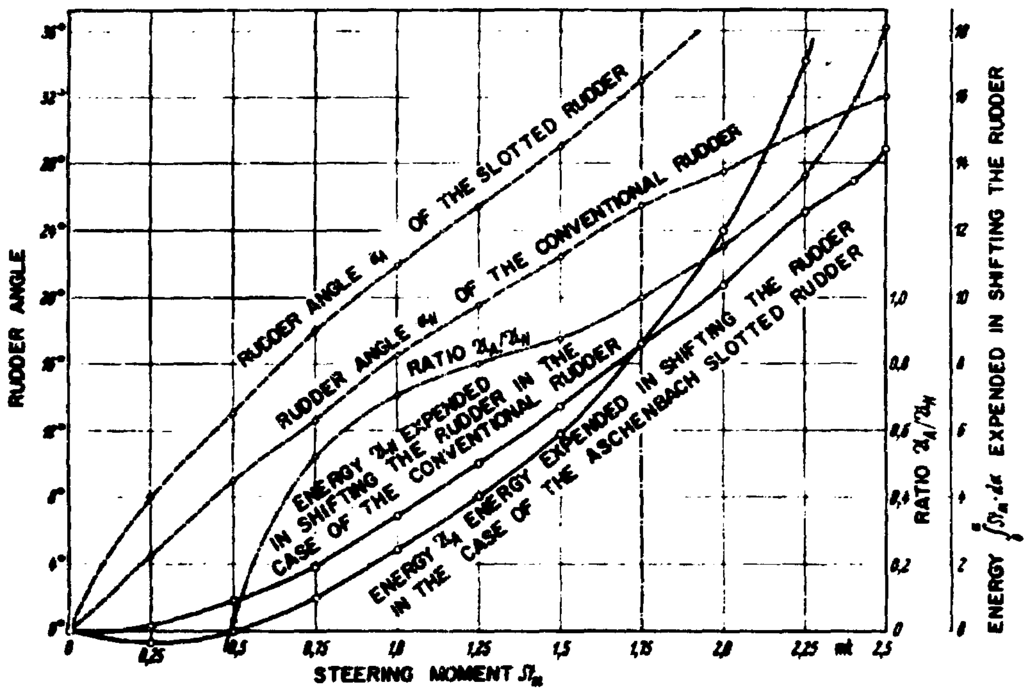

Figure 4 - Energy Expended in Shifting the Rudder for both Rudder Types

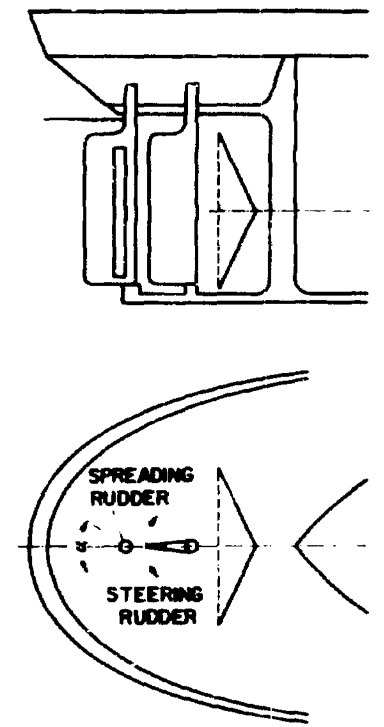

Figure 5 - Sketch of Rudder Arrangement

Figure 4. It will be seen that up to a rudder angle of 20 deg, the Aschenbach-slotted rudder can be shifted more easily with equal rudder efficiency.

It should be pointed out that these tests with elements were not intended to determine optimum rudder arrangements but only to compare the conventional rudder with a slotted rudder designed on the spur of the moment. The slotted rudder should have been adapted to the hull. This is proved by my design for concrete tankers whose rudders were adapted to the form of the ship and as a result, exhibited a comparatively smaller head resistance both in the experimental tank at the Berlin Research Institute for Hydraulic Engineering and Shipbuilding and on the river Danube.

During the test runs along a sinuous course, the rudder is shifted to zero, whereupon it is shifted to port or starboard by means of a steering engine and the sheering of the model out of course is observed. Once the model has reached a course angle of 10 deg, the rudder is shifted to the opposite course and the measuring process is repeated. By carrying out this maneuver several times, we obtain the Z-maneuver for 10-, 20-, and 30-deg rudder angle. If the rudder is shifted in intervals from one hard-over position to the other (from full-right to full-left rudder), a turbulent flow is produced about the rudder which does not calm down very quickly; in the case of the moving ship, on the other hand, an almost laminar flow occurs since the rudder is shifted slowly with the result that the streamlining of the rudder stands out more prominently compared to the unstreamlined conventional rudder just as the existence of a slot becomes more prominent, too.

Although these tests demonstrated a certain superiority of the slotted rudder, it would nevertheless be a good idea if the author of the paper would extend his investigations to include this type of rudder also since in wartime not all of my proposals, objections, and modifications could be taken into consideration.

The other patent referred to concerned a twin 'spreading rudder' ('Spreizdoppelruder,' "spreading double rudder") which is to serve the purpose of roll quenching. According to the intensity of the seaway, the angle of spread (or flare) α is adjusted, and by means of the twin rudder, that half of the rudder which is effective in a given case can reduce the

yawing of the ship and thus the rolling as well since the yawing and rolling motions are coupled with one another through the path of the center of gravity; the result is that steering the ship along a straight course must also have the effect of damping the rolling of the ship, at least the rolling oscillations, at the same time.

The steering rudder does not participate in this; the spreading rudder, however, which may be installed fore or aft of the steering rudder is controlled by a gyroscope which shifts it accordingly. In a calm sea, the angle α may be set at zero.

Figure 5 shows a sketch of the arrangement. It has not been executed as yet. However, since it is simpler than other stabilizers, I should like to recommend that the author include this rudder arrangement in future tests.

Prof. G. Weinblum, Dr. Eng., Dr. Eng. h.c., Hamburg
(Word of appreciation).

Although the somewhat unfortunate time history may have tired you perhaps, you have nevertheless gained the impression how much work may be accomplished in this field, already regarded as classical, and how much has actually been accomplished by Mr. Thieme. The latter now resembles a sponge which is sucked full of useful information; hence, we may expect a number of interesting results from him in the course of the next few years. I believe that I speak for all present when I say that we are very grateful to Mr. Thieme for his fundamental and practically interesting presentation; thus we conclude the present lecture (Lively applause).

Dr. J. Richter, Dr. Eng., Berlin (submitted in writing).

First of all, I wish to express my appreciation to Mr. Thieme for his report. He may be certain that not only naval architects but also marine engineers and electrical engineers are keenly interested in this work.

I was particularly interested in the difference in the turning ability of the small ship model in comparison to the full-scale ship if the rudder is dimensioned according to scale and if one is governed by Froude's law when determining the model speed. In one individual case, I have

ascertained that for a scale of length of 1:75, the turning ability of the model fell 16 percent below the turning ability of the full-scale ship. I am sure that the author can furnish information as to the size of the model rudder required in order to predict the actual turning ability of a full-scale ship from steering tests with models.

Dipl.-Ing. H. Thieme (Written reply)

The two proposals made by Dr. Aschenbach—slotted rudder and spreading rudder—had not previously come to my attention nor presumably to many in this audience; hence, this presentation of his proposals will contribute to many additional lines of reasoning in the rudder development. What is common to both proposals from the hydrodynamic standpoint is that they concern the problem of the tandem rudder. Inasmuch as few data exist on this subject, I had already taken this project into consideration for further programs. Thus, the recommendation of Dr. Aschenbach falls on somewhat prepared ground.

I should like to point out, however, that I do not expect any advantage can be gained by using a slotted rudder. The superiority of this form as obtained in the rudder moment for equal efficiency in the lower angle range is based less on the superior quality of this arrangement than on the arbitrary underbalancing of the barge rudder used for comparison.

I have some reservations on accepting the conjecture regarding the dynamically obtained flow condition on the model rudder and the laminar condition on the ship rudder.

In conclusion, I wish to express my keen appreciation to Dr. Aschenbach for sharing his experiences with us and for his suggestions.

The question raised by Dr. Richter with regard to the methods of accounting for scale effect on the rudder efficiency broadens the scope of the subject in a natural and weldome manner. Hence, I am doubly grateful to him for his observation.

Let me first turn to Dr. Richter's statement that in one case he observed that the turning ability of the model amounted to only 84 percent of the turning ability of the ship. In a study of 11 ships of all possible types and various rudder angles, Suarez and Strumpf (Davidson Laboratory

Note No. 548) determined the ratios of the turning ability between model and ship to be between 0.7 and 1.14, in which case the values below 1 are altogether preponderant. Hence, Dr. Richter's observation lies within the range of statistically normal expectation.

The following scale effects may have an effect on the magnitude of the force to be expected on the rudder:

1. Apart from undesirable and extreme laminar effects, the wake on the rudder is generally greater for the model than for the ship.

2. For rudders in the propeller slipstream, we must always assume a greater velocity increment for the free-running models than for the ship. This effect is thus the opposite of the one referred to under 1. Hence, the final result may lie in both directions.

3. In the case of similar flow conditions, the smooth model rudder with a smaller Reynolds number normally shows smaller force coefficients in all cases than the rougher ship rudder with a greater Reynolds number; from this, too, we may therefore expect a contribution in terms of a reduction of the ratio of the turning ability.

In the normal case, no suitably computed corrections are made in model tests because of the considerable difficulties encountered in estimating these effects in advance. In case of . given advance estimation the ratio of the turning ability to be expected under 1. may be guarded against by a dissimilar enlargement of the rudder area on the model or--in case one is restricted to fairly moderate rudder deflections--by replacing the streamline model rudder by a plate model rudder.

Although this goes somewhat beyond the question raised by Dr. Richter, but I want to avoid having the reader jump to any oversimplified analogy conclusions. Hence, I wish to add immediately that theoretically the change in the course stability as well as in the yaw-checking ability may be expected to amount to no more than approximately one-half the magnitude owing to the scale between model and ship in view of 1. and 2.; This result is obtained if consideration is given to the change of the flow angles on the rudder which is brought about by the scale effects.

INITIAL DISTRIBUTION

Copies	
6	CHBUSHIPS 2 Tech Info Br (Code 210L) 1 Lab Mgt (Code 320) 1 Mach, Sci & Res Sec (Code 436) 2 Sci & Res Sec (Code 442)
20	DDC
4	CNO 2 (Op 922) 2 (Op 923M3)
1	Special Libraries Assoc. 31 East 10th St New York, N.Y. 10003

Unclassified
Security Classification

DOCUMENT CONTROL DATA - R&D

(Security classification of title, body of abstract and indexing annotation must be entered when the overall report is classified)

1. ORIGINATING ACTIVITY (Corporate author) David Taylor Model Basin	2a. REPORT SECURITY CLASSIFICATION Unclassified 2b. GROUP

3. REPORT TITLE

DESIGN OF SHIP RUDDERS (Zur Formgebung von Schiffsrudern)

4. DESCRIPTIVE NOTES (Type of report and inclusive dates)

Translation

5. AUTHOR(S) (Last name, first name, initial)

Thieme, H.

6. REPORT DATE	7a. TOTAL NO. OF PAGES	7b. NO. OF REFS
November 1965	69	30

8a. CONTRACT OR GRANT NO. b. PROJECT NO. c. d.	9a. ORIGINATOR'S REPORT NUMBER(S) Translation 321 9b. OTHER REPORT NO(S) (Any other numbers that may be assigned this report)

10. AVAILABILITY/LIMITATION NOTICES

Foreign announcement and dissemination of this report by DDC is not authorized.

11. SUPPLEMENTARY NOTES	12. SPONSORING MILITARY ACTIVITY

13. ABSTRACT

Starting from present day criteria for the choice of the size and arrangement of rudders, this paper discusses the suitable streamlining of guiding-head and balanced rudders. In addition to a purely visual comparison of conventional (usual) and newly developed profiles, the report includes profile offsets that have not been published previously and contrasts the form parameters of various rudder profiles which are based on a familiar mathematical method of profile representation. Comparative studies of several familiar foreign rudder profiles and of rudder profiles which have been developed in the Shipbuilding Institute in recent years indicate that the modern profiles definitely improve rudder efficiency, both when the ship is moving astern and ahead; this also applies to bow rudder profiles. The influence of the thickness ratio (proportion of thickness to length) in the case of plate rudders--which has not been established experimentally in publications thus far--is indicated in all additional test series. To illustrate the possibilities of subsequently improving the rudder profile either in efficiency or balancing, the use of a rudder wedge arrangement, with and without profile shortening, is discussed and examples are given from a special experimental investigation.

DD FORM 1 JAN 64 1473

Unclassified
Security Classification

Unclassified
Security Classification

14. KEY WORDS	LINK A ROLE	LINK A WT	LINK B ROLE	LINK B WT	LINK C ROLE	LINK C WT
Rudder Arrangement						
Structural Design						
Hydromechanic Aspects						
Comparison of Profile Forms						
Wind-Tunnel Tests						
Alteration of Rudder Characteristics						
Guiding head rudder						

INSTRUCTIONS

1. ORIGINATING ACTIVITY: Enter the name and address of the contractor, subcontractor, grantee, Department of Defense activity or other organization (*corporate author*) issuing the report.

2a. REPORT SECURITY CLASSIFICATION: Enter the overall security classification of the report. Indicate whether "Restricted Data" is included. Marking is to be in accordance with appropriate security regulations.

2b. GROUP: Automatic downgrading is specified in DoD Directive 5200.10 and Armed Forces Industrial Manual. Enter the group number. Also, when applicable, show that optional markings have been used for Group 3 and Group 4 as authorized.

3. REPORT TITLE: Enter the complete report title in all capital letters. Titles in all cases should be unclassified. If a meaningful title cannot be selected without classification, show title classification in all capitals in parenthesis immediately following the title.

4. DESCRIPTIVE NOTES: If appropriate, enter the type of report, e.g., interim, progress, summary, annual, or final. Give the inclusive dates when a specific reporting period is covered.

5. AUTHOR(S): Enter the name(s) of author(s) as shown on or in the report. Enter last name, first name, middle initial. If military, show rank and branch of service. The name of the principal author is an absolute minimum requirement.

6. REPORT DATE: Enter the date of the report as day, month, year, or month, year. If more than one date appears on the report, use date of publication.

7a. TOTAL NUMBER OF PAGES: The total page count should follow normal pagination procedures, i.e., enter the number of pages containing information.

7b. NUMBER OF REFERENCES: Enter the total number of references cited in the report.

8a. CONTRACT OR GRANT NUMBER: If appropriate, enter the applicable number of the contract or grant under which the report was written.

8b, 8c, & 8d. PROJECT NUMBER: Enter the appropriate military department identification, such as project number, subproject number, system numbers, task number, etc.

9a. ORIGINATOR'S REPORT NUMBER(S): Enter the official report number by which the document will be identified and controlled by the originating activity. This number must be unique to this report.

9b. OTHER REPORT NUMBER(S): If the report has been assigned any other report numbers (*either by the originator or by the sponsor*), also enter this number(s).

10. AVAILABILITY/LIMITATION NOTICES: Enter any limitations on further dissemination of the report, other than those imposed by security classification, using standard statements such as:

(1) "Qualified requesters may obtain copies of this report from DDC."

(2) "Foreign announcement and dissemination of this report by DDC is not authorized."

(3) "U. S. Government agencies may obtain copies of this report directly from DDC. Other qualified DDC users shall request through ________________."

(4) "U. S. military agencies may obtain copies of this report directly from DDC. Other qualified users shall request through ________________."

(5) "All distribution of this report is controlled. Qualified DDC users shall request through ________________."

If the report has been furnished to the Office of Technical Services, Department of Commerce, for sale to the public, indicate this fact and enter the price, if known.

11. SUPPLEMENTARY NOTES: Use for additional explanatory notes.

12. SPONSORING MILITARY ACTIVITY: Enter the name of the departmental project office or laboratory sponsoring (*paying for*) the research and development. Include address.

13. ABSTRACT: Enter an abstract giving a brief and factual summary of the document indicative of the report, even though it may also appear elsewhere in the body of the technical report. If additional space is required, a continuation sheet shall be attached.

It is highly desirable that the abstract of classified reports be unclassified. Each paragraph of the abstract shall end with an indication of the military security classification of the information in the paragraph, represented as (*TS*), (*S*), (*C*), or (*U*).

There is no limitation on the length of the abstract. However, the suggested length is from 150 to 225 words.

14. KEY WORDS: Key words are technically meaningful terms or short phrases that characterize a report and may be used as index entries for cataloging the report. Key words must be selected so that no security classification is required. Identifiers, such as equipment model designation, trade name, military project code name, geographic location, may be used as key words but will be followed by an indication of technical context. The assignment of links, roles, and weights is optional.

Unclassified
Security Classification

David Taylor Model Basin. Translation 321.
DESIGN OF SHIP RUDDERS (ZUR FORMGEBUNG VON SCHIFFSRUDERN), by H. Thieme. Presented in supplements to the Main Convention, Hamburg, 1961 (Jahrbuch der Schiffbautechnischen Gesellschaft, v.56, 1962). Translated by E. N. Labouvie.
Nov 1965. viii, 69p., illus., graphs, tabs., refs.
UNCLASSIFIED

Starting from present day criteria for the choice of the size and arrangement of rudders, this paper discusses the suitable streamlining of guiding-head and balanced rudders. In addition to a purely visual comparison of conventional (usual) and newly developed profiles, the report includes profile offsets that have not been published previously and contrasts the form parameters of various rudder

1. Rudders--Development
2. Rudders--Design
3. Wedges--Applications
I. Thieme, H.

David Taylor Model Basin. Translation 321.
DESIGN OF SHIP RUDDERS (ZUR FORMGEBUNG VON SCHIFFSRUDERN), by H. Thieme. Presented in supplements to the Main Convention, Hamburg, 1961 (Jahrbuch der Schiffbautechnischen Gesellschaft, v.56, 1962). Translated by E. N. Labouvie.
Nov 1965. viii, 69p., illus., graphs, tabs., refs.
UNCLASSIFIED

Starting from present day criteria for the choice of the size and arrangement of rudders, this paper discusses the suitable streamlining of guiding-head and balanced rudders. In addition to a purely visual comparison of conventional (usual) and newly developed profiles, the report includes profile offsets that have not been published previously and contrasts the form parameters of various rudder

1. Rudders--Development
2. Rudders--Design
3. Wedges--Applications
I. Thieme, H.

David Taylor Model Basin. Translation 321.
DESIGN OF SHIP RUDDERS (ZUR FORMGEBUNG VON SCHIFFSRUDERN), by H. Thieme. Presented in supplements to the Main Convention, Hamburg, 1961 (Jahrbuch der Schiffbautechnischen Gesellschaft, v.56, 1962). Translated by E. N. Labouvie.
Nov 1965. viii, 69p., illus., graphs, tabs., refs.
UNCLASSIFIED

Starting from present day criteria for the choice of the size and arrangement of rudders, this paper discusses the suitable streamlining of guiding-head and balanced rudders. In addition to a purely visual comparison of conventional (usual) and newly developed profiles, the report includes profile offsets that have not been published previously and contrasts the form parameters of various rudder

1. Rudders--Development
2. Rudders--Design
3. Wedges--Applications
I. Thieme, H.

David Taylor Model Basin. Translation 321.
DESIGN OF SHIP RUDDERS (ZUR FORMGEBUNG VON SCHIFFSRUDERN), by H. Thieme. Presented in supplements to the Main Convention, Hamburg, 1961 (Jahrbuch der Schiffbautechnischen Gesellschaft, v.56, 1962). Translated by E. N. Labouvie.
Nov 1965. viii, 69p., illus., graphs, tabs., refs.
UNCLASSIFIED

Starting from present day criteria for the choice of the size and arrangement of rudders, this paper discusses the suitable streamlining of guiding-head and balanced rudders. In addition to a purely visual comparison of conventional (usual) and newly developed profiles, the report includes profile offsets that have not been published previously and contrasts the form parameters of various rudder

1. Rudders--Development
2. Rudders--Design
3. Wedges--Applications
I. Thieme, H.

profiles which are based on a familiar mathematical method of profile representation. Comparative studies of several familiar foreign rudder profiles and of rudder profiles which have been developed in the Shipbuilding Institute in recent years indicate that the modern profiles definitely improve rudder efficiency, both when the ship is moving astern and ahead; this also applies to bow rudder profiles. The influence of the thickness ratio (proportion of thickness to length) in the case of plate rudders--which has not been established experimentally in publications thus far--is indicated in an additional test series. To illustrate the possibilities of subsequently improving the rudder profile either in efficiency or balancing, the use of a rudder wedge arrangement, with and without profile shortening, is discussed and examples are given from a special experimental investigation.

profiles which are based on a familiar mathematical method of profile representation. Comparative studies of several familiar foreign rudder profiles and of rudder profiles which have been developed in the Shipbuilding Institute in recent years indicate that the modern profiles definitely improve rudder efficiency, both when the ship is moving astern and ahead; this also applies to bow rudder profiles. The influence of the thickness ratio (proportion of thickness to length) in the case of plate rudders--which has not been established experimentally in publications thus far--is indicated in an additional test series. To illustrate the possibilities of subsequently improving the rudder profile either in efficiency or balancing, the use of a rudder wedge arrangement, with and without profile shortening, is discussed and examples are given from a special experimental investigation.

profiles which are based on a familiar mathematical method of profile representation. Comparative studies of several familiar foreign rudder profiles and of rudder profiles which have been developed in the Shipbuilding Institute in recent years indicate that the modern profiles definitely improve rudder efficiency, both when the ship is moving astern and ahead; this also applies to bow rudder profiles. The influence of the thickness ratio (proportion of thickness to length) in the case of plate rudders--which has not been established experimentally in publications thus far--is indicated in an additional test series. To illustrate the possibilities of subsequently improving the rudder profile either in efficiency or balancing, the use of a rudder wedge arrangement, with and without profile shortening, is discussed and examples are given from a special experimental investigation.

profiles which are based on a familiar mathematical method of profile representation. Comparative studies of several familiar foreign rudder profiles and of rudder profiles which have been developed in the Shipbuilding Institute in recent years indicate that the modern profiles definitely improve rudder efficiency, both when the ship is moving astern and ahead; this also applies to bow rudder profiles. The influence of the thickness ratio (proportion of thickness to length) in the case of plate rudders--which has not been established experimentally in publications thus far--is indicated in an additional test series. To illustrate the possibilities of subsequently improving the rudder profile either in efficiency or balancing, the use of a rudder wedge arrangement, with and without profile shortening, is discussed and examples are given from a special experimental investigation.